

PSP/IS⊙IS Energetic Particle Data - User Guide

Prepared by: Bala Poduval, Jonathan Niehof & Wouter de Wet
Bala.Poduval@unh.edu; Jonathan.Niehof@unh.edu; Wouter.deWet@unh.edu

Release Version – Release 6

November 16, 2020

Contents

1	INTRODUCTION	1
1.1	Terms of Use: IS \odot IS Data	1
1.2	Release Notes	2
1.2.1	Release 1	2
1.2.2	Release 2	2
1.2.3	Release 3	3
1.2.4	Release 4	3
1.2.5	Release 5	4
1.2.6	Release 6	4
1.3	Photon Contamination	4
1.3.1	Photons and Dust	5
1.3.2	Look Directions	5
1.3.3	Energy Ranges	5
1.3.4	Proxies	6
1.3.5	Summary	6
2	SUMMARY: SCIENCE DATA	7
2.1	EPI-Lo Science Data	7
2.1.1	File: psp_isois-epilo_l2-ic	8
2.1.2	File: psp_isois-epilo_l2-pe	9
2.2	EPI-Hi Science Data	9
2.2.1	File: psp_isois-epihi_l2-het-rates10	10
2.2.2	File: psp_isois-epihi_l2-het-rates300	12
2.2.3	File: psp_isois-epihi_l2-het-rates3600	12
2.2.4	File: psp_isois-epihi_l2-het-rates60	21
2.2.5	File: psp_isois-epihi_l2-let1-rates10	29
2.2.6	File: psp_isois-epihi_l2-let1-rates300	30
2.2.7	File: psp_isois-epihi_l2-let1-rates3600	30
2.2.8	File: psp_isois-epihi_l2-let1-rates60	37
2.2.9	File: psp_isois-epihi_l2-let2-rates10	42
2.2.10	File: psp_isois-epihi_l2-let2-rates300	43
2.2.11	File: psp_isois-epihi_l2-let2-rates3600	43
2.2.12	File: psp_isois-epihi_l2-let2-rates60	48
2.2.13	File: psp_isois-epihi_l2-second-rates	52
3	GENERAL LIST OF VARIABLES	53
3.1	psp_isois-epihi_l2-het-rates10	53
3.2	psp_isois-epihi_l2-het-rates300	53
3.3	psp_isois-epihi_l2-het-rates3600	54
3.4	psp_isois-epihi_l2-het-rates60	56
3.5	psp_isois-epihi_l2-let1-rates10	58
3.6	psp_isois-epihi_l2-let1-rates300	59
3.7	psp_isois-epihi_l2-let1-rates3600	60

3.8	psp_isois-epihi_l2-let1-rates60	62
3.9	psp_isois-epihi_l2-let2-rates10	64
3.10	psp_isois-epihi_l2-let2-rates300	65
3.11	psp_isois-epihi_l2-let2-rates3600	65
3.12	psp_isois-epihi_l2-let2-rates60	67
3.13	psp_isois-epihi_l2-second-rates	68
3.14	psp_isois-epilo_l2-ic	69
3.15	psp_isois-epilo_l2-pe	70
3.16	psp_isois_l2-summary	71
4	CDF CONTENTS	72
4.1	psp_isois_l2-summary	72
4.1.1	Primary variables	72
4.1.2	Other data	72
4.1.3	Other support	73
4.2	psp_isois-epilo_l2-ic	73
4.2.1	Primary variables	73
4.2.2	Other data	74
4.2.3	Other support	84
4.3	psp_isois-epilo_l2-pe	84
4.3.1	Primary variables	84
4.3.2	Other data	84
4.3.3	Other support	90
4.4	psp_isois-epihi_l2-het-rates10	90
4.4.1	Primary variables	91
4.4.2	Other data	91
4.4.3	Other support	94
4.5	psp_isois-epihi_l2-het-rates300	94
4.5.1	Primary variables	94
4.5.2	Other data	94
4.5.3	Other support	99
4.6	psp_isois-epihi_l2-het-rates3600	99
4.6.1	Primary variables	99
4.6.2	Other data	100
4.6.3	Other support	115
4.7	psp_isois-epihi_l2-het-rates60	115
4.7.1	Primary variables	116
4.7.2	Other data	117
4.7.3	Other support	126
4.8	psp_isois-epihi_l2-let1-rates10	126
4.8.1	Primary variables	127
4.8.2	Other data	127
4.8.3	Other support	130
4.9	psp_isois-epihi_l2-let1-rates300	130
4.9.1	Primary variables	130

4.9.2	Other data	130
4.9.3	Other support	137
4.10	psp_isois-epihi_l2-let1-rates3600	137
4.10.1	Primary variables	137
4.10.2	Other data	139
4.10.3	Other support	155
4.11	psp_isois-epihi_l2-let1-rates60	155
4.11.1	Primary variables	155
4.11.2	Other data	157
4.11.3	Other support	168
4.12	psp_isois-epihi_l2-let2-rates10	168
4.12.1	Primary variables	168
4.12.2	Other data	169
4.12.3	Other support	170
4.13	psp_isois-epihi_l2-let2-rates300	170
4.13.1	Primary variables	171
4.13.2	Other data	171
4.13.3	Other support	174
4.14	psp_isois-epihi_l2-let2-rates3600	174
4.14.1	Primary variables	175
4.14.2	Other data	176
4.14.3	Other support	184
4.15	psp_isois-epihi_l2-let2-rates60	184
4.15.1	Primary variables	184
4.15.2	Other data	185
4.15.3	Other support	191
4.16	psp_isois-epihi_l2-second-rates	191
4.16.1	Primary variables	191
4.16.2	Other data	191
4.16.3	Other support	196
5	EPI-Lo DECODER RING	197
6	ACRONYMS	199
	REFERENCES	199

List of Tables

2.1.1	psp_isois-epilo_l2-ic	8
2.1.2	psp_isois-epilo_l2-pe	9
2.2.1	psp_isois-epihi_l2-het-rates10	11
2.2.2	psp_isois-epihi_l2-het-rates300	12
2.2.3	psp_isois-epihi_l2-het-rates3600	13
2.2.4	psp_isois-epihi_l2-het-rates3600 contd	14

2.2.5	psp_isois-epihi_l2-het-rates3600 contd	14
2.2.6	psp_isois-epihi_l2-het-rates3600 contd	15
2.2.7	psp_isois-epihi_l2-het-rates3600 contd	16
2.2.8	psp_isois-epihi_l2-het-rates3600 contd	17
2.2.9	psp_isois-epihi_l2-het-rates3600 contd	18
2.2.10	psp_isois-epihi_l2-het-rates3600 contd	19
2.2.11	psp_isois-epihi_l2-het-rates3600 contd	20
2.2.12	psp_isois-epihi_l2-het-rates60	21
2.2.13	psp_isois-epihi_l2-het-rates60 contd	22
2.2.14	psp_isois-epihi_l2-het-rates60 contd	22
2.2.15	psp_isois-epihi_l2-het-rates60 contd	23
2.2.16	psp_isois-epihi_l2-het-rates60 contd	24
2.2.17	psp_isois-epihi_l2-het-rates60 contd	25
2.2.18	psp_isois-epihi_l2-het-rates60 contd	26
2.2.19	psp_isois-epihi_l2-het-rates60 contd	27
2.2.20	psp_isois-epihi_l2-het-rates60 contd	28
2.2.21	psp_isois-epihi_l2-let1-rates10	29
2.2.22	psp_isois-epihi_l2-let1-rates300	30
2.2.23	psp_isois-epihi_l2-let1-rates3600	31
2.2.24	psp_isois-epihi_l2-let1-rates3600 contd	31
2.2.25	psp_isois-epihi_l2-let1-rates3600 contd	32
2.2.26	psp_isois-epihi_l2-let1-rates3600 contd	33
2.2.27	psp_isois-epihi_l2-let1-rates3600 contd	34
2.2.28	psp_isois-epihi_l2-let1-rates3600 contd	34
2.2.29	psp_isois-epihi_l2-let1-rates3600 contd	35
2.2.30	psp_isois-epihi_l2-let1-rates3600 contd	35
2.2.31	psp_isois-epihi_l2-let1-rates3600 contd	35
2.2.32	psp_isois-epihi_l2-let1-rates3600 contd	36
2.2.33	psp_isois-epihi_l2-let1-rates60	37
2.2.34	psp_isois-epihi_l2-let1-rates60 contd	38
2.2.35	psp_isois-epihi_l2-let1-rates60 contd	38
2.2.36	psp_isois-epihi_l2-let1-rates60 contd	39
2.2.37	psp_isois-epihi_l2-let1-rates60 contd	39
2.2.38	psp_isois-epihi_l2-let1-rates60 contd	40
2.2.39	psp_isois-epihi_l2-let1-rates60 contd	41
2.2.40	psp_isois-epihi_l2-let2-rates10	42
2.2.41	psp_isois-epihi_l2-let2-rates300	43
2.2.42	psp_isois-epihi_l2-let2-rates3600	44
2.2.43	psp_isois-epihi_l2-let2-rates3600 contd	44
2.2.44	psp_isois-epihi_l2-let2-rates3600 contd	45
2.2.45	psp_isois-epihi_l2-let2-rates3600 contd	46
2.2.46	psp_isois-epihi_l2-let2-rates3600 contd	46
2.2.47	psp_isois-epihi_l2-let2-rates3600 contd	47
2.2.48	psp_isois-epihi_l2-let2-rates3600 contd	47
2.2.49	psp_isois-epihi_l2-let2-rates3600 contd	48

2.2.50	psp_isois-epihi_l2-let2-rates60	48
2.2.51	psp_isois-epihi_l2-let2-rates60 contd	49
2.2.52	psp_isois-epihi_l2-let2-rates60 contd	49
2.2.53	psp_isois-epihi_l2-let2-rates60 contd	50
2.2.54	psp_isois-epihi_l2-let2-rates60 contd	50
2.2.55	psp_isois-epihi_l2-let2-rates60 contd	51
2.2.56	psp_isois-epihi_l2-let2-rates60 contd	51
2.2.57	psp_isois-epihi_l2-second-rates	52

List of Figures

1	EPI-Lo Instrument	7
2	EPI-Lo Skymap	8
3	EPI-Hi Instrument & FOV	10
4	EPI-Lo Decoder Ring	197

PSP/IS⊙IS Energetic Particle Data - User Guide

November 16, 2020

INTRODUCTION

This user guide contains detailed information on the various quantities measured by the Integrated Science Investigation of the Sun (IS⊙IS) instrument suite on board the Parker Solar Probe (PSP) and how to access them from the data repository. These are the Level 2 data from the EPI-Lo (Energetic Particle Instrument - Low Energy) and EPI-Hi (Energetic Particle Instrument - High Energy) instruments. This document is divided into seven sections, including this introduction and references. Also included in the Introduction is an account of photon contamination (§ 1.3). The terms of using the PSP/IS⊙IS data is presented in § 1.1. The various properties of the solar energetic particles detected in a wide range of energies and the associated attributes such as cadence, energy bins, look directions and sectors in each CDF file that are useful for science analysis are tabulated and presented in § 2. All the variables currently available in the data repository for the scientific community are listed in § 3 and § 4 consists of a compilation of all the information of the variables from the metadata in each CDF file. The variables listed in § 3 are dynamically linked to their detailed descriptions in § 4. The EPI-Lo Decoder Ring is presented in § 5 and a list acronyms in § 6, followed by References.

TERMS OF USE: IS⊙IS DATA

Production of Integrated Science Investigation of the Sun (IS⊙IS) data is funded as part of NASA's Parker Solar Probe mission under contract NNN06AA01C. Use of any IS⊙IS data should include the following acknowledgement and also refer to the publication provided below.

Acknowledgement:

“Thanks to the Integrated Science Investigation of the Sun (IS⊙IS) Science Team (PI: David McComas, Princeton University).”

Reference Publication:

McComas, D. J. et al. (2016), Integrated Science Investigation of the Sun (IS⊙IS): Design of the Energetic Particle Investigation, *Space Science Reviews*, 204, 187–256, doi:10.1007/s11214-014-0059-1.

RELEASE NOTES

RELEASE 1

Released 2019-11-15.

Proper analysis of this first release of the data requires knowledge of several caveats and possible instrumental effects.

- Pitch angles are using preliminary calibrations from the FIELDS magnetic field instrument. This may result in errors in pitch angle determination up to about 1.5 degrees.
- EPI-Hi and EPI-Lo data use different units for energies and thus for fluxes. EPI-Hi data are reported MeV for protons and electrons, and MeV/nuc for heavy ions. EPI-Lo uses keV for all species except for time-of-flight only data, which uses keV/nuc. These differences are important when combining data across the two sensors.
- Ions heavier than helium and electrons are likely to have substantial background, including from other species, and are thus provided as count rates only until commissioning of these species can be completed for inclusion in a future release.
- EPI-Hi data below approximately 2MeV may be subject to instrumental effects that are currently being quantified. At these energies, the incident energy may be under reported by as much as 10% and the flux may be underreported by as much as 30%.
- EPI-Hi hourly (3600) data is compiled on the hour according to the spacecraft clock. The first integration after turn-on may be substantially shorter than an hour depending on when turn-on occurred. This may result in poor counting statistics from a short integration and unrealistic spectra for this first integration. The same effect is present, but less apparent, for the first integration of shorter periods.
- Spacecraft position is provided for every timebase in a file. Position is in HCI (variable names starting with HCI_R, HCI_Lat, HCI_Lon for each timebase) and HGC (names starting with HGC_R, HGC_Lat, HGC_Lon). Particle flow direction for each look direction is provided as unit vectors in HCI and RTN, as well as pitch angle, also on every timebase; variable names start with HCI, RTN, and PA.

RELEASE 2

Released 2020-01-27.

This release extends the dataset through 2019-10-10 (after third encounter). Files included cover the entire mission; thus it supersedes release 1. Contact the SOC for access to release 1 data if needed for comparison.

- Pitch angles for 2019 use updated FIELDS calibrations. The 2018 pitch angles have not changed from release 1, as FIELDS calibrations from 2018 required no updating.
- The summary product (psp_isois_12-summary) includes a new variable, A_Heavy_Rate_TS. This is a total heavy-ion count rate from the EPI-Hi LET1A telescope.

RELEASE 3

Released 2020-04-14.

This release extends the dataset through 2020-01-06. This includes the end of Orbit 3 and beginning of Orbit 4, including Venus Flyby 2, but with no new encounter data. Files included cover the entire mission; thus it supersedes previous releases. Contact the SOC for access to release 1 and 2 data if needed for comparison.

- Much of the CDF metadata has been updated to provide better descriptions and make data easier to find. In particular, pitch angle and related pointing data are tagged as data rather than support_data to make them more visible in many tools. Variable names have not been changed.
- Updated calibration tables for EPI-Lo have been applied. This results in small (a few percent) changes in energy channels and fluxes throughout the mission.

RELEASE 4

Released 2020-08-04.

This release extends the dataset through 2020-04-29. This includes Encounter 4 and the rest of orbit 4. Files included cover the entire mission; thus this release supersedes all previous releases. Contact the SOC for access to release 1-3 data if needed for comparison.

- The EPI-Hi instrument was off for operational reasons from 2019-10-07 through 2020-02-12.
- Due to a dust impact on 2019-04-03 around 16:45Z, look direction 31 of the EPI-Lo TOF-only products (channel T) is highly susceptible to UV photon contamination after this time (see <http://dx.doi.org/10.3847/1538-4365/ab643d>). Release 3 removed calibrated fluxes for this look direction after this time. In release 4, L31 is also excluded from count rate products that are summed over look direction. This includes H_CountRate_ChanT_SP in psp_isois_12-summary and related quicklook plots. This exclusion is for all time, so that rates before and after the dust impact can be compared. Look directions 34 and 35, although they retain intact foils, can also be heavily contaminated by UV and are excluded from summed count rate products as well.
- During the EPI-Lo high voltage ramp-up immediately after turn-on (approximately 15 minutes), count rates and fluxes are not accurate measurements of the incident population. These periods have been filtered out from the flux and count rate variables.
- All pitch angle variables now have a corresponding “spiral angle” variable, containing the angle the particle flow direction makes with the outward nominal Parker Spiral. “Nominal” is defined as $400\text{km/s } v_{\text{sw}}$ with corotation breakdown at $10R_{\text{S}}$. For EPI-Lo, these variables are named like SA_ChanX; for EPI-Hi, names are similar to LET1_A_SA and LET1_A_R1_SECT_SA (for non-sectored and sectored rates, respectively.)
- Many small metadata updates have been made for greater clarity; variable names remain the same.

- EPI-Hi energy unit labeling is consistent (MeV/nuc for ions heavier than protons; MeV for all else) and all energy labels have consistent formatting.

RELEASE 5

Released 2020-09-24.

This release includes data through 2020-04-29, with no additional dates since release 4. This includes Encounter 4 and the rest of orbit 4. Files included cover the entire mission; thus this release supersedes all previous releases. Contact the SOC for access to release 1-4 data if needed for comparison.

- Release 4 was made using the EPI-Lo calibration data from release 2; release 5 uses the latest calibration data. This results in small (a few percent) changes in energy channels and fluxes throughout the mission, similar to release 3.
- Release 4 also included fluxes for look direction 31 of the time-of-flight products after the dust impact on 2019-04-03; these fluxes are largely from UV photon contamination and should not be used. They are properly filtered from release 5.
- EPI-Hi data are the same as release 4, but the files are reproduced in release 5 to avoid confusion.
- IS \odot IS summary data are largely the same as release 4, but may have small changes in energy channels in the variables related to EPI-Lo.

RELEASE 6

Released 2020-11-16.

This release extends the dataset through 2020-08-13. This includes Encounter 5 and the rest of orbit 5. Files included cover the entire mission; thus this release supersedes all previous releases. Contact the SOC for access to release 1-5 data if needed for comparison.

- Data may include brief periods of counts generated internally to the instrument for calibration purposes. These will be filtered in a future release and are noted in the Data Anomalies & Quality list (<https://spp-isois.sr.unh.edu/Released-Data-Anomalies-and-Quality-Notes.html>).
- Pitch angles for the periods 2019 Jan through Aug and 2020 Jan through Feb were added for this release.

PHOTON CONTAMINATION

EPI-Lo was designed to investigate the physics of energetic particles, however in the special lowest-energy “time-of-flight only” product used in this study, it also responds to solar photons in a subset of approximately sunward-looking apertures lacking special light-attenuating foils. This topic is discussed in detail by [Hill et al. \(2019\)](#) but we provide some details here.

PHOTONS AND DUST

The EPI-Lo design is robust against the detrimental effects of ambient dust or light entering any of EPI-Lo’s eighty apertures. The mitigation for light contamination includes employing thicker start foils in the six look directions dominated by photospheric light that is Thomson scattering off electrons near the Sun, and thus visible away from the solar disk where there is no shielding from PSP’s thermal protection system (TPS). In addition to thicker foils, we employ baffles and multiple coincidence logic to cut down photon contamination. Also, to protect against dust and resulting dust–hole–admitted light, an extra “collimator foil” was added to all collimator turrets so that pinholes from dust impacts either penetrate only the collimator foil (for the smallest dust grains ≤ 100 nm) or only admit light from very tiny solid angles where these holes line up, resulting in a greatly reduced geometry factor for post-impact light contamination than would occur with only one foil. The first dust impact directly detectable by EPI-Lo (i.e., an impact resulting in noticeable light–admitting damage) took place after the second perihelion on 2019–04–03 (DOY 093) 16:45 in the L31 direction (see Figure 2 for description of EPI-Lo look directions). This L31 hole resulted in elevated photon background in one look direction but at a level that has not diminish EPI-Lo’s scientific capabilities. This dust impact is discussed in more detail by [Szalay et al. \(2019\)](#).

LOOK DIRECTIONS

We divided the field of view (FOV) into three independent sets of look directions: the generally sunward-looking Bright Look directions with very clear photon viewing (composed of the look directions L22, L25, L34–L37, L44, and L46); the Dim Look directions surrounding the bright area, where there are reduced indications of photons (composed of look directions L24, L26, L27, L41, L45, L47); and the Dark Look direction region, where there is no strong sign of photons (composed of the apertures that are neither the bright look direction or the dim look direction lists and which are mostly composed of wedges W0, W1, and W5–W7, which look away from the Sun). Explicitly, the list of dark look directions is L00–L21, L23, L28–L33, L38–L40, L42, L43, and L48–L79, with the sum of the Bright, Dim, and Dark look directions incorporating all 80 apertures. Although the bright look directions are roughly those most directed at the Sun, an important distinction is that the six apertures closest to the Sun with thicker light-blocking start foils (L23, L30–L33, and L40) are not included in the bright FOV or dim FOV because the thick foils effectively block the scattered light.

ENERGY RANGES

In addition to the division of the FOV, the energy channels are also split into three independent ranges: Low Energy (channels T030 and T031, 1–4 keV/nuc detected energy, based on the TOF measurement, corresponding to incident energies below 34 keV when H is assumed), where accidentals dominate during quiet times; Medium Energy (channels T016–T029, 4–350 keV/nuc detected and 34–370 keV for incident H), where foreground ion measurements are the strongest; and High Energy (channels T001–T015, 350 keV/nuc – 37 MeV/nuc detected and 370 keV – 39 MeV for incident H), where crosstalk events dominate during quiet times. Although the upper energy limit is high, no ions were detected above a few hundred keV/nuc (confirmed by EPI-Hi observations). The reason that accidental coincidences are associated with lower energy intensifications is because randomly distributed start and stop events that accidentally satisfy the TOF logic result in a flat distribution in TOF-space, but because of the inverse square relationship between energy and

TOF, a large fraction of the longer end of the TOF range corresponds to a small, low-energy range of energies.

PROXIES

With these definitions we found that a good proxy for the clean ion signal is found by combining Low Energy/Dark Look Directions, Medium-Energy/Dim Look Directions, and Medium-Energy/Dark Look Directions and a good proxy for photon contamination is the Low-Energy/Bright Look Direction measurements. That is, Ion Proxy = Low Dark + Medium Dim + Medium Dark and Photon Proxy = Low Bright.

SUMMARY

EPI-Lo measures ion intensity, energy, composition, and anisotropy, by design, and also responds to photons that are most likely scattered by zodiacal dust. Utilizing thicker start foils to suppress photon contamination unfortunately degrades low-energy ion response, so this mitigation was used sparingly; consequently, there are several generally sunward apertures with thin start foils where photons produce backgrounds, mostly through accidental coincidence of uncorrelated transmitted photon start and stop triggers. The result is that EPI-Lo responds to SEPs and solar photons, and through directional and energy filtering as well as accidental coincidence calculations, the ion signal can be largely separated from the photon backgrounds, as we have detailed.

SUMMARY: SCIENCE DATA

In this section, the energetic particle measurements of *PSP/IS⊙IS* that are useful for science investigations are presented. The various quantities measured by the EPI-Lo (Energetic Particle Instrument - Low Energy) and EPI-Hi (Energetic Particle Instrument - High Energy) instruments are tabulated in Tables 2.1.1 – 2.2.57.

EPI-LO SCIENCE DATA

Figure 1 shows the EPI-Lo instrument layout and Figure 2 depicts the view of the sky of the 80 apertures. The files containing the EPI-Lo data are named as: <mission>_<suite-instrument>_<data level>_<file-descriptor> (e.g., *psp_isois-epilo_l2_ic*). There are four primary science data files corresponding to the four modes (depicted by <file-descriptor>) of observation: ion composition (ic), ion energy (ie), particle composition (pc) and particle energy (pe). The tables in this section summarize the science data available for the following EPI-Lo data files:

psp_isois-epilo_l2-ic (ion composition)
psp_isois-epilo_l2-pe (particle energy)

Species without energy ranges specified are measured in this mode but are not yet commissioned. They will be included in future releases.

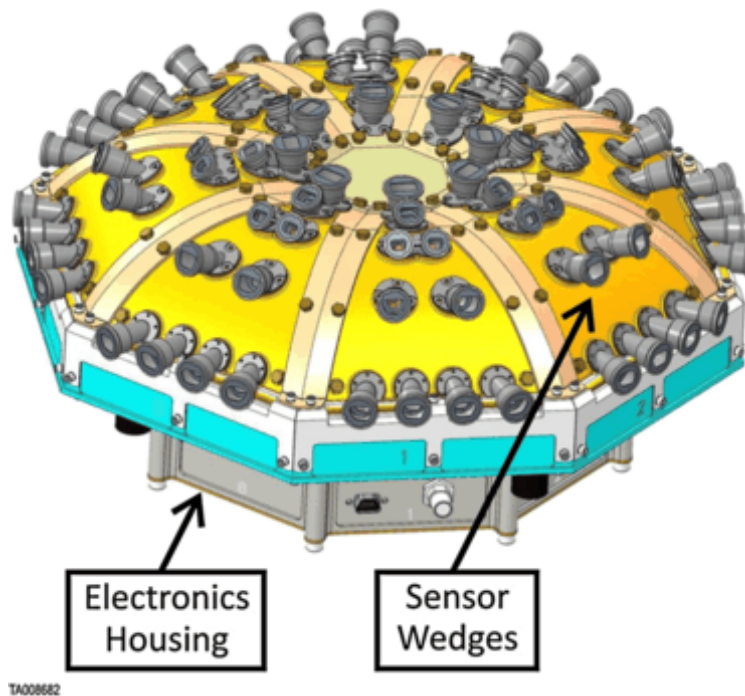


Figure 1: The EPI-Lo Instrument (see [McComas et al., 2016](#), for details).

FILE: PSP_ISOIS-EPILO_L2-IC

This file contains the EPI-Lo ion composition (ic) data for various particle species such as C, Fe, H, ³He, ⁴He, Mg, O and Si. The variable name is structured as <species>_<quantity>_<channel>, where, <species> is one of the particle species; <quantity> takes ‘Counts’, ‘CountRate’ (counts/s) or ‘Flux’ (cm⁻² sr⁻¹ sec⁻¹ keV⁻¹); and <channel> takes one of the values in Column 2. The Columns ‘Look Direction’ and ‘Energy’ imply the available look directions (0 – 79) and energy ranges, respectively, in the data file. For details on look directions, see [McComas et al. \(2016\)](#). Examples: C_CountRate_ChanD; H_Flux_ChanT.

Species	Channel	Size	Count Rate		Counts		Flux	
			Look Direction 80	Energy (keV) (bins)	Look Direction 80	Energy (keV) (bins)	Look Direction 80	Energy (keV) (bins)
C	D	80x48	0 – 79	206 – 17560 (21)	0 – 79	206 – 17560 (21)	0 – 79	206 – 17560 (21)
Fe	C	80x48	0 – 79	466 – 20709 (41)	0 – 79	466 – 20709 (41)	0 – 79	466 – 20709 (41)
H	R	80x48	0 – 79	62 – 83 (41)	0 – 79	62 – 8320 (41)	0 – 79	62 – 8320 (41)
	P	80x48	0 – 79	70 – 8320 (15)	0 – 79	70 – 8320 (15)	0 – 79	70 – 8320 (15)
	T	80x48	0 – 79	30 – 47318 (32)	0 – 79	30 – 47318 (32)	0 – 79	30 – 47318 (32)
He3	D	80x48	0 – 79	87 – 18514 (46)	0 – 79	87 – 18514 (46)	0 – 79	87 – 18514 (46)
He4	C	80x48	0 – 79	73 – 18518 (46)	0 – 79	73 – 18518 (46)	0 – 79	73 – 18518 (46)
Mg	D	80x48	0 – 79	–	0 – 79	–	0 – 79	–
O	C	80x48	0 – 79	233 – 19119 (41)	0 – 79	233 – 19119 (41)	0 – 79	233 – 19119 (41)
Si	D	80x48	0 – 79	594 – 18650 (15)	0 – 79	594 – 18650 (15)	0 – 79	594 – 18650 (15)

Table 2.1.1: PSP_ISOIS-EPILO_L2-IC: The EPI-Lo ion composition (ic) data for C, Fe, H, He3, He4, Mg, O and Si in channels D, C, R, P and T.

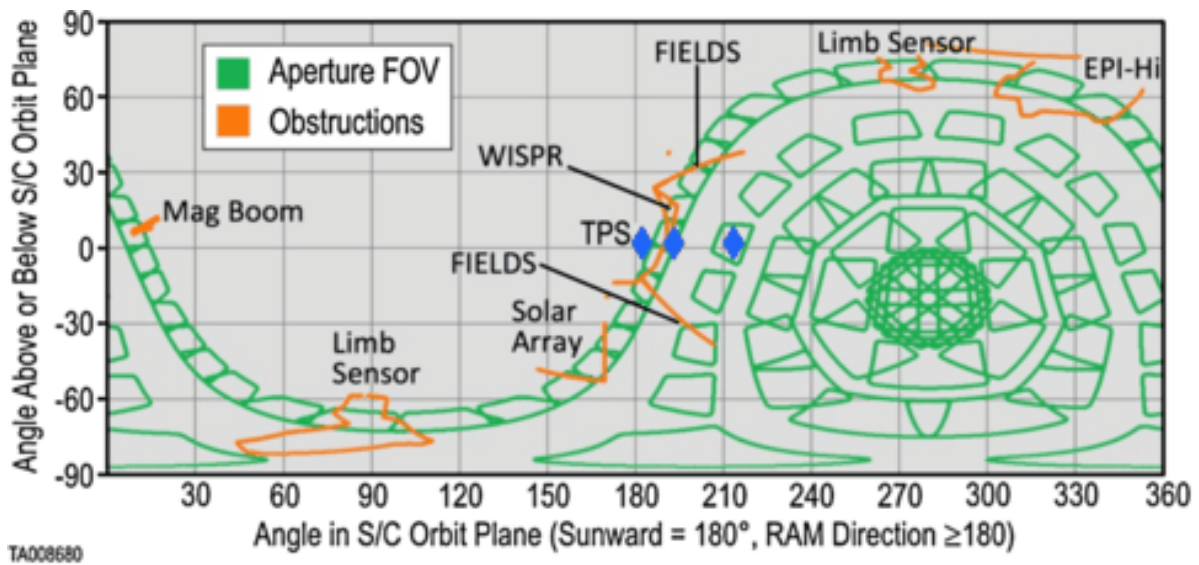


Figure 2: EPI-Lo Skymap (see [McComas et al., 2016](#), for details).

FILE: PSP_ISOIS-EPILO_L2-PE

EPI-Lo particle energy (pe) data for different particle species, C, electron, H, ^3He , He, and O. The general form of the variable name is: <species>_<quantity>_<channel>. Here, <species> refers to one of the particle species; <quantity> takes ‘Counts’, ‘CountRate’ (counts/s) or ‘Flux’ ($\text{cm}^{-2} \text{sr}^{-1} \text{sec}^{-1} \text{keV}^{-1}$); and <channel> takes to one of the values in Column 2.

Examples: C_Flux_ChanN; O_Counts_ChanX; Electron_CountRate_ChanE.

Species	Channel	Size	Count Rate		Counts		Flux	
			Look Direction (bins)	Energy (keV) (bins)	Look Direction (bins)	Energy (keV) (bins)	Look Direction (bins)	Energy (keV) (bins)
C	X	8 x 48	0 – 7 (8)	–	0 – 7 (8)	–	0 – 7 (8)	–
electron	E	8 x 48	0 – 7 (8)	27 – 375 (16)	0 – 7 (8)	27 – 375 (16)	0 – 7 (8)	27 – 375 (16)
	G	80 x 48	0 – 79 (80)	27 – 375 (16)	0 – 79 (80)	27 – 375 (16)	0 – 79 (80)	27 – 375 (16)
	F	8 x 48	0 – 7 (8)	33 – 375 (9)	0 – 7 (8)	33 – 375 (9)	0 – 7 (8)	33 – 375 (9)
H	E	8 x 48	0 – 7 (8)	–	0 – 7 (8)	–	0 – 7 (8)	–
	F	80 x 48	0 – 79 (80)	–	0 – 79 (80)	–	0 – 79 (80)	–
	F	8 x 48	0 – 7 (8)	–	0 – 7 (8)	–	0 – 7 (8)	–
	X	8 x 64	0 – 7 (8)	–	0 – 7 (8)	–	0 – 7 (8)	–
^3He	X	8 x 48	0 – 7 (8)	–	0 – 7 (8)	–	0 – 7 (8)	–
He	X	8 x 48	0 – 7 (8)	–	0 – 7 (8)	–	0 – 7 (8)	–
O	X	8 x 48	0 – 7 (8)	–	0 – 7 (8)	–	0 – 7 (8)	–

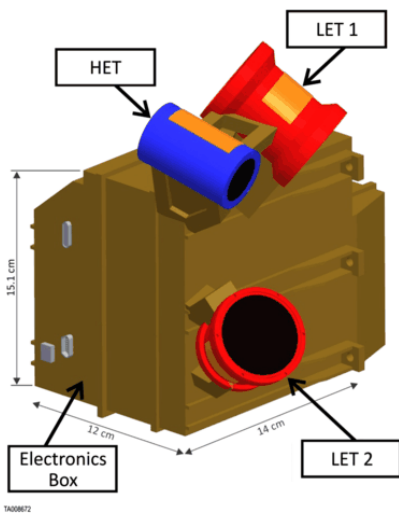
Table 2.1.2: PSP_ISOIS-EPILO_L2-PE. The EPI-Lo particle energy (pe) data for electron, H, ^3He , He and O in channels X, E, G, F and X.

EPI-HI SCIENCE DATA

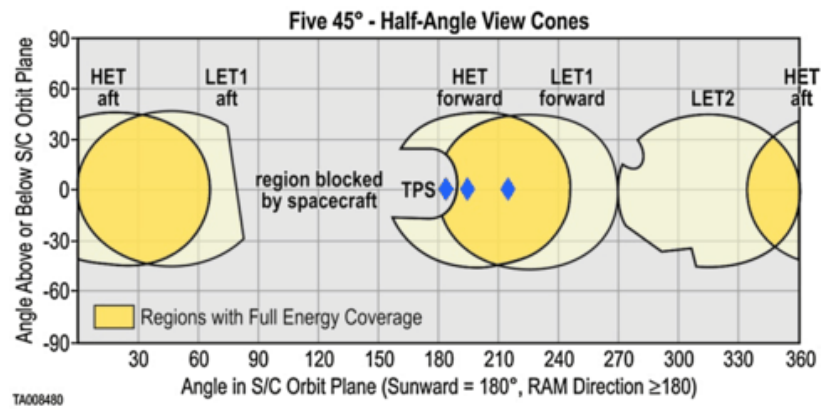
The following tables summarize the science data for the EPI-Hi Instrument. The files are named as: <mission>_<suite-instrument>_<data level>_<file-descriptor>. The EPI-Hi instrument consists of three telescopes HET, LET1 and LET2. The HET and LET1 telescopes have two sides (A, B) and let2 has one side (C). Sides A on LET1 and HET look sunward along the Parker Spiral and sides B on LET1 and HET look antisunward. Side C LET2 looks in the spacecraft ram direction. Full pointing information (RTN/HCI) is available in the L2 files (see [McComas et al., 2016](#), and [Figure 3](#)). The numerical values following rates in the <file-descriptor> represent the cadence in seconds (e.g., rates10; rates300). If no value is present, the cadence is assumed to be 1 second. Listed below are the EPI-Hi data files. The 60 s cadence products containing only the engineering singles are excluded from public release.

EPI-Hi science rates are accumulated at several cadences. The 10 s and 1 s rates are an encounter-only product. The 60 s rates are also, at a baseline, encounter-only. The 3600 s rates are the main cruise phase product. EPI-Hi produces several engineering rates that overflow their counters when accumulated for 3600 s. For those, a 1/60 sample of the 60 s rates are included in cruise data. The 60 s products are thus produced for the whole mission but those containing no science data are excluded from the public release.

HET	LET1	LET2
psp_isois-epihi_l2-het-rates10	psp_isois-epihi_l2-let1-rates10	psp_isois-epihi_l2-let2-rates10
psp_isois-epihi_l2-het-rates300	psp_isois-epihi_l2-let1-rates300	psp_isois-epihi_l2-let2-rates300
psp_isois-epihi_l2-het-rates3600	psp_isois-epihi_l2-let1-rates3600	psp_isois-epihi_l2-let2-rates3600
psp_isois-epihi_l2-het-rates60	psp_isois-epihi_l2-let1-rates60	psp_isois-epihi_l2-let2-rates60
HET, LET1 & LET2		psp_isois-epihi_l2-second-rates



(a) EPI-Hi Instrument.



(b) EPI-Hi field of view.

Figure 3: The EPI-Hi instrument and field of view. Sides A on LET1 and HET look sunward along the Parker Spiral while sides B on LET1 and HET look antisunward. Side C on LET2 looks in the spacecraft *ram* direction. Full pointing information (RTN/HCI) is available in the L2 files (see [McComas et al., 2016](#), for details on the sides A, B and C given in the tables.)

FILE: PSP_ISOIS-EPIHI_L2-HET-RATES10

This file contains the 10 s data of energetic particle Counts, Flux ($\text{cm}^{-2} \text{sr}^{-1} \text{MeV}^{-1}$) and Count Rate (counts/s) for electrons, H, He and NEUT_DET for sides A and B, for different ranges (R1 – R7) of the High Energy Telescope (HET). The naming convention of the variables in the data files is: <side>_<species>_<quantity> for those quantities independent of range. Here, <side> stands for A or B; <species> stands for the particle species (electrons, H, He, etc.); and <quantity> represents Counts (not used in variable names, in general), Flux or Rate. For those parameters

measured as a function of range, the naming convention is: <range><side>_<species>_<quantity>, where, <range> goes from R1 to R7 and <side> takes either A or B. Variable names without ranges (e.g., A_Electrons_Flux) or with double digit range (e.g., R17) have the values integrated over all the available ranges (R1 to R7, in general).

Examples: A_H (measured quantity is “counts”); A_Electrons_Flux; R1A_Electrons_Rate.

Side	Range	Quantity	Electrons		H		He		NEUT_DET	
			E-bins	E-range (MeV/nuc) (bins)	E-bins	E-range (MeV/nuc) (bins)	E-bins	E-range (MeV/nuc) (bins)	E-bins	E-range (MeV/nuc) (bins)
A/B		Count	16	1 - 9 (16)	11	10 - 59 (11)	12	10 - 70 (12)	35	0 - 495 (35)
		Flux	16	1 - 9 (16)	11	10 - 59 (11)	12	10 - 70 (12)		
		Count Rate	16	1 - 9 (16)	11	10 - 59 (11)	12	10 - 70 (12)	35	0 - 495 (35)
	R1	Count	12	1 - 4 (12)	7	9 - 25 (7)	8	9 - 29 (8)		
		Flux	12	1 - 4 (12)	7	9 - 25 (7)	8	9 - 29 (8)		
		Count Rate	12	1 - 4 (12)	7	9 - 25 (7)	8	9 - 29 (8)		
	R2	Count	12	1 - 4 (12)	7	15 - 42 (7)	8	15 - 50 (8)		
		Flux	12	1 - 4 (12)	7	15 - 42 (7)	8	15 - 50 (8)		
		Count Rate	12	1 - 4 (12)	7	15 - 42 (7)	8	15 - 50 (8)		
	R3	Count	10	1 - 5 (10)	6	21 - 50 (6)	7	21 - 59 (7)		
		Flux	10	1 - 5 (10)	6	21 - 50 (6)	7	21 - 59 (7)		
		Count Rate	10	1 - 5 (10)	6	21 - 50 (6)	7	21 - 59 (7)		
	R4	Count	10	1 - 6 (10)	4	29 - 50 (4)	5	29 - 59 (5)		
		Flux	10	1 - 6 (10)	4	29 - 50 (4)	5	29 - 59 (5)		
		Count Rate	10	1 - 6 (10)	4	29 - 50 (4)	5	29 - 59 (5)		
	R5	Count	9	2 - 7 (9)	4	35 - 59 (4)	5	35 - 70 (5)		
		Flux	9	2 - 7 (9)	4	35 - 59 (4)	5	35 - 70 (5)		
		Count Rate	9	2 - 7 (9)	4	35 - 59 (4)	5	35 - 70 (5)		
	R6	Count	9	2 - 9 (9)	4	35 - 59 (4)	5	35 - 70 (5)		
		Flux	9	2 - 9 (9)	4	35 - 59 (4)	5	35 - 70 (5)		
		Count Rate	9	2 - 9 (9)	4	35 - 59 (4)	5	35 - 70 (5)		
	R7	Count	9	3 - 10 (9)	4	42 - 70 (4)	5	42 - 83 (5)		
		Flux	9	3 - 10 (9)	4	42 - 70 (4)	5	42 - 83 (5)		
		Count Rate	9	3 - 10 (9)	4	42 - 70 (4)	5	42 - 83 (5)		

Table 2.2.1: PSP_ISOIS-EPIHI_L2-HET-RATES10. The 10 s HET data of particle Counts, Flux and Count Rate for electrons, H, He and NEUT_DET for sides A and B, and for ranges R1 – R7.

FILE: PSP_ISOIS-EPIHI_L2-HET-RATES300

This file provides the 300 s rates of energetic particle Counts, Flux ($\text{cm}^{-2} \text{sr}^{-1} \text{sec}^{-1} \text{MeV}^{-1}$) and Count Rate (counts/s) for CNO, FeGroup and NetoSi ions for ranges R1 – R7 of the High Energy Telescope (HET) for sides A and B. The variables (summarized in Table 2.2.2) are named as: <side>_<species>_<quantity> for those quantities independent of range. Here, <side> stands for A or B; <species> stands for the particle species (CNO_SECT, FeGroup_SECT and NetoSi_SECT), and <quantity> represents Counts (not used in the variable names, in general), Flux or Rate. Examples: A_CNO_SECT (measured quantity is “counts”); A_FeGroup_SECT_Flux; A_NetoSi_SECT_Rate.

Side	Quantity	CNO_SECT			FeGroup_SECT			NetoSi_SECT		
		E-bins	E-range (MeV/nuc)	Sectors (bins)	E-bins	E-range (MeV/nuc)	Sectors (bins)	E-bins	E-range (MeV/nuc)	Sectors (bins)
A/B	Count	2	36 – 68	0 – 8 (9)	1	81 – 81	0 – 8 (9)	1	57 – 57	0 – 8 (9)
	Flux	2	36 – 68	0 – 8 (9)	1 1	81 – 81	0 – 8 (9)	1 1	57 – 57	0 – 8 (9)
	Count Rate	2	36 – 68	0 – 8 (9)	1 1	81 – 81	0 – 8 (9)	1 1	57 – 57	0 – 8 (9)
ENB_SECT - measured quantity is Count; Size 1 X 25; E-bins: 1; E-range: 12 - 12; Sectors: 0 -8 (9).										

Table 2.2.2: PSP_ISOIS-EPIHI_L2-HET-RATES300. The 300 s cadence HET data of particle Counts, Flux and Count Rate for CNO, FeGroup and NetoSi ions for sides A and B, and integrated over ranges R1 – R7.

FILE: PSP_ISOIS-EPIHI_L2-HET-RATES3600

In this file, the 3600 s cadence data of particle Counts, Flux ($\text{cm}^{-2} \text{sr}^{-1} \text{sec}^{-1} \text{MeV}^{-1}$) and Count Rate (counts/s) measured by High Energy Telescope (HET) are available. The names of variables (summarized in Tables 2.2.3 – 2.2.11) follow the general pattern: <side>_<species>_<quantity>, where, <side> stands for A or B; <species> stands for the particle species (Al, Ar, C, etc., in column 2); and <quantity> represents Counts, Flux or Count Rate. Note that “Count” is not used in the variable names, in general. Variable names without ranges (e.g., A_C) or with double digit range (e.g., R17) have the values integrated over all the available ranges (R1 to R7, in general: e.g., B_H_SECT_Flux has values averaged over R1 – R7 in Table 2.2.3). Examples: A_C, NEUT1, NEUT2_DET, (measured quantity is “counts”); B_FeGroup_SECT_Flux; PENA_C_Rate; R1A_32to50_Flux.

Side	Species	Count			Flux			Count Rate		
		Size (bins)	Range SECT (bins)	Energy (MeV/nuc)	Size (bins)	Range SECT (bins)	Energy (MeV/nuc)	Size (bins)	Range SECT (bins)	Energy (MeV/nuc)
A/B	Al	15	–	21 – 236	15	–	21 – 236	15	–	21 – 236
	Ar	15	–	25 – 280	15	–	25 – 280	15	–	25 – 280
	C	15	–	12 – 140	15	–	12 – 140	15	–	12 – 140
	CNO_SECT	2x25 (2 bins)	R17 0 – 8 (9)	36 – 68	2x25 (2 bins)	R17 0 – 8 (9)	36 – 68	2x25 (2 bins)	R17 0 – 8 (9)	36 – 68
	Ca	15	–	25 – 280	15	–	25 – 280	15	–	25 – 280
	Cr	16	–	25 – 333	16	–	25 – 333	16	–	25 – 333
	Electrons	19	–	0 – 10	19	–	0 – 10	19	–	0 – 10
	Electron_SECT	2x25 (2 bins)	R17 0 – 8 (9)	2 – 3	2x25 (2 bins)	R17 0 – 8 (9)	3 – 3	2x25 (2 bins)	R17 0 – 8 (9)	2 – 3
	Fe	15	–	29 - 333	15	–	29 – 333	15	–	29 – 333
	FeGroup_SECT	1x25 (1 bin)	R17 0 – 8 (9)	81 – 81	1x25 (1 bin)	R17 0 – 8 (9)	81 – 81	1x25 (1 bin)	R17 0 – 8 (9)	81 – 81
	H	15	–	7 – 83	15	–	7 – 83	15	–	7 – 83
	H_SECT	2x25 (2 bins)	R17 0 – 8 (9)	18 – 34	2x25 (2 bins)	R17 0 – 8 (9)	18 – 34	2x25 (2 bins)	R17 0 – 8 (9)	18 – 34
	He	16	–	7 – 99	16	–	7 – 99	16	–	7 - 99
	He_SECT	2x25 (2 bins)	R17 0 – 8 (9)	18 – 34	2x25 (2 bins)	R17 0 – 8 (9)	18 – 34	2x25 (2 bins)	R17 0 – 8 (9)	18 – 34
	Mg	15	–	21 – 236	15	–	21 – 236	15	–	21 – 236
	N	15	–	12 – 140	15	–	12 – 140	15	–	12 – 140
	Na	15	–	18 – 198	15	–	18 – 198	15	–	18 – 198
	Ne	15	–	18 – 198	15	–	18 – 198	15	–	18 – 198
	NetoSi_SECT	1x25 (1 bin)	R17 0 – 8 (9)	57 – 57	1x25 (1 bin)	R17 0 – 8 (9)	57 – 57	1x25 (1 bin)	R17 0 – 8 (9)	57 – 57
	Ni	15	–	29 - 333	15	–	29 – 333	15	–	29 – 333
O	15	–	15 - 167	15	–	15 – 167	15	–	15 – 167	
S	16	–	21 – 280	16	–	21 – 280	16	–	21 – 280	
Si	15	–	21 – 236	15	–	21 – 236	15	–	21 – 236	
	NEUT1	35x21	–	0 – 495	–	–	–	35x21	–	0 – 495
	NEUT2_DET	35x6	–	0 – 495	–	–	–	35x6	–	0 – 495

Table 2.2.3: PSP_ISOIS-EPIHI_L2-HET-RATES3600. The 3600 s cadence HET data of the particle Counts, Flux and Count Rates for different particle species for sides A and B and ranges R1 – R7. R17 implies integration of the measured values over ranges R1 – R7.

Side	Species	Count		Count Rate	
		Size (bins)	Energy (MeV/nuc)	Size (bins)	Energy (MeV/nuc)
A/B	PENx_C	9	45 – 583	9	45 – 583
	PENx_Fe	9	108 – 793	9	108 – 793
	PENx_H	9	27 – 521	9	27 – 521
	PENx_He	9	27 – 521	9	27 – 521
	PENx_Mg	9	64 – 646	9	64 – 646
	PENx_N	9	45 – 583	9	45 – 583
	PENx_Ne	8	64 – 612	8	64 – 612
	PENx_O	9	54 – 612	9	54 – 612
	PENx_Si	9	76 – 687	9	76 – 687

Table 2.2.4: PSP_ISOIS-EPIHI_L2-HET-RATES3600 (contd.). Here, ‘x’ stands for sides A & B.

Side	Species	Count		Flux		Count Rate	
		Size (bins)	Energy (MeV/nuc)	Size (bins)	Energy (MeV/nuc)	Size (bins)	Energy (MeV/nuc)
A/B	xxx_29to32	6	14 – 538	6	14 – 538	6	14 – 538
	xxx_32to50	6	14 – 538	6	14 – 538	6	14 – 538
	xxx_Al	11	10 – 476	11	10 – 476	11	10 – 476
	xxx_Ar	11	11 – 484	11	11 – 484	11	11 – 484
	xxx_C	12	6 – 463	12	6 – 463	12	6 – 463
	xxx_Ca	11	11 – 484	11	11 – 484	11	11 – 484
	xxx_Cr	12	11 – 495	12	11 – 495	12	11 – 495
	xxx_Electrons	15	0 – 433	15	0 – 433	15	0 – 433
	xxx_Fe	11	14 – 495	11	14 – 495	11	14 – 495
	xxx_H	11	4 – 447	11	4 – 447	11	4 – 447
	xxx_He	12	4 – 450	12	4 – 450	12	4 – 450
	xxx_He_BIN	5x16 (5)	9 – 32	–	–	–	–
	xxx_He_BIN (MASS)	16 bins	–	–	–	–	–
		0 – 15 seg	–	–	–	–	–
	xxx_Mg	11	10 – 476	11	10 – 476	11	10 – 476
	xxx_N	12	6 – 463	12	6 – 463	12	6 – 463
	xxx_Na	11	8 – 469	11	8 – 469	11	8 – 469
	xxx_Ne	11	8 – 469	11	8 – 469	11	8 – 469
	xxx_Ne_BIN	4x8 (4)	23 – 65	–	–	–	–
	xxx_Ne_BIN (MASS)	8 bins	–	–	–	–	–
		0 – 7 seg	–	–	–	–	–
xxx_Ni	12	14 – 507	12	14 – 507	12	14 – 507	
xxx_O	11	7 – 463	11	7 – 463	11	7 – 463	
xxx_S	12	10 – 484	12	10 – 484	12	10 – 484	
xxx_Si	11	10 – 476	11	10 – 476	11	10 – 476	
xxx_gt50	6	14 – 538	6	14 – 538	6	14 – 538	

Table 2.2.5: PSP_ISOIS-EPIHI_L2-HET-RATES3600 (contd.). Here ‘xxx’ stands for R1A & R1B.

Side	Species	Count		Flux		Count Rate	
		Size (bins)	Energy (MeV/nuc)	Size (bins)	Energy (MeV/nuc)	Size (bins)	Energy (MeV/nuc)
A/B	xxx_29to32	5	23 – 538	5	23 – 538	5	23 – 538
	xxx_32to50	5	23 – 538	5	23 – 538	5	23 – 538
	xxx_Al	11	14 – 495	11	14 – 495	11	14 – 495
	xxx_Ar	11	19 – 521	11	19 – 521	11	19 – 521
	xxx_C	11	10 – 476	11	10 – 476	11	10 – 476
	xxx_Ca	11	19 – 521	11	19 – 521	11	19 – 521
	xxx_Cr	12	19 – 538	12	19 – 538	12	19 – 538
	xxx_Electrons	15	0 – 433	15	0 – 433	15	0 – 433
	xxx_Fe	11	23 – 538	11	23 – 538	11	23 – 538
	xxx_H	11	6 – 457	11	6 – 457	11	6 – 457
	xxx_He	12	6 – 463	12	6 – 463	12	6 – 463
	xxx_He_BIN xxx_He_BIN (MASS)	4x16 (4) 16 bins 0 – 15 seg	16 – 46 – –	– – –	– – –	– – –	– – –
	xxx_Mg	11	14 – 495	11	14 – 495	11	14 – 495
	xxx_N	11	10 – 476	11	10 – 476	11	10 – 476
	xxx_Na	11	14 – 495	11	14 – 495	11	14 – 495
	xxx_Ne	11	14 – 495	11	14 – 495	11	14 – 495
	xxx_Ne_BIN xxx_Ne_BIN (MASS)	4x8 (4) 8 bins 0 – 7 seg	32 – 92 – –	– – –	– – –	– – –	– – –
	xxx_Ni	11	23 – 538	11	23 – 538	11	23 – 538
	xxx_O	11	11 – 484	11	11 – 484	11	11 – 484
	xxx_S	12	16 – 521	12	16 – 521	12	16 – 521
xxx_Si	11	16 – 507	11	16 – 507	11	16 – 507	
xxx_gt50	5	23 – 538	5	23 – 538	5	23 – 538	

Table 2.2.6: PSP_ISOIS-EPIHI_L2-HET-RATES3600 (contd.). Here, ‘xxx’ stands for R2A and R2B.

Side	Species	Count		Flux		Count Rate	
		Size (bins)	Energy (MeV/nuc)	Size (bins)	Energy (MeV/nuc)	Size (bins)	Energy (MeV/nuc)
A/B	xxx_29to32	5	38 – 612	5	38 – 612	5	38 – 612
	xxx_32to50	5	38 – 612	5	38 – 612	5	38 – 612
	xxx_Al	9	23 – 507	9	23 – 507	9	23 – 507
	xxx_Ar	9	32 – 538	9	32 – 538	9	32 – 538
	xxx_C	9	16 – 484	9	16 – 484	9	16 – 484
	xxx_Ca	9	32 – 538	9	32 – 538	9	32 – 538
	xxx_Cr	10	32 – 559	10	32 – 559	10	32 – 559
	xxx_Electrons	13	1 – 433	13	1 – 433	13	1 – 433
	xxx_Fe	10	32 – 559	10	32 – 559	10	32 – 559
	xxx_H	10	8 – 463	10	8 – 463	10	8 – 463
	xxx_He	11	8 – 469	11	8 – 469	11	8 – 469
	xxx_He_BIN xxx_He_BIN (MASS)	4x16 (4) 16 bins 0 - 15 seg	23 – 65 – –	– – –	– – –	– – –	– – –
	xxx_Mg	9	23 – 507	9	23 – 507	9	23 – 507
	xxx_N	9	16 – 484	9	16 – 484	9	16 – 484
	xxx_Na	10	19 – 507	10	19 – 507	10	19 – 507
	xxx_Ne	10	19 – 507	10	19 – 507	10	19 – 507
	xxx_Ne_BIN xxx_Ne_BIN (MASS)	4x8 (4) 8 bins 0 - 7 seg	46 – 130 – –	– – –	– – –	– – –	– – –
	xxx_Ni	10	32 – 559	10	32 – 559	10	32 – 559
	xxx_O	9	19 – 495	9	19 – 495	9	19 – 495
	xxx_S	10	27 – 538	10	27 – 538	10	27 – 538
xxx_Si	9	27 – 521	9	27 – 521	9	27 – 521	
xxx_gt50	5	38 – 612	5	38 – 612	5	38 – 612	

Table 2.2.7: PSP_ISOIS-EPIHI_L2-HET-RATES3600 (contd.). Here, ‘xxx’ stands for R3A and R3B.

Side	Species	Count		Flux		Count Rate	
		Size (bins)	Energy (MeV/nuc)	Size (bins)	Energy (MeV/nuc)	Size (bins)	Energy (MeV/nuc)
A/B	xxx_29to32	5	38 – 612	5	38 – 612	5	38 – 612
	xxx_32to50	5	38 – 612	5	38 – 612	5	38 – 612
	xxx_Al	9	27 – 521	9	27 – 521	9	27 – 521
	xxx_Ar	8	38 – 538	8	38 – 538	8	38 – 538
	xxx_C	9	19 – 495	9	19 – 495	9	19 – 495
	xxx_Ca	8	38 – 538	8	38 – 538	8	38 – 538
	xxx_Cr	9	38 – 559	9	38 – 559	9	38 – 559
	xxx_Electrons	12	1 – 434	12	1 – 434	12	1 – 434
	xxx_Fe	8	45 – 559	8	45 – 559	8	45 – 559
	xxx_H	8	11 – 463	8	11 – 463	8	11 – 463
	xxx_He	9	11 – 469	9	11 – 469	9	11 – 469
	xxx_He_BIN xxx_He_BIN (MASS)	3x16 (3) 16 bins 0 - 15 seg	32 – 65 – –	– – –	– – –	– – –	– – –
	xxx_Mg	9	27 – 521	9	27 – 521	9	27 – 521
	xxx_N	9	19 – 495	9	19 – 495	9	19 – 495
	xxx_Na	8	27 – 507	8	27 – 507	8	27 – 507
	xxx_Ne	8	27 – 507	8	27 – 507	8	27 – 507
	xxx_Ne_BIN xxx_Ne_BIN (MASS)	3x8 (3) 8 bins 0 - 7 seg	65 – 130 – –	– – –	– – –	– – –	– – –
	xxx_Ni	9	45 – 583	9	45 – 583	9	45 – 583
	xxx_O	8	23 – 495	8	23 – 495	8	23 – 495
	xxx_S	9	32 – 538	9	32 – 538	9	32 – 538
xxx_Si	9	32 – 538	9	32 – 538	9	32 – 538	
xxx_gt50	5	38 – 612	5	38 – 612	5	38 – 612	

Table 2.2.8: PSP_ISOIS-EPIHI_L2-HET-RATES3600 (contd.). Here, ‘xxx’ stands for R4A and R4B.

Side	Species	Count		Flux		Count Rate	
		Size (bins)	Energy (MeV/nuc)	Size (bins)	Energy (MeV/nuc)	Size (bins)	Energy (MeV/nuc)
A/B	xxx_29to32	4	64 – 612	4	64 – 612	4	64 – 612
	xxx_32to50	4	64 – 612	4	64 – 612	4	64 – 612
	xxx_Al	9	32 – 538	9	32 – 538	9	32 – 538
	xxx_Ar	8	45 – 559	8	45 – 559	8	45 – 559
	xxx_C	8	23 – 495	8	23 – 495	8	23 – 495
	xxx_Ca	8	45 – 559	8	45 – 559	8	45 – 559
	xxx_Cr	9	45 – 583	9	45 – 583	9	45 – 583
	xxx_Electrons	11	1 – 435	11	1 – 435	11	1 – 435
	xxx_Fe	8	54 – 583	8	54 – 583	8	54 – 583
	xxx_H	8	14 – 469	8	14 – 469	8	14 – 469
	xxx_He	9	14 – 476	9	14 – 476	9	14 – 476
	xxx_He_BIN xxx_He_BIN (MASS)	3x16 (3) 16 bins 0 - 15 seg	32 – 65 – –	– – –	– – –	– – –	– – –
	xxx_Mg	9	32 – 538	9	32 – 538	9	32 – 538
	xxx_N	8	23 – 495	8	23 – 495	8	23 – 495
	xxx_Na	8	32 – 521	8	32 – 521	8	32 – 521
	xxx_Ne	8	32 – 521	8	32 – 521	8	32 – 521
	xxx_Ne_BIN xxx_Ne_BIN (MASS)	2x8 (2) 8 bins 0 - 7 seg	92 – 130 – –	– – –	– – –	– – –	– – –
	xxx_Ni	9	54 – 612	9	54 – 612	9	54 – 612
	xxx_O	8	27 – 507	8	27 – 507	8	27 – 507
	xxx_S	9	38 – 559	9	38 – 559	9	38 – 559
xxx_Si	8	38 – 538	8	38 – 538	8	38 – 538	
xxx_gt50	4	64 – 612	4	64 – 612	4	64 – 612	

Table 2.2.9: PSP_ISOIS-EPIHI_L2-HET-RATES3600 (contd.). Here, ‘xxx’ stands for R5A and R5B.

Side	Species	Count		Flux		Count Rate	
		Size (bins)	Energy (MeV/nuc)	Size (bins)	Energy (MeV/nuc)	Size (bins)	Energy (MeV/nuc)
A/B	xxx_29to32	4	64 – 612	4	64 – 612	4	64 – 612
	xxx_32to50	4	64 – 612	4	64 – 612	4	64 – 612
	xxx_Al	8	38 – 538	8	38 – 538	8	38 – 538
	xxx_Ar	9	45 – 583	9	45 – 583	9	45 – 583
	xxx_C	8	27 – 507	8	27 – 507	8	27 – 507
	xxx_Ca	9	45 – 583	9	45 – 583	9	45 – 583
	xxx_Cr	10	45 – 612	10	45 – 612	10	45 – 612
	xxx_Electrons	11	1 – 435	11	1 – 435	11	1 – 435
	xxx_Fe	9	54 – 612	9	54 – 612	9	54 – 612
	xxx_H	8	14 – 469	8	14 – 469	8	14 – 469
	xxx_He	9	14 – 476	9	14 – 476	9	14 – 476
	xxx_He_BIN xxx_He_BIN (MASS)	3x16 (3) 16 bins 0 - 15 seg	32 – 65 – –	– – –	– – –	– – –	– – –
	xxx_Mg	8	38 – 538	8	38 – 538	8	38 – 538
	xxx_N	8	27 – 507	8	27 – 507	8	27 – 507
	xxx_Na	8	38 – 538	8	38 – 538	8	38 – 538
	xxx_Ne	8	38 – 538	8	38 – 538	8	38 – 538
	xxx_Ne_BIN xxx_Ne_BIN (MASS)	3x8 (3) 8 bins 0 - 7 seg	92 – 184 – –	– – –	– – –	– – –	– – –
	xxx_Ni	9	54 – 612	9	54 – 612	9	54 – 612
	xxx_O	8	32 – 521	8	32 – 521	8	32 – 521
	xxx_S	9	45 – 583	9	45 – 583	9	45 – 583
xxx_Si	8	45 – 559	8	45 – 559	8	45 – 559	
xxx_gt50	4	64 – 612	4	64 – 612	4	64 – 612	

Table 2.2.10: PSP_ISOIS-EPIHI_L2-HET-RATES3600 (contd.). Here, ‘xxx’ stands for R6A and R6B.

Side	Species	Count		Flux		Count Rate	
		Size (bins)	Energy (MeV/nuc)	Size (bins)	Energy (MeV/nuc)	Size (bins)	Energy (MeV/nuc)
A/B	xxx_29to32	4	64 – 612	4	64 – 612	4	64 – 612
	xxx_32to50	4	64 – 612	4	64 – 612	4	64 – 612
	xxx_Al	8	45 – 559	8	45 – 559	8	45 – 559
	xxx_Ar	7	64 – 583	7	64 – 583	7	64 – 583
	xxx_C	7	32 – 507	7	32 – 507	7	32 – 507
	xxx_Ca	7	64 – 583	7	64 – 583	7	64 – 583
	xxx_Cr	8	64 – 612	8	64 – 612	8	64 – 612
	xxx_Electrons	11	1 – 436	11	1 – 436	11	1 – 436
	xxx_Fe	8	64 – 612	8	64 – 612	8	64 – 612
	xxx_H	8	16 – 476	8	16 – 476	8	16 – 476
	xxx_He	9	16 – 484	9	16 – 484	9	16 – 484
	xxx_He_BIN xxx_He_BIN (MASS)	2x16 (2) 16 bins 0 - 15 seg	46 – 65 – –	– – –	– – –	– – –	– – –
	xxx_Mg	8	45 – 559	8	45 – 559	8	45 – 559
	xxx_N	7	32 – 507	7	32 – 507	7	32 – 507
	xxx_Na	8	38 – 538	8	38 – 538	8	38 – 538
	xxx_Ne	8	38 – 538	8	38 – 538	8	38 – 538
	xxx_Ne_BIN xxx_Ne_BIN (MASS)	3x8 (3) 8 bins 0 - 7 seg	92 – 184 – –	– – –	– – –	– – –	– – –
	xxx_Ni	8	64 – 612	8	64 – 612	8	64 – 612
	xxx_O	7	38 – 521	7	38 – 521	7	38 – 521
	xxx_S	8	54 – 583	8	54 – 583	8	54 – 583
xxx_Si	7	54 – 559	7	54 – 559	7	54 – 559	
xxx_gt50	4	64 – 612	4	64 – 612	4	64 – 612	

Table 2.2.11: PSP_ISOIS-EPIHI_L2-HET-RATES3600 (contd.). Here, ‘xxx’ stands for R7A and R7B.

FILE: PSP_ISOIS-EPIHI_L2-HET-RATES60

This file contains the 60-second cadence data of particle Counts, Flux ($\text{cm}^{-2} \text{sr}^{-1} \text{sec}^{-1} \text{MeV}^{-1}$) and Count Rate (counts/s) for Al, Ar, C, Ca, Cr, Electrons, Fe, H, He, Mg, N, Na, Ne, Ni, O, S and Si ions for ranges R1 – R7) of the High Energy Telescope (HET) for sides A and B. The measured values are summarized in Tables 2.2.12 – 2.2.20. The variable names follow the structure: <side>_<species>_<quantity>, where, <side> stands for A or B; <species> stands for the particle species; and <quantity> represents Counts (not used in the variable names, in general), Flux or Count Rate. Variable names without ranges (e.g., A_C) or with double digit range (e.g., R17) have their values integrated over all the available ranges (R1 to R7, in general).

Examples: A_Fe (measured quantity is “counts”); B_Electron_SECT_Flux; PENB_Mg_Flux; R7A_Ni_Rate.

Side	Species	Count			Flux			Count Rate		
		Size (bins)	Range SECT (bins)	Energy (MeV/nuc)	Size (bins)	Range SECT (bins)	Energy (MeV/nuc)	Size (bins)	Range SECT (bins)	Energy (MeV/nuc)
A/B	Al	15	–	21 – 236	15	–	21 – 236	15	–	21 – 236
	Ar	15	–	25 – 280	15	–	25 – 280	15	–	25 – 280
	C	15	–	12 – 140	15	–	12 – 140	15	–	12 – 140
	Ca	15	–	25 – 280	15	–	25 – 280	15	–	25 – 280
	Cr	16	–	25 – 333	16	–	25 – 333	16	–	25 – 333
	Electrons	19	–	0 – 10	19	–	0 – 10	19	–	0 – 10
	Electron_SECT	2x25 (2 bins)	R17 0 – 8 (9)	2 – 3	2x25 (2 bins)	R17 0 – 8 (9)	3 – 3	2x25 (2 bins)	R17 0 – 8 (9)	2 – 3
	Fe	15	–	29 – 333	15	–	29 – 333	15	–	29 – 333
	H	15	–	7 – 83	15	–	7 – 83	15	–	7 – 83
	H_SECT	2x25 (2 bins)	R17 0 – 8 (9)	18 – 34	2x25 (2 bins)	R17 0 – 8 (9)	18 – 34	2x25 (2 bins)	R17 0 – 8 (9)	18 – 34
	He	16	–	7 – 99	16	–	7 – 99	16	–	7 – 99
	He_SECT	2x25 (2 bins)	R17 0 – 8 (9)	18 – 34	2x25 (2 bins)	R17 0 – 8 (9)	18 – 34	2x25 (2 bins)	R17 0 – 8 (9)	18 – 34
	Mg	15	–	21 – 236	15	–	21 – 236	15	–	21 – 236
	N	15	–	12 – 140	15	–	12 – 140	15	–	12 – 140
	Na	15	–	18 – 198	15	–	18 – 198	15	–	18 – 198
	Ne	15	–	18 – 198	15	–	18 – 198	15	–	18 – 198
	Ni	15	–	29 – 333	15	–	29 – 333	15	–	29 – 333
	O	15	–	15 – 167	15	–	15 – 167	15	–	15 – 167
	S	16	–	21 – 280	16	–	21 – 280	16	–	21 – 280
Si	15	–	21 – 236	15	–	21 – 236	15	–	21 – 236	

Table 2.2.12: PSP_ISOIS-EPIHI_HET-RATES60. The HET 60 s cadence data for various particle species. R17 implies integration of the measured values over ranges R1 – R7.

Side	Species	Count		Count Rate	
		Size (bins)	Energy (MeV/nuc)	Size (bins)	Energy (MeV/nuc)
A/B	PENx_C	9	45 – 583	9	45 – 583
	PENx_Fe	9	108 – 793	9	108 – 793
	PENx_H	9	27 – 521	9	27 – 521
	PENx_He	9	27 – 521	9	27 – 521
	PENx_Mg	9	64 – 646	9	64 – 646
	PENx_N	9	45 – 583	9	45 – 583
	PENx_Ne	8	64 – 612	8	64 – 612
	PENx_O	9	54 – 612	9	54 – 612
	PENx_Si	9	76 – 687	9	76 – 687

Table 2.2.13: PSP_ISOIS-EPIHI_L2-HET-RATES60 (contd.). Here, ‘x’ stands for sides A & B.

Side	Species	Count		Flux		Count Rate	
		Size (bins)	Energy (MeV/nuc)	Size (bins)	Energy (MeV/nuc)	Size (bins)	Energy (MeV/nuc)
A/B	xxx_29to32	6	14 – 538	6	14 – 538	6	14 – 538
	xxx_32to50	6	14 – 538	6	14 – 538	6	14 – 538
	xxx_Al	11	10 – 476	11	10 – 476	11	10 – 476
	xxx_Ar	11	11 – 484	11	11 – 484	11	11 – 484
	xxx_C	12	6 – 463	12	6 – 463	12	6 – 463
	xxx_Ca	11	11 – 484	11	11 – 484	11	11 – 484
	xxx_Cr	12	11 – 495	12	11 – 495	12	11 – 495
	xxx_Electrons	15	0 – 433	15	0 – 433	15	0 – 433
	xxx_Fe	11	14 – 495	11	14 – 495	11	14 – 495
	xxx_H	11	4 – 447	11	4 – 447	11	4 – 447
	xxx_He	12	4 – 450	12	4 – 450	12	4 – 450
	xxx_Mg	11	10 – 476	11	10 – 476	11	10 – 476
	xxx_N	12	6 – 463	12	6 – 463	12	6 – 463
	xxx_Na	11	8 – 469	11	8 – 469	11	8 – 469
	xxx_Ne	11	8 – 469	11	8 – 469	11	8 – 469
	xxx_Ni	12	14 – 507	12	14 – 507	12	14 – 507
	xxx_O	11	7 – 463	11	7 – 463	11	7 – 463
	xxx_S	12	10 – 484	12	10 – 484	12	10 – 484
	xxx_Si	11	10 – 476	11	10 – 476	11	10 – 476
	xxx_gt50	6	14 – 538	6	14 – 538	6	14 – 538

Table 2.2.14: PSP_ISOIS-EPIHI_HET-RATES60 (contd.). Here, ‘xxx’ stands for R1A and R1B.

Side	Species	Count		Flux		Count Rate	
		Size (bins)	Energy (MeV/nuc)	Size (bins)	Energy (MeV/nuc)	Size (bins)	Energy (MeV/nuc)
A/B	xxx_29to32	5	23 – 538	5	23 – 538	5	23 – 538
	xxx_32to50	5	23 – 538	5	23 – 538	5	23 – 538
	xxx_Al	11	14 – 495	11	14 – 495	11	14 – 495
	xxx_Ar	11	19 – 521	11	19 – 521	11	19 – 521
	xxx_C	11	10 – 476	11	10 – 476	11	10 – 476
	xxx_Ca	11	19 – 521	11	19 – 521	11	19 – 521
	xxx_Cr	12	19 – 538	12	19 – 538	12	19 – 538
	xxx_Electrons	15	0 – 433	15	0 – 433	15	0 – 433
	xxx_Fe	11	23 – 538	11	23 – 538	11	23 – 538
	xxx_H	11	6 – 457	11	6 – 457	11	6 – 457
	xxx_He	12	6 – 463	12	6 – 463	12	6 – 463
	xxx_He_BIN xxx_He_BIN (MASS)	4x16 (4) 16 bins 0 – 15 seg	16 – 46 – –	– – –	– – –	– – –	– – –
	xxx_Mg	11	14 – 495	11	14 – 495	11	14 – 495
	xxx_N	11	10 – 476	11	10 – 476	11	10 – 476
	xxx_Na	11	14 – 495	11	14 – 495	11	14 – 495
	xxx_Ne	11	14 – 495	11	14 – 495	11	14 – 495
	xxx_Ne_BIN xxx_Ne_BIN (MASS)	4x8 (4) 8 bins 0 – 7 seg	32 – 92 – –	– – –	– – –	– – –	– – –
	xxx_Ni	11	23 – 538	11	23 – 538	11	23 – 538
	xxx_O	11	11 – 484	11	11 – 484	11	11 – 484
	xxx_S	12	16 – 521	12	16 – 521	12	16 – 521
xxx_Si	11	16 – 507	11	16 – 507	11	16 – 507	
xxx_gt50	5	23 – 538	5	23 – 538	5	23 – 538	

Table 2.2.15: PSP_ISOIS-EPIHI_L2-HET-RATES60 (contd.). Here, ‘xxx’ stands for R2A and R2B.

Side	Species	Count		Flux		Count Rate	
		Size (bins)	Energy (MeV/nuc)	Size (bins)	Energy (MeV/nuc)	Size (bins)	Energy (MeV/nuc)
A/B	xxx_29to32	5	38 – 612	5	38 – 612	5	38 – 612
	xxx_32to50	5	38 – 612	5	38 – 612	5	38 – 612
	xxx_Al	9	23 – 507	9	23 – 507	9	23 – 507
	xxx_Ar	9	32 – 538	9	32 – 538	9	32 – 538
	xxx_C	9	16 – 484	9	16 – 484	9	16 – 484
	xxx_Ca	9	32 – 538	9	32 – 538	9	32 – 538
	xxx_Cr	10	32 – 559	10	32 – 559	10	32 – 559
	xxx_Electrons	13	1 – 433	13	1 – 433	13	1 – 433
	xxx_Fe	10	32 – 559	10	32 – 559	10	32 – 559
	xxx_H	10	8 – 463	10	8 – 463	10	8 – 463
	xxx_He	11	8 – 469	11	8 – 469	11	8 – 469
	xxx_He_BIN xxx_He_BIN (MASS)	4x16 (4) 16 bins 0 – 15 seg	23 – 65 – –	– – –	– – –	– – –	– – –
	xxx_Mg	9	23 – 507	9	23 – 507	9	23 – 507
	xxx_N	9	16 – 484	9	16 – 484	9	16 – 484
	xxx_Na	10	19 – 507	10	19 – 507	10	19 – 507
	xxx_Ne	10	19 – 507	10	19 – 507	10	19 – 507
	xxx_Ne_BIN xxx_Ne_BIN (MASS)	4x8 (4) 8 bins 0 – 7 seg	46 – 130 – –	– – –	– – –	– – –	– – –
	xxx_Ni	10	32 – 559	10	32 – 559	10	32 – 559
	xxx_O	9	19 – 495	9	19 – 495	9	19 – 495
	xxx_S	10	27 – 538	10	27 – 538	10	27 – 538
	xxx_Si	9	27 – 521	9	27 – 521	9	27 – 521
xxx_gt50	5	38 – 612	5	38 – 612	5	38 – 612	

Table 2.2.16: PSP_ISOIS-EPIHI_L2-HET-RATES60 (contd.). Here, ‘xxx’ stands for R3A and R3B.

Side	Species	Count		Flux		Count Rate	
		Size (bins)	Energy (MeV/nuc)	Size (bins)	Energy (MeV/nuc)	Size (bins)	Energy (MeV/nuc)
A/B	xxx_29to32	5	38 – 612	5	38 – 612	5	38 – 612
	xxx_32to50	5	38 – 612	5	38 – 612	5	38 – 612
	xxx_Al	9	27 – 521	9	27 – 521	9	27 – 521
	xxx_Ar	8	38 – 538	8	38 – 538	8	38 – 538
	xxx_C	9	19 – 495	9	19 – 495	9	19 – 495
	xxx_Ca	8	38 – 538	8	38 – 538	8	38 – 538
	xxx_Cr	9	38 – 559	9	38 – 559	9	38 – 559
	xxx_Electrons	12	1 – 434	12	1 – 434	12	1 – 434
	xxx_Fe	8	45 – 559	8	45 – 559	8	45 – 559
	xxx_H	8	11 – 463	8	11 – 463	8	11 – 463
	xxx_He	9	11 – 469	9	11 – 469	9	11 – 469
	xxx_He_BIN xxx_He_BIN (MASS)	3x16 (3) 16 bins 0 – 15 seg	32 – 65 – –	– – –	– – –	– – –	– – –
	xxx_Mg	9	27 – 521	9	27 – 521	9	27 – 521
	xxx_N	9	19 – 495	9	19 – 495	9	19 – 495
	xxx_Na	8	27 – 507	8	27 – 507	8	27 – 507
	xxx_Ne	8	27 – 507	8	27 – 507	8	27 – 507
	xxx_Ne_BIN xxx_Ne_BIN (MASS)	3x8 (3) 8 bins 0 – 7 seg	65 – 130 – –	– – –	– – –	– – –	– – –
	xxx_Ni	9	45 – 583	9	45 – 583	9	45 – 583
	xxx_O	8	23 – 495	8	23 – 495	8	23 – 495
	xxx_S	9	32 – 538	9	32 – 538	9	32 – 538
xxx_Si	9	32 – 538	9	32 – 538	9	32 – 538	
xxx_gt50	5	38 – 612	5	38 – 612	5	38 – 612	

Table 2.2.17: PSP_ISOIS-EPIHI_L2-HET-RATES60 (contd.). Here, ‘xxx’ stands for R4A and R4B.

Side	Species	Count		Flux		Count Rate	
		Size (bins)	Energy (MeV/nuc)	Size (bins)	Energy (MeV/nuc)	Size (bins)	Energy (MeV/nuc)
A/B	xxx_29to32	4	64 – 612	4	64 – 612	4	64 – 612
	xxx_32to50	4	64 – 612	4	64 – 612	4	64 – 612
	xxx_Al	9	32 – 538	9	32 – 538	9	32 – 538
	xxx_Ar	8	45 – 559	8	45 – 559	8	45 – 559
	xxx_C	8	23 – 495	8	23 – 495	8	23 – 495
	xxx_Ca	8	45 – 559	8	45 – 559	8	45 – 559
	xxx_Cr	9	45 – 583	9	45 – 583	9	45 – 583
	xxx_Electrons	11	1 – 435	11	1 – 435	11	1 – 435
	xxx_Fe	8	54 – 583	8	54 – 583	8	54 – 583
	xxx_H	8	14 – 469	8	14 – 469	8	14 – 469
	xxx_He	9	14 – 476	9	14 – 476	9	14 – 476
	xxx_He_BIN xxx_He_BIN (MASS)	3x16 (3) 16 bins 0 - 15 seg	32 – 65 – –	– – –	– – –	– – –	– – –
	xxx_Mg	9	32 – 538	9	32 – 538	9	32 – 538
	xxx_N	8	23 – 495	8	23 – 495	8	23 – 495
	xxx_Na	8	32 – 521	8	32 – 521	8	32 – 521
	xxx_Ne	8	32 – 521	8	32 – 521	8	32 – 521
	xxx_Ne_BIN xxx_Ne_BIN (MASS)	2x8 (2) 8 bins 0 - 7 seg	92 – 130 – –	– – –	– – –	– – –	– – –
	xxx_Ni	9	54 – 612	9	54 – 612	9	54 – 612
	xxx_O	8	27 – 507	8	27 – 507	8	27 – 507
	xxx_S	9	38 – 559	9	38 – 559	9	38 – 559
xxx_Si	8	38 – 538	8	38 – 538	8	38 – 538	
xxx_gt50	4	64 – 612	4	64 – 612	4	64 – 612	

Table 2.2.18: PSP_ISOIS-EPIHI_L2-HET-RATES60 (contd.). Here, ‘xxx’ stands for R5A and R5B.

Side	Species	Count		Flux		Count Rate	
		Size (bins)	Energy (MeV/nuc)	Size (bins)	Energy (MeV/nuc)	Size (bins)	Energy (MeV/nuc)
A/B	xxx_29to32	4	64 – 612	4	64 – 612	4	64 – 612
	xxx_32to50	4	64 – 612	4	64 – 612	4	64 – 612
	xxx_Al	8	38 – 538	8	38 – 538	8	38 – 538
	xxx_Ar	9	45 – 583	9	45 – 583	9	45 – 583
	xxx_C	8	27 – 507	8	27 – 507	8	27 – 507
	xxx_Ca	9	45 – 583	9	45 – 583	9	45 – 583
	xxx_Cr	10	45 – 612	10	45 – 612	10	45 – 612
	xxx_Electrons	11	1 – 435	11	1 – 435	11	1 – 435
	xxx_Fe	9	54 – 612	9	54 – 612	9	54 – 612
	xxx_H	8	14 – 469	8	14 – 469	8	14 – 469
	xxx_He	9	14 – 476	9	14 – 476	9	14 – 476
	xxx_He_BIN xxx_He_BIN (MASS)	3x16 (3) 16 bins 0 – 15 seg	32 – 65 – –	– – –	– – –	– – –	– – –
	xxx_Mg	8	38 – 538	8	38 – 538	8	38 – 538
	xxx_N	8	27 – 507	8	27 – 507	8	27 – 507
	xxx_Na	8	38 – 538	8	38 – 538	8	38 – 538
	xxx_Ne	8	38 – 538	8	38 – 538	8	38 – 538
	xxx_Ne_BIN xxx_Ne_BIN (MASS)	3x8 (3) 8 bins 0 – 7 seg	92 – 184 – –	– – –	– – –	– – –	– – –
	xxx_Ni	9	54 – 612	9	54 – 612	9	54 – 612
	xxx_O	8	32 – 521	8	32 – 521	8	32 – 521
	xxx_S	9	45 – 583	9	45 – 583	9	45 – 583
xxx_Si	8	45 – 559	8	45 – 559	8	45 – 559	
xxx_gt50	4	64 – 612	4	64 – 612	4	64 – 612	

Table 2.2.19: PSP_ISOIS-EPIHI_L2-HET-RATES60 (contd.). Here, ‘xxx’ stands for R6A and R6B.

Side	Species	Count		Flux		Count Rate	
		Size (bins)	Energy (MeV/nuc)	Size (bins)	Energy (MeV/nuc)	Size (bins)	Energy (MeV/nuc)
A/B	xxx_29to32	4	64 – 612	4	64 – 612	4	64 – 612
	xxx_32to50	4	64 – 612	4	64 – 612	4	64 – 612
	xxx_Al	8	45 – 559	8	45 – 559	8	45 – 559
	xxx_Ar	7	64 – 583	7	64 – 583	7	64 – 583
	xxx_C	7	32 – 507	7	32 – 507	7	32 – 507
	xxx_Ca	7	64 – 583	7	64 – 583	7	64 – 583
	xxx_Cr	8	64 – 612	8	64 – 612	8	64 – 612
	xxx_Electrons	11	1 – 436	11	1 – 436	11	1 – 436
	xxx_Fe	8	64 – 612	8	64 – 612	8	64 – 612
	xxx_H	8	16 – 476	8	16 – 476	8	16 – 476
	xxx_He	9	16 – 484	9	16 – 484	9	16 – 484
	xxx_He_BIN xxx_He_BIN (MASS)	2x16 (2) 16 bins 0 - 15 seg	46 – 65 – –	– – –	– – –	– – –	– – –
	xxx_Mg	8	45 – 559	8	45 – 559	8	45 – 559
	xxx_N	7	32 – 507	7	32 – 507	7	32 – 507
	xxx_Na	8	38 – 538	8	38 – 538	8	38 – 538
	xxx_Ne	8	38 – 538	8	38 – 538	8	38 – 538
	xxx_Ne_BIN xxx_Ne_BIN (MASS)	3x8 (3) 8 bins 0 - 7 seg	92 – 184 – –	– – –	– – –	– – –	– – –
	xxx_Ni	8	64 – 612	8	64 – 612	8	64 – 612
	xxx_O	7	38 – 521	7	38 – 521	7	38 – 521
	xxx_S	8	54 – 583	8	54 – 583	8	54 – 583
xxx_Si	7	54 – 559	7	54 – 559	7	54 – 559	
xxx_gt50	4	64 – 612	4	64 – 612	4	64 – 612	

Table 2.2.20: PSP_ISOIS-EPIHI_L2-HET-RATES60 (contd.). Here, ‘xxx’ stands for R7A and R7B.

FILE: PSP_ISOIS-EPIHI_L2-LET1-RATES10

This file contains the 10-second cadence data of particle Counts, Flux ($\text{cm}^{-2} \text{sr}^{-1} \text{sec}^{-1} \text{MeV}^{-1}$) and Count Rate (counts/s) for Electrons, H and He ions for various ranges (R1 – R7) of the Low Energy Telescope (LET1), for sides A and B. The measured values are summarized in Table 2.2.21. The variable names follow the pattern: <side>_<species>_<quantity>, where, <side> stands for A or B; <species> stands for the particle species; and <quantity> represents Counts (not used in the variable names, in general), Flux or Count Rate, for variables independent of range (R1, R2, etc.). The variables for different ranges has the structure: <range><side>_<species>_<quantity>. For electrons, the structure is: <Electrons>_<range><side>. Variable names without ranges (e.g., A_C) or with double digit range (e.g., R17) have the values integrated over all the available ranges (e.g., R1 to R7, in general).

Examples: A_Fe (measured quantity is “count”); Electrons_R6B_Rate; and R1A_He_Rate.

Side	Range	Quantity	Electrons		H		He	
			E-bins	E-range (MeV/nuc) (bins)	E-bins	E-range (MeV/nuc) (bins)	E-bins	E-range (MeV/nuc) (bins)
A/B	R1	Count			16	1 - 12 (16)	20	1 - 25 (20)
		Flux			16	1 - 12 (16)	20	1 - 25 (20)
		Count Rate			16	1 - 12 (16)	20	1 - 25 (20)
		Count			8	1 - 3 (8)	8	1 - 3 (8)
		Flux			8	1 - 3 (8)	8	1 - 3 (8)
		Count Rate			8	1 - 3 (8)	8	1 - 3 (8)
		Count			13	2 - 12 (13)	13	2 - 15 (13)
		Flux			13	2 - 12 (13)	13	2 - 15 (13)
		Count Rate			13	2 - 12 (13)	13	2 - 15 (13)
	Count	10	1 - 3 (10)					
	Flux							
	Count Rate	10	1 - 3 (10)					
	Count	10	1 - 4 (10)					
	Flux							
	Count Rate	10	1 - 4 (10)					
	Count	9	1 - 4 (9)					
	Flux							
	Count Rate	9	1 - 4 (9)					
	Count	8	2 - 5 (8)				3	21 - 29 (3)
	Flux						3	21 - 29 (3)
	Count Rate	8	2 - 5 (8)				3	21 - 29 (3)
	Count							
	Flux							
	Count Rate							

Table 2.2.21: PSP_ISOIS-EPIHI_L2-LET1-RATES10. The LET1 10 s data of various energetic particle species.

FILE: PSP_ISOIS-EPIHI_L2-LET1-RATES300

This file contains the 300 s cadence data of particle Counts, Flux ($\text{cm}^{-2} \text{sr}^{-1} \text{MeV}^{-1}$) and Count Rate (counts/s) for various particle species for ranges R1 & R26 (integrated over ranges R2 to R6) measured by the Low Energy Telescope (LET1), for sides A and B. The measured values are summarized in Table 2.2.22. The variable nomenclature is: <range><side>_<species>_<quantity>, where, <range> denotes the range (R1 to R7), <side> stands for A or B; <species> takes one of the particle species; and <quantity> represents Counts (not used in variable names, in general), Flux or Count Rate. Variable names without ranges (e.g., A_C) or with double digit range (e.g., R26) have the values integrated over all the available ranges (e.g., R2 to R6).

Examples: R1B_NetoSi_SECT_Rate; R26A_CNO_SECT_Flux.

Side	Range	Quantity	CNO_SECT			FeGroup_SECT			NetoSi_SECT		
			E-bins	E-range (MeV/nuc)	Sectors (bins)	E-bins	E-range (MeV/nuc)	Sectors (bins)	E-bins	E-range (MeV/nuc)	Sectors (bins)
A/B	R1	Count	1	3 - 3	0 - 8 (9)	1	3 - 3	0 - 8 (9)	1	3 - 3	0 - 8 (9)
		Flux	1	3 - 3	0 - 8 (9)	1	3 - 3	0 - 8 (9)	1	3 - 3	0 - 8 (9)
		Count Rate	1	3 - 3	0 - 8 (9)	1	3 - 3	0 - 8 (9)	1	3 - 3	0 - 8 (9)
A/B	R26	Count	3	6 - 24	0 - 24 (25)	3	6 - 24	0 - 24 (25)	3	6 - 24	0 - 24 (25)
		Flux	3	6 - 24	0 - 24 (25)	3	6 - 24	0 - 24 (25)	3	6 - 24	0 - 24 (25)
		Count Rate	3	6 - 24	0 - 24 (25)	3	6 - 24	0 - 24 (25)	3	6 - 24	0 - 24 (25)
R1 ENB_SECT - measured quantity is Counts; Size 3 x 9; E-bins: 3; E-range: 1 - 2 (MeV/nuc); Sectors: 0 - 8 (9).											
R26 ENB_SECT - measured quantity is Counts; Size 4 x 25; E-bins: 4; E-range: 2 - 12 (MeV/nuc); Sectors: 0 - 24 (25).											

Table 2.2.22: PSP_ISOIS-EPIHI_L2-LET1-RATES300. The LET1 300 s cadence measurements of various energetic particle species for ranges R1 and integrated over ranges R2 – R6 (R26).

FILE: PSP_ISOIS-EPIHI_L2-LET1-RATES3600

This file contains the 3600 s cadence measurements of particle Counts, Count Rate (counts/sec) and Flux ($\text{cm}^{-2} \text{sr}^{-1} \text{MeV}^{-1}$) for Al, Ar, C, Ca, Cr, Fe, H, He, Mg, N, Na, Ne, Ni, O, S and Si by the Low Energy Telescope (LET1), for sides A and B for different ranges (R1 – R6). The measured values are summarized in Tables 2.2.23 – 2.2.32 and the variables are named as: <side>_<species>_<quantity>. Here, <side> stands for A or B; <species> stands for the particle species; and <quantity> represents Counts (not used in variable names, in general), Flux or Rate. Variable names without ranges (e.g., A_C) or with double digit range (e.g., R35) have their values integrated over all the available ranges (e.g., R3 to R5).

Examples: A_C_Flux; PENB_C_Rate; R1A_32to50_Flux; Electrons_R5B.

Side	Species	Count		Flux		Count Rate	
		Size (bins)	Energy (MeV/nuc)	Size (bins)	Energy (MeV/nuc)	Size (bins)	Energy (MeV/nuc)
A/B	Al	28	1 – 118	28	1 – 118	28	1 – 118
	Ar	29	1 – 140	29	1 – 140	29	1 – 140
	C	27	1 – 99	27	1 – 99	27	1 – 99
	Ca	30	1 – 140	30	1 – 140	30	1 – 140
	Cr	31	1 – 140	31	1 – 140	31	1 – 140
	Fe	32	1 – 167	32	1 – 167	32	1 – 167
	H	25	1 – 42	25	1 – 42	25	1 – 42
	He	26	1 – 50	26	1 – 50	26	1 – 50
	Mg	28	1 – 118	28	1 – 118	28	1 – 118
	N	27	1 – 99	27	1 – 99	27	1 – 118
	Na	28	1 – 118	28	1 – 118	28	1 – 118
	Ne	28	1 – 118	28	1 – 118	28	1 – 118
	Ni	33	1 – 198	33	1 – 198	33	1 – 198
	O	28	1 – 118	28	1 – 118	33	1 – 118
S	29	1 – 140	29	1 – 140	29	1 – 140	
Si	29	1 – 140	29	1 – 140	29	1 – 140	

Table 2.2.23: PSP_ISOIS-EPIHI_L2-LET1-RATES3600. The 3600 s cadence LET1 data for various particle species for sides A and B.

Side	Species	Count		Count Rate	
		Size (bins)	Energy (MeV/nuc)	Size (bins)	Energy (MeV/nuc)
A/B	PENx_C	11	23 – 364	11	23 – 364
	PENx_Fe	11	45 – 471	11	45 – 471
	PENx_He	11	11 – 310	11	11 – 310
	PENx_Mg	10	38 – 408	10	38 – 408
	PENx_N	11	23 – 364	11	23 – 364
	PENx_Ne	11	27 – 384	11	27 – 384
	PENx_O	11	27 – 384	11	27 – 384
	PENx_Si	10	38 – 408	11	38 – 408

Table 2.2.24: PSP_ISOIS-EPIHI_L2-LET1-RATES3600 (contd.). Here ‘x’ denotes sides A & B.

Side	Species	Count			Flux			Count Rate		
		Size (bins)	Range SECT (bins)	Energy (MeV/nuc)	Size (bins)	Range SECT (bins)	Energy (MeV/nuc)	Size (bins)	Range SECT (bins)	Energy (MeV/nuc)
A/B	xxx_29to32	7	29 – 32	0 – 264	7	29 – 32	0 – 264	7	29 – 32	0 – 264
	xxx_32to50	7	32 – 50	0 – 264	7	32 – 50	0 – 264	7	32 – 50	0 – 264
	xxx_Al	14	–	1 – 260	14	–	1 – 260	14	–	1 – 260
	xxx_Ar	15	–	1 – 261	15	–	1 – 261	15	–	1 – 261
	xxx_C	12	–	1 – 259	12	–	1 – 259	12	–	1 – 259
	xxx_Ca	16	–	1 – 261	16	–	1 – 262	16	–	1 – 261
	xxx_CNO_SECT	1x9 (1 bin)	R1 0 – 8 (9)	3 – 3	1x9 (1 bin)	R1 0 – 8 (9)	3 – 3	1x9 (1 bin)	R1 0 – 8 (9)	3 – 3
	xxx_Cr	17	–	1 – 261	17	–	1 – 261	17	–	1 – 261
	xxx_Fe	17	–	1 – 261	17	–	1 – 261	17	–	1 – 261
	xxx_FeGroup_SECT	1x9 (1 bin)	R1 0 – 8 (9)	3 – 3	1x9 (1 bin)	R1 0 – 8 (9)	3 – 3	1x9 (1 bin)	R1 0 – 8 (9)	3 – 3
	xxx_H	12	–	0 – 258	12	–	0 – 258	12	–	0 – 258
	xxx_H_SECT	1x9 (1 bin)	R1 0 – 8 (9)	2 – 2	1x9 (1 bin)	R1 0 – 8 (9)	2 – 2	1x9 (1 bin)	R1 0 – 8 (9)	2 – 2
	xxx_He	12	–	0 – 258	12	–	0 – 258	12	–	0 – 258
	xxx_He_SECT	1x9 (1 bin)	R1 0 – 8 (9)	2 – 2	1x9 (1 bin)	R1 0 – 8 (9)	2 – 2	1x9 (1 bin)	R1 0 – 8 (9)	2 – 2
	xxx_He_BIN xxx_He_BIN (MASS)	5x16 (5) 16 bins 0 – 15 seg	– – –	1 – 3 – –	– – –	– – –	– – –	– – –	– – –	– – –
	xxx_Mg	14	–	1 – 260	14	–	1 – 260	14	–	1 – 260
	xxx_N	12	–	1 – 259	12	–	1 – 259	12	–	1 – 259
	xxx_Na	13	–	1 – 259	13	–	1 – 259	12	–	1 – 259
	xxx_Ne	13	–	1 – 259	13	–	1 – 259	13	–	1 – 259
	xxx_Ne_BIN xxx_Ne_BIN (MASS)	5x8 (5) 8 bins 0 – 7 seg	– – –	1 – 6 – –	– – –	– – –	– – –	– – –	– – –	– – –
	xxx_Ni	17	–	1 – 261	17	–	1 – 261	17	–	1 – 261
	xxx_O	13	–	1 – 259	13	–	1 – 259	13	–	1 – 259
	xxx_S	15	–	1 – 261	15	–	1 – 261	15	–	1 – 261
	xxx_Si	14	–	1 – 260	14	–	1 – 260	14	–	1 – 260
	xxx_NetoSi_SECT	1x9 (1 bin)	R1 0 – 8 (9)	3 – 3	1x9 (1 bin)	R1 0 – 8 (9)	3 – 3	1x9 (1 bin)	R1 0 – 8 (9)	3 – 3
	xxx_gt50	7	–	0 – 264	7	–	0 – 264	7	–	0 – 264

Table 2.2.25: PSP_ISOIS-EPIHI_L2-LET1-RATES3600 (contd.). Here, ‘xxx’ denotes R1A and R1B.

Side	Species	Count		Flux		Count Rate	
		Size (bins)	Energy (MeV/nuc)	Size (bins)	Energy (MeV/nuc)	Size (bins)	Energy (MeV/nuc)
A/B	xxx_29to32	8	1 – 320	8	1 – 320	8	1 – 320
	xxx_32to50	8	1 – 320	8	1 – 320	8	1 – 320
	xxx_Al	18	2 – 279	18	2 – 279	18	2 – 279
	xxx_Ar	20	2 – 288	20	2 – 288	20	2 – 288
	xxx_C	18	1 – 272	18	1 – 272	18	1 – 272
	xxx_Ca	20	2 – 288	20	2 – 288	20	2 – 288
	xxx_Cr	20	2 – 288	20	2 – 288	20	2 – 288
	xxx_Fe	20	2 – 288	20	2 – 288	20	2 – 288
	xxx_H	17	1 – 264	17	1 – 264	17	1 – 264
	xxx_He	17	1 – 266	17	1 – 266	17	1 – 266
	xxx_He_BIN xxx_He_BIN (MASS)	7x16 (7) 16 bins 0 – 15 seg	2 – 16 – –	– – –	– – –	– – –	– – –
	xxx_Mg	18	2 – 279	18	2 – 279	18	2 – 279
	xxx_N	18	1 – 272	18	1 – 272	18	1 – 272
	xxx_Na	18	1 – 275	18	1 – 275	18	1 – 275
	xxx_Ne	18	1 – 275	18	1 – 275	18	1 – 275
	xxx_Ne_BIN xxx_Ne_BIN (MASS)	8x8 (8) 8 bins 0 – 7 seg	3 – 32 – –	– – –	– – –	– – –	– – –
	xxx_Ni	21	2 – 294	21	2 – 294	21	2 – 294
	xxx_O	17	1 – 272	17	1 – 272	17	1 – 272
	xxx_S	20	2 – 288	20	2 – 288	20	2 – 288
	xxx_Si	18	2 – 279	18	2 – 279	18	2 – 279
xxx_gt50	8	1 – 320	8	1 – 320	8	1 – 320	

Table 2.2.26: PSP_ISOIS-EPIHI_L2-LET1-RATES3600 (contd.). Here, ‘xxx’ denotes R2A and R2B.

Side	Species	Count		Count Rate	
		Size (bins)	Energy (MeV/nuc)	Size (bins)	Energy (MeV/nuc)
A/B	Electrons_xxx	15	0 – 6	15	0 – 6
	xxx_He_BIN	5x16 (5)	8 – 32	–	–
	xxx_He_BIN (MASS)	16 bins 0 - 15 seg	–	–	–
	xxx_Ne_BIN	6x8 (4)	16 – 92	–	–
	xxx_Ne_BIN (MASS)	8 bins 0 - 7 seg	–	–	–

Table 2.2.27: PSP_ISOIS-EPIHI_L2-LET1-RATES3600 (contd.). Here, ‘xxx’ stands for R3A and R3B.

Side	Species	Count		Flux		Count Rate	
		Size (bins)	Energy (MeV/nuc)	Size (bins)	Energy (MeV/nuc)	Size (bins)	Energy (MeV/nuc)
A/B	xxxx_29to32	6	8 – 384	6	8 – 384	6	8 – 384
	xxxx_32to50	6	8 – 384	6	8 – 384	6	8 – 384
	xxxx_Al	13	8 – 310	13	8 – 310	13	8 – 310
	xxxx_Ar	13	10 – 320	13	10 – 320	13	10 – 320
	xxxx_C	14	5 – 294	14	5 – 294	14	5 – 294
	xxxx_Ca	14	10 – 332	14	10 – 332	14	10 – 332
	xxxx_Cr	14	10 – 332	14	10 – 332	14	10 – 332
	xxxx_Fe	14	10 – 332	14	10 – 332	14	10 – 332
	xxxx_H	13	3 – 275	13	3 – 275	13	3 – 275
	xxxx_He	14	3 – 279	14	3 – 279	14	3 – 279
	xxxx_Mg	13	8 – 310	13	8 – 310	13	8 – 310
	xxxx_N	14	5 – 294	14	5 – 294	14	5 – 294
	xxxx_Na	14	7 – 310	14	7 – 310	14	7 – 310
	xxxx_Ne	14	7 – 310	14	7 – 310	14	7 – 310
	xxxx_Ni	15	10 – 347	15	10 – 347	15	10 – 347
	xxxx_O	14	6 – 301	14	6 – 301	14	6 – 301
	xxxx_S	13	10 – 320	13	10 – 320	13	10 – 320
	xxxx_Si	14	8 – 320	14	8 – 320	14	8 – 320
xxxx_gt50	6	8 – 384	6	8 – 384	6	8 – 384	

Table 2.2.28: PSP_ISOIS-EPIHI_L2-LET1-RATES3600 (contd.). Here, ‘xxxx’ stands for R35A and R35B which implies the values are integratd over ranges R3 – R5 for sides A and B.

Side	Species	Count		Count Rate	
		Size (bins)	Energy (MeV/nuc)	Size (bins)	Energy (MeV/nuc)
A/B	Electrons_xxx	16	0 – 7	16	0 – 7

Table 2.2.29: PSP_ISOIS-EPIHI_L2-LET1-RATES3600 (contd.). Here, ‘xxx’ stands for R4A and R4B.

Side	Species	Count		Count Rate	
		Size (bins)	Energy (MeV/nuc)	Size (bins)	Energy (MeV/nuc)
A/B	Electrons_xxx	15	1 – 7	15	1 – 7

Table 2.2.30: PSP_ISOIS-EPIHI_L2-LET1-RATES3600 (contd.). Here, ‘xxx’ stands for R5A and R5B.

Side	Species	Count	
		Size (bins)	Energy (MeV/nuc)
A/B	xxxx_He_BIN xxxx_He_BIN (MASS)	5x16 (5) 16 bins 0 - 15 seg	16 – 92
	xxxx_Ne_BIN xxxx_Ne_BIN (MASS)	6x8 (6) 8 bins 0 - 7 seg	16 – 92

Table 2.2.31: PSP_ISOIS-EPIHI_L2-LET1-RATES3600 (contd.). Here, ‘xxxx’ stands for R45A and R45B and the values are integrated over ranges R4 – R5.

Side	Species	Count		Flux		Count Rate	
		Size (bins)	Energy (MeV/nuc)	Size (bins)	Energy (MeV/nuc)	Size (bins)	Energy (MeV/nuc)
A/B	xxx_29to32	4	32 – 384	4	32 – 384	4	32 – 384
	xxx_32to50	4	32 – 384	4	32 – 384	4	32 – 384
	xxx_Al	8	23 – 320	8	23 – 320	8	23 – 320
	xxx_Ar	7	32 – 332	7	32 – 332	7	32 – 332
	xxx_C	9	16 – 310	9	16 – 310	9	16 – 310
	xxx_Ca	7	32 – 332	7	32 – 332	7	32 – 332
	xxx_Cr	7	32 – 332	7	32 – 332	7	32 – 332
	Electrons_xxx	13	1 – 7	–	–	13	1 – 7
	xxx_Fe	7	38 – 347	7	38 – 347	7	38 – 347
	xxx_H	8	8 – 279	8	8 – 279	8	8 – 279
	xxx_He	9	8 – 283	9	8 – 283	9	8 – 283
	xxx_He_BIN	3x16 (3)	23 – 46	–	–	–	–
	xxx_He_BIN (MASS)	16 bins	–	–	–	–	–
		0 - 15 seg	–	–	–	–	–
	xxx_Mg	8	23 – 320	8	23 – 320	8	23 – 320
	xxx_N	9	16 – 310	9	16 – 310	9	16 – 310
	xxx_Na	9	19 – 320	9	19 – 320	9	19 – 320
	xxx_Ne	9	19 – 320	9	19 – 320	9	19 – 320
	xxx_Ne_BIN	3x8 (3)	46 – 92	–	–	–	–
	xxx_Ne_BIN (MASS)	8 bins	–	–	–	–	–
	0 - 7 seg	–	–	–	–	–	
xxx_Ni	8	38 – 364	8	38 – 364	8	38 – 364	
xxx_O	9	19 – 320	9	19 – 320	9	19 – 320	
xxx_S	7	32 – 332	7	32 – 332	7	32 – 332	
xxx_Si	8	27 – 332	8	27 – 332	8	27 – 332	
xxx_gt50	4	32 – 384	4	32 – 384	4	32 – 384	

Table 2.2.32: PSP_ISOIS-EPIHI_L2-LET1-RATES3600 (contd.). Here, ‘xxx’ stands for R6A and R6B.

FILE: PSP_ISOIS-EPIHI_L2-LET1-RATES60

This file contains the LET1 (Low Energy Telescope) 60 s cadence measurements of particle Counts, Flux ($\text{cm}^{-2} \text{sr}^{-1} \text{sec}^{-1} \text{MeV}^{-1}$) and Count Rate (counts/s) of Al, Ar, C, Ca, Cr, Fe, H, He, Mg, N, Na, Ne, Ni, O, S and Si for sides A and B. The values of these variables are summarized in Tables 2.2.33 – 2.2.39. The variables are named as: <side>_<species>_<quantity>, where, <side> stands for A or B; <species> stands for the particle species; and <quantity> represents Count, Flux or Rate (“Count” is not used in the variable names, in general). Variable names without ranges (e.g. A_C) or with double digit range (e.g. R35) have the values integrated over all the available ranges (e.g. R3 to R5).

Examples: A_C_Flux, PENB_C_Rate, R1A_32to50_Flux.

Side	Species	Counts		Flux		Count Rate	
		Size (bins)	Energy (MeV/nuc)	Size (bins)	Energy (MeV/nuc)	Size (bins)	Energy (MeV/nuc)
A/B	Al	28	1 – 118	28	1 – 118	28	1 – 118
	Ar	29	1 – 140	29	1 – 140	29	1 – 140
	C	27	1 – 99	27	1 – 99	27	1 – 99
	Ca	30	1 – 140	30	1 – 140	30	1 – 140
	Cr	31	1 – 140	31	1 – 140	31	1 – 140
	Fe	32	1 – 167	32	1 – 167	32	1 – 167
	H	25	1 – 42	25	1 – 42	25	1 – 42
	He	26	1 – 50	26	1 – 50	26	1 – 50
	Mg	28	1 – 118	28	1 – 118	28	1 – 118
	N	27	1 – 99	27	1 – 99	27	1 – 99
	Na	28	1 – 118	28	1 – 118	28	1 – 118
	Ne	28	1 – 118	28	1 – 118	28	1 – 118
	Ni	33	1 – 198	33	1 – 198	33	1 – 198
	O	28	1 – 118	28	2 – 118	28	1 – 118
	S	29	1 – 140	29	1 – 140	29	1 – 140
Si	29	1 – 140	29	1 – 140	29	1 – 140	

Table 2.2.33: PSP_ISOIS-EPIHI_L2-LET1-RATES60. The LET1 measurements of different particle species at a cadence of 60 s for sides A and B.

Side	Species	Count		Count Rate	
		Size (bins)	Energy (MeV/nuc)	Size (bins)	Energy (MeV/nuc)
A/B	PENx_C	9	45 – 583	9	45 – 583
	PENx_Fe	9	108 – 793	9	108 – 793
	PENx_H	9	27 – 521	9	27 – 521
	PENx_He	9	27 – 521	9	27 – 521
	PENx_Mg	9	64 – 646	9	64 – 646
	PENx_N	9	45 – 583	9	45 – 583
	PENx_Ne	8	64 – 612	8	64 – 612
	PENx_O	9	54 – 612	9	54 – 612
	PENx_Si	9	76 – 687	9	76 – 687

Table 2.2.34: PSP_ISOIS-EPIHI_L2-LET1-RATES60 (contd.). Here, ‘x’ stands for sides A & B.

Side	Species	Count			Flux			Count Rate		
		Size (bins)	Range SECT (bins)	Energy (MeV/nuc)	Size (bins)	Range SECT (bins)	Energy (MeV/nuc)	Size (bins)	Range SECT (bins)	Energy (MeV/nuc)
A/B	xxx_29to32	7	–	0 – 264	7	–	0 – 264	7	–	0 – 264
	xxx_32to50	7	–	0 – 264	7	–	0 – 264	7	–	0 – 264
	xxx_Al	14	–	1 – 260	14	–	1 – 260	14	–	1 – 260
	xxx_Ar	15	–	1 – 261	15	–	1 – 261	15	–	1 – 261
	xxx_C	12	–	1 – 259	12	–	1 – 259	12	–	1 – 259
	xxx_Ca	16	–	1 – 261	16	–	1 – 261	16	–	1 – 261
	xxx_Cr	17	–	1 – 261	17	–	1 – 261	17	–	1 – 261
	xxx_Fe	17	–	1 – 261	17	–	1 – 261	17	–	1 – 261
	xxx_H	12	–	0 – 258	12	–	0 – 258	12	–	0 – 258
	xxx_H_SECT	1x9 (1 bin)	R1 0 – 8 (9)	2 – 2	1x9 (1 bin)	R1 0 – 8 (9)	2 – 2	1x9 (1 bin)	R1 0 – 8 (9)	2 – 2
	xxx_He	12	–	0 – 258	12	–	0 – 258	12	–	0 – 258
	xxx_He_SECT	1x9 (1 bin)	R1 0 – 8 (9)	2 – 2	1x9 (1 bin)	R1 0 – 8 (9)	2 – 2	1x9 (1 bin)	R1 0 – 8 (9)	2 – 2
	xxx_Mg	14	–	1 – 260	14	–	1 – 260	14	–	1 – 260
	xxx_N	12	–	1 – 259	12	–	1 – 259	12	–	1 – 259
	xxx_Na	13	–	1 – 259	13	–	1 – 259	13	–	1 – 259
	xxx_Ne	13	–	1 – 259	13	–	1 – 259	13	–	1 – 259
	xxx_Ni	17	–	1 – 261	17	–	1 – 261	17	–	1 – 261
	xxx_O	13	–	1 – 259	13	–	1 – 259	13	–	1 – 259
	xxx_S	15	–	1 – 259	15	–	1 – 259	15	–	1 – 259
	xxx_Si	14	–	1 – 260	14	–	1 – 260	14	–	1 – 260
xxx_gt50	7	–	0 – 264	7	–	0 – 264	7	–	0 – 264	

Table 2.2.35: PSP_ISOIS-EPIHI_L2-LET1-RATES60 (contd.). Here, ‘xxx’ stands for R1A and R1B.

Side	Species	Count			Flux (1/cm ² sr sec MeV)			Count Rate		
		Size (bins)	Range SECT (bins)	Energy (MeV/nuc)	Size (bins)	Range SECT (bins)	Energy (MeV/nuc)	Size (bins)	Range SECT (bins)	Energy (MeV/nuc)
	xxxx_H_SECT	3x25 (3 bins)	R26 0 – 24 (25)	3 – 12	3x25 (3 bins)	R26 0 – 24	3 – 12	3x25 (3 bins)	R26 0 – 24 (25)	3 – 12
A/B	xxxx_He_SECT	3x25 (3 bins)	R26 0 – 24 (25)	3 – 12	3x25 (3 bins)	R26 0 – 24 (25)	3 – 12	3x25 (3 bins)	R26 0 – 24 (25)	3 – 12
	xxxx_ENA_SECT	8 x 25 (8 bins)	R26 0 – 24 (25)	3 – 12 – –	– – –	– – –	– – –	– – –	– – –	– – –

Table 2.2.36: PSP_ISOIS-EPIHI_L2-LET1-RATES60 (contd.). Here, ‘xxxx’ stands for R26A and R26B. The variables have values integrated over ranges R2 – R6.

Side	Species	Count		Flux		Count Rate	
		Size (bins)	Energy (MeV/nuc)	Size (bins)	Energy (MeV/nuc)	Size (bins)	Energy (MeV/nuc)
A/B	xxx_29to32	8	1 – 320	8	1 – 320	8	1 – 320
	xxx_32to50	8	1 – 320	8	1 – 320	8	1 – 320
	xxx_Al	18	2 – 279	18	2 – 279	18	2 – 279
	xxx_Ar	20	2 – 288	20	2 – 288	20	2 – 288
	xxx_C	18	1 – 272	18	1 – 272	18	1 – 272
	xxx_Ca	20	2 – 288	20	2 – 288	20	2 – 288
	xxx_Cr	20	2 – 288	20	2 – 288	20	2 – 288
	xxx_Fe	20	2 – 288	20	2 – 288	20	2 – 288
	xxx_H	17	1 – 264	17	1 – 264	17	1 – 264
	xxx_He	17	1 – 266	17	1 – 266	17	1 – 266
	xxx_Mg	18	2 – 279	18	2 – 279	18	2 – 279
	xxx_N	18	1 – 272	18	2 – 272	18	2 – 272
	xxx_Na	18	1 – 275	18	1 – 275	18	1 – 275
	xxx_Ne	18	1 – 275	18	1 – 275	18	1 – 275
	xxx_Ni	21	2 – 294	21	2 – 294	21	2 – 294
	xxx_O	17	1 – 272	17	1 – 272	17	1 – 272
	xxx_S	20	2 – 288	20	2 – 288	20	2 – 288
	xxx_Si	18	2 – 279	18	2 – 279	18	2 – 279
xxx_gt50	8	1 – 320	8	1 – 320	8	1 – 320	

Table 2.2.37: PSP_ISOIS-EPIHI_L2-LET1-RATES60 (contd.). Here, ‘xxx’ stands for R2A and R2B.

Side	Species	Count		Flux		Count Rate	
		Size (bins)	Energy (MeV/nuc)	Size (bins)	Energy (MeV/nuc)	Size (bins)	Energy (MeV/nuc)
A/B	xxxx_29to32	6	8 – 384	6	8 – 384	6	8 – 384
	xxxx_32to50	6	8 – 384	6	8 – 384	6	8 – 384
	xxxx_Al	13	8 – 310	13	8 – 310	13	8 – 310
	xxxx_Ar	13	10 – 320	13	10 – 320	13	10 – 320
	xxxx_C	14	5 – 294	14	5 – 294	14	5 – 294
	xxxx_Ca	14	10 – 332	14	10 – 332	14	10 – 332
	xxxx_Cr	14	10 – 332	14	10 – 332	14	10 – 332
	xxxx_Fe	14	10 – 332	14	10 – 332	14	10 – 332
	xxxx_H	13	3 – 275	13	3 – 275	13	3 – 275
	xxxx_He	14	3 – 279	14	3 – 279	14	3 – 279
	xxxx_Mg	13	8 – 310	13	8 – 310	13	8 – 310
	xxxx_N	14	5 – 294	14	5 – 294	14	5 – 294
	xxxx_Na	14	7 – 310	14	7 – 310	14	7 – 310
	xxxx_Ne	14	7 – 310	14	7 – 310	14	7 – 310
	xxxx_Ni	15	10 – 347	15	10 – 347	15	10 – 347
	xxxx_O	14	6 – 301	14	6 – 301	14	6 – 301
	xxxx_S	13	10 – 320	13	10 – 320	13	10 – 320
	xxxx_Si	14	8 – 320	14	8 – 320	14	8 – 320
xxxx_gt50	6	8 – 384	6	8 – 384	6	8 – 384	

Table 2.2.38: PSP_ISOIS-EPIHI_L2-LET1-RATES60 (contd.). Here, ‘xxxx’ stands for R35A and R35B. The values are integrated over ranges R3 – R5.

Side	Species	Count		Flux		Count Rate	
		Size (bins)	Energy (MeV/nuc)	Size (bins)	Energy (MeV/nuc)	Size (bins)	Energy (MeV/nuc)
A/B	xxx_29to32	4	32 – 384	4	32 – 384	4	32 – 384
	xxx_32to50	4	32 – 384	4	32 – 384	4	32 – 384
	xxx_Al	8	23 – 320	8	23 – 320	8	23 – 320
	xxx_Ar	7	32 – 332	7	32 – 332	7	32 – 332
	xxx_C	9	16 – 310	9	16 – 310	9	16 – 310
	xxx_Ca	7	32 – 332	7	32 – 332	7	32 – 332
	xxx_Cr	7	32 – 332	7	32 – 332	7	32 – 332
	Electrons_xxx	13	1 – 7	–	–	13	1 – 7
	xxx_Fe	7	38 – 347	7	38 – 347	7	38 – 347
	xxx_H	8	8 – 279	8	8 – 279	8	8 – 279
	xxx_He	9	8 – 283	9	8 – 283	9	8 – 283
	xxx_He_BIN xxx_He_BIN (MASS)	3x16 (3) 16 bins 0 – 15 seg	23 – 46 – –	– – –	– – –	– – –	– – –
	xxx_Mg	8	23 – 320	8	23 – 320	8	23 – 320
	xxx_N	9	16 – 310	9	16 – 310	9	16 – 310
	xxx_Na	9	19 – 320	9	19 – 320	9	19 – 320
	xxx_Ne	9	19 – 320	9	19 – 320	9	19 – 320
	xxx_Ne_BIN xxx_Ne_BIN (MASS)	3x8 (3) 8 bins 0 – 7 seg	46 – 92 – –	– – –	– – –	– – –	– – –
	xxx_Ni	8	38 – 364	8	38 – 364	8	38 – 364
	xxx_O	9	19 – 320	9	19 – 320	9	19 – 320
	xxx_S	7	32 – 332	7	32 – 332	7	32 – 332
xxx_Si	8	27 – 332	8	27 – 332	8	27 – 332	
xxx_gt50	4	32 – 384	4	32 – 384	4	32 – 384	

Table 2.2.39: PSP_ISOIS-EPIHI_L2-LET1-RATES60 (contd.). Here, ‘xxx’ stands for R6A and R6B.

FILE: PSP_ISOIS-EPIHI_L2-LET2-RATES10

This file contains the 10-second cadence data of particle Counts, Flux ($\text{cm}^{-2} \text{sr}^{-1} \text{sec}^{-1} \text{MeV}^{-1}$) and Count Rate (counts/s) for Electrons, H and He ions for various ranges (R1 – R7) of the single-sided (depicted as C) Low Energy Telescope (LET2). Table 2.2.40 summarizes the measured values. The variable names follow the structure: <side>_<species>_<quantity>, where, <side> stands for C; <species> stands for the particle species, and <quantity> represents Counts (not used in the variable names, in general), Flux or Rate for those variables independent of range. The variable names for different ranges (R1 – R5) are of the form: <range><side>_<species>_<quantity>. For electrons, the structure is: <Electrons>_<range><side>. Variable names without ranges (e.g., A_C) or with double digit range (e.g., R17) have the values integrated over all the available ranges (e.g., R1 to R7).

Examples: C_He (measured quantity is “count”); Electrons_R3C_Rate; R1C_He_Rate.

Side	Range	Quantity	Electrons		H		He	
			E-bins	E-range (MeV/nuc) (bins)	E-bins	E-range (MeV/nuc) (bins)	E-bins	E-range (MeV/nuc) (bins)
C		Count			16	1 - 12 (16)	20	1 - 25 (20)
		Flux			16	1 - 12 (16)	20	1 - 25 (20)
		Count Rate			16	1 - 12 (16)	20	1 - 25 (20)
	R1	Count			8	1 - 3 (8)	8	1 - 3 (8)
		Flux			8	1 - 3 (8)	8	1 - 3 (8)
		Count Rate			8	1 - 3 (8)	8	1 - 3 (8)
	R2	Count			13	2 - 12 (13)	13	2 - 15 (13)
		Flux			13	2 - 12 (13)	13	2 - 15 (13)
		Count Rate			13	2 - 12 (13)	13	2 - 15 (13)
	R35	Count			5	7 - 15 (5)	9	7 - 29 (9)
		Flux			5	7 - 15 (5)	9	7 - 29 (9)
		Count Rate			5	7 - 15 (5)	9	7 - 29 (9)
	R3	Count	10	1 - 3 (10)				
		Flux						
		Count Rate	10	1 - 3 (10)				
	R4	Count	10	1 - 4 (10)				
		Flux						
		Count Rate	10	1 - 4 (10)				
	R5	Count	9	1 - 4 (9)				
		Flux						
		Count Rate	9	1 - 4 (9)				

Table 2.2.40: PSP_ISOIS-EPIHI_L2-LET2-RATES10. The 10 s cadence data of LET2 for various energetic particle species.

FILE: PSP_ISOIS-EPIHI_L2-LET2-RATES300

This file contains the 300 s cadence data of particle Counts, Flux ($\text{cm}^{-2} \text{sr}^{-1} \text{sec}^{-1} \text{MeV}^{-1}$) and Count Rate (counts/s) for various particle species for ranges R1 & R26 (integrated over Ranges 2 – 6) measured by the single-sided (named C) Low Energy Telescope (LET2). The measured values are summarized in Table 2.2.41. The variable naming is: <range><side>_<species>_<quantity>, where, <range> denotes the range (R1 and R26), <side> stands for C; <species> takes one of the particle species; and <quantity> represents Counts (not used in variable names, in general), Flux or Rate. Variable names without ranges (e.g., A_C) or with double digit range (e.g., R25) have the values integrated over all the available ranges (e.g., R2 to R5).

Examples: R1C_NetoSi_SECT_Rate; R25C_CNO_SECT_Flux.

Side	Range	Quantity	CNO_SECT			FeGroup_SECT			NetoSi_SECT		
			E-bins	E-range (MeV/nuc)	Sectors (bins)	E-bins	E-range (MeV/nuc)	Sectors (bins)	E-bins	E-range (MeV/nuc)	Sectors (bins)
C	R1	Count	1	3 - 3	0 - 8 (9)	1	3 - 3	0 - 8 (9)	1	3 - 3	0 - 8 (9)
		Flux	1	3 - 3	0 - 8 (9)	1	3 - 3	0 - 8 (9)	1	3 - 3	0 - 8 (9)
		Count Rate	1	3 - 3	0 - 8 (9)	1	3 - 3	0 - 8 (9)	1	3 - 3	0 - 8 (9)
C	R26	Count	3	6 - 24	0 - 24 (25)	3	6 - 24	0 - 24 (25)	3	6 - 24	0 - 24 (25)
		Flux	3	6 - 24	0 - 24 (25)	3	6 - 24	0 - 24 (25)	3	6 - 24	0 - 24 (25)
		Count Rate	3	6 - 24	0 - 24 (25)	3	6 - 24	0 - 24 (25)	3	6 - 24	0 - 24 (25)
R1 ENB_SECT – measured quantity is Counts; Size 3 x 9; E-bins: 3; E-range: 1 - 2 (MeV/nuc); Sectors: 0 - 8 (9).											
R26 ENB_SECT – measured quantity is Counts; Size 4 x 25; E-bins: 4; E-range: 2 - 12 (MeV/nuc); Sectors: 0 - 24 (25).											

Table 2.2.41: PSP_ISOIS-EPIHI_L2-LET2-RATES300. The LET2 300 s cadence measurements of various energetic particle species for ranges R1 and integrated over ranges R2 – R6 (R26).

FILE: PSP_ISOIS-EPIHI_L2-LET2-RATES3600

This file contains the 3600 s cadence data of particle Counts, Flux ($\text{cm}^{-2} \text{sr}^{-1} \text{sec}^{-1} \text{MeV}^{-1}$) and Count Rate (counts/s) for Al, Ar, C, Ca, Cr, Fe, H, He, Mg, N, Na, Ne, Ni, O, S and Si by the single sided (depicted as C) Low Energy Telescope (LET2). The measured values of these variables are summarized in Tables 2.2.42 – 2.2.49. The variables are named as: <side>_<species>_<quantity>, where, <side> stands for C; <species> represents the particle species; and <quantity> denotes Counts (not used in the variable names, in general), Flux or Rate. Variable names without ranges (e.g. C_Al) or with double digit range (e.g. R25) have the values integrated over all the available ranges (e.g. R2 to R5).

Examples: C_Si_Flux; PENB_C_Rate; R1C_32to50_Flux; Electrons_R5C.

Side	Species	Count		Flux		Count Rate	
		Size (bins)	Energy (MeV/nuc)	Size (bins)	Energy (MeV/nuc)	Size (bins)	Energy (MeV/nuc)
C	Al	27	1 – 99	27	1 – 99	27	1 – 99
	Ar	29	1 – 118	28	1 – 118	28	1 – 118
	C	25	1 – 70	25	1 – 70	25	1 – 70
	Ca	30	1 – 140	30	1 – 140	30	1 – 140
	Cr	31	1 – 140	31	1 – 140	31	1 – 140
	Fe	31	1 – 140	31	1 – 140	31	1 – 140
	H	24	1 – 35	24	1 – 35	24	1 – 35
	He	25	1 – 42	25	1 – 42	25	1 – 42
	Mg	27	1 – 99	27	1 – 99	27	1 – 99
	N	25	1 – 70	25	1 – 70	25	1 – 70
	Na	27	1 – 99	27	1 – 99	27	1 – 99
	Ne	27	1 – 99	27	1 – 99	27	1 – 99
	Ni	32	1 – 167	32	1 – 167	32	1 – 167
	O	26	1 – 83	26	1 – 83	26	1 – 83
	S	28	1 – 118	28	1 – 118	28	1 – 118
Si	28	1 – 117	28	1 – 118	28	1 – 118	

Table 2.2.42: PSP_ISOIS-EPIHI_L2-LET2-RATES3600. The 3600 s cadence data for various particle species for the single-sided (side C) telescope LET2.

Side	Species	Count		Count Rate	
		Size (bins)	Energy (MeV/nuc)	Size (bins)	Energy (MeV/nuc)
C	PENx_C	11	23 – 364	11	23 – 364
	PENx_Fe	11	45 – 471	11	45 – 471
	PENx_He	11	11 – 310	11	11 – 310
	PENx_Mg	10	38 – 408	10	38 – 408
	PENx_N	11	23 – 364	11	23 – 364
	PENx_Ne	11	27 – 384	11	27 – 384
	PENx_O	11	27 – 384	11	27 – 384
	PENx_Si	10	38 – 408	11	38 – 408

Table 2.2.43: PSP_ISOIS-EPIHI_L2-LET2-RATES3600 (contd.). Here, ‘x’ stands for side C.

Side	Species	Count			Flux			Count Rate		
		Size (bins)	Range SECT (bins)	Energy (MeV/nuc)	Size (bins)	Range SECT (bins)	Energy (MeV/nuc)	Size (bins)	Range SECT (bins)	Energy (MeV/nuc)
C	xxx_29to32	7	29 – 32	0 – 264	7	29 – 32	0 – 264	7	29 – 32	0 – 264
	xxx_32to50	7	32 – 50	0 – 264	7	32 – 50	0 – 264	7	32 – 50	0 – 264
	xxx_Al	14	–	1 – 260	14	–	1 – 260	14	–	1 – 260
	xxx_Ar	15	–	1 – 261	15	–	1 – 261	15	–	1 – 261
	xxx_C	12	–	1 – 259	12	–	1 – 259	12	–	1 – 259
	xxx_Ca	16	–	1 – 261	16	–	1 – 262	16	–	1 – 261
	xxx_CNO_SECT	1x9 (1 bin)	R1 0 – 8 (9)	3 – 3	1x9 (1 bin)	R1 0 – 8 (9)	3 – 3	1x9 (1 bin)	R1 0 – 8 (9)	3 – 3
	xxx_Cr	17	–	1 – 261	17	–	1 – 261	17	–	1 – 261
	xxx_Fe	17	–	1 – 261	17	–	1 – 261	17	–	1 – 261
	xxx_FeGroup_SECT	1x9 (1 bin)	R1 0 – 8 (9)	3 – 3	1x9 (1 bin)	R1 0 – 8 (9)	3 – 3	1x9 (1 bin)	R1 0 – 8 (9)	3 – 3
	xxx_H	12	–	0 – 258	12	–	0 – 258	12	–	0 – 258
	xxx_H_SECT	1x9 (1 bin)	R1 0 – 8 (9)	2 – 2	1x9 (1 bin)	R1 0 – 8 (9)	2 – 2	1x9 (1 bin)	R1 0 – 8 (9)	2 – 2
	xxx_He	12	–	0 – 258	12	–	0 – 258	12	–	0 – 258
	xxx_He_SECT	1x9 (1 bin)	R1 0 – 8 (9)	2 – 2	1x9 (1 bin)	R1 0 – 8 (9)	2 – 2	1x9 (1 bin)	R1 0 – 8 (9)	2 – 2
	xxx_He_BIN xxx_He_BIN (MASS)	5x16 (5) 16 bins 0 – 15 seg	– – –	1 – 3 – –	– – –	– – –	– – –	– – –	– – –	– – –
	xxx_Mg	14	–	1 – 260	14	–	1 – 260	14	–	1 – 260
	xxx_N	12	–	1 – 259	12	–	1 – 259	12	–	1 – 259
	xxx_Na	13	–	1 – 259	13	–	1 – 259	12	–	1 – 259
	xxx_Ne	13	–	1 – 259	13	–	1 – 259	13	–	1 – 259
	xxx_Ne_BIN xxx_Ne_BIN (MASS)	5x8 (5) 8 bins 0 – 7 seg	– – –	1 – 6 – –	– – –	– – –	– – –	– – –	– – –	– – –
	xxx_Ni	17	–	1 – 261	17	–	1 – 261	17	–	1 – 261
	xxx_O	13	–	1 – 259	13	–	1 – 259	13	–	1 – 259
	xxx_S	15	–	1 – 261	15	–	1 – 261	15	–	1 – 261
	xxx_Si	14	–	1 – 260	14	–	1 – 260	14	–	1 – 260
xxx_NetoSi_SECT	1x9 (1 bin)	R1 0 – 8 (9)	3 – 3	1x9 (1 bin)	R1 0 – 8 (9)	3 – 3	1x9 (1 bin)	R1 0 – 8 (9)	3 – 3	
xxx_gt50	7	–	0 – 264	7	–	0 – 264	7	–	0 – 264	

Table 2.2.44: PSP_ISOIS-EPIHI_L2-LET2-RATES3600 (contd.). Here, ‘xxx’ stands for R1C.

Side	Species	Count			Flux			Count Rate		
		Size (bins)	Range SECT (bins)	Energy (MeV/nuc)	Size (bins)	Range SECT (bins)	Energy (MeV/nuc)	Size (bins)	Range SECT (bins)	Energy (MeV/nuc)
C	xxxx_CNO_SECT	3x25 (3 bins)	R25 0 – 24 (25)	6 – 24	3x25 (3 bins)	R25 0 – 24 (25)	6 – 24	3x25 (3 bins)	R25 0 – 24 (25)	6 – 24
	xxxx_FeGroup_SECT	3x25 (3 bins)	R25 0 – 24 (25)	6 – 24	3x25 (3 bins)	R25 0 – 24 (25)	6 – 24	3x25 (3 bins)	R25 0 – 24 (25)	6 – 24
	xxxx_H_SECT	3x25 (3 bins)	R25 0 – 24 (25)	3 – 12	3x25 (3 bins)	R25 0 – 24 (25)	3 – 12	3x25 (3 bins)	R25 0 – 24 (25)	3 – 12
	xxxx_He_SECT	3x25 (3 bins)	R25 0 – 24 (25)	3 – 12	3x25 (3 bins)	R25 0 – 24 (25)	3 – 12	3x25 (3 bins)	R25 0 – 24 (25)	3 – 12
	xxxx_NetoSi_SECT	3x25 (3 bins)	R25 0 – 24 (25)	6 – 24	3x25 (3 bins)	R25 0 – 24 (25)	6 – 24	3x25 (3 bins)	R25 0 – 24 (25)	6 – 24

Table 2.2.45: PSP_ISOIS-EPIHI_L2-LET2-RATES3600 (contd.). Here, ‘xxxx’ stands for R25C and the values are integrated over ranges R2 – R5.

Side	Species	Count		Flux		Count Rate	
		Size (bins)	Energy (MeV/nuc)	Size (bins)	Energy (MeV/nuc)	Size (bins)	Energy (MeV/nuc)
C	xxx_29to32	8	1 – 320	8	1 – 320	8	1 – 320
	xxx_32to50	8	1 – 320	8	1 – 320	8	1 – 320
	xxx_Al	18	2 – 279	18	2 – 279	18	2 – 279
	xxx_Ar	20	2 – 288	20	2 – 288	20	2 – 288
	xxx_C	18	1 – 272	18	1 – 272	18	1 – 272
	xxx_Ca	20	2 – 288	20	2 – 288	20	2 – 288
	xxx_Cr	20	2 – 288	20	2 – 288	20	2 – 288
	xxx_Fe	20	2 – 288	20	2 – 288	20	2 – 288
	xxx_H	17	1 – 264	17	1 – 264	17	1 – 264
	xxx_He	17	1 – 266	17	1 – 266	17	1 – 266
	xxx_He_BIN	7x16 (7)	2 – 16	–	–	–	–
	xxx_He_BIN (MASS)	16 bins	–	–	–	–	–
		0 – 15 seg	–	–	–	–	–
	xxx_Mg	18	2 – 279	18	2 – 279	18	2 – 279
	xxx_N	18	1 – 272	18	1 – 272	18	1 – 272
	xxx_Na	18	1 – 275	18	1 – 275	18	1 – 275
	xxx_Ne	18	1 – 275	18	1 – 275	18	1 – 275
	xxx_Ne_BIN	8x8 (8)	3 – 32	–	–	–	–
	xxx_Ne_BIN (MASS)	8 bins	–	–	–	–	–
		0 – 7 seg	–	–	–	–	–
xxx_Ni	21	2 – 294	21	2 – 294	21	2 – 294	
xxx_O	17	1 – 272	17	1 – 272	17	1 – 272	
xxx_S	20	2 – 288	20	2 – 288	20	2 – 288	
xxx_Si	18	2 – 279	18	2 – 279	18	2 – 279	
xxx_gt50	8	1 – 320	8	1 – 320	8	1 – 320	

Table 2.2.46: PSP_ISOIS-EPIHI_L2-LET2-RATES3600 (contd.). Here, ‘xxx’ stands for R2C.

Side	Species	Count		Count Rate	
		Size (bins)	Energy (MeV/nuc)	Size (bins)	Energy (MeV/nuc)
C	Electrons_R3C	15	0 – 6	15	0 – 6
	R3C_He_BIN	5x16 (5)	8 – 32	–	–
	R3C_He_BIN (MASS)	16 bins	–	–	–
		0 – 15 seg	–	–	–
	R3C_Ne_BIN	6x8 (6)	16 – 92	–	–
	R3C_Ne_BIN (MASS)	8 bins	–	–	–
		0 – 7 seg	–	–	–
	Electrons_R4C	16	0 – 7	16	0 – 7
	Electrons_R5C	15	1 – 7	15	1 – 7

Table 2.2.47: PSP_ISOIS-EPIHI_L2-LET2-RATES3600 (contd.). LET2 electron measurements for ranges R3, R4 and R5.

Side	Species	Count		Flux		Count Rate	
		Size (bins)	Energy (MeV/nuc)	Size (bins)	Energy (MeV/nuc)	Size (bins)	Energy (MeV/nuc)
C	xxxx_29to32	6	8 – 384	6	8 – 384	6	8 – 384
	xxxx_32to50	6	8 – 384	6	8 – 384	6	8 – 384
	xxxx_Al	13	8 – 310	13	8 – 310	13	8 – 310
	xxxx_Ar	13	10 – 320	13	10 – 320	13	10 – 320
	xxxx_C	14	5 – 294	14	5 – 294	14	5 – 294
	xxxx_Ca	14	10 – 332	14	10 – 332	14	10 – 332
	xxxx_Cr	14	10 – 332	14	10 – 332	14	10 – 332
	xxxx_Fe	14	10 – 332	14	10 – 332	14	10 – 332
	xxxx_H	13	3 – 275	13	3 – 275	13	3 – 275
	xxxx_He	14	3 – 279	14	3 – 279	14	3 – 279
	xxxx_Mg	13	8 – 310	13	8 – 310	13	8 – 310
	xxxx_N	14	5 – 294	14	5 – 294	14	5 – 294
	xxxx_Na	14	7 – 310	14	7 – 310	14	7 – 310
	xxxx_Ne	14	7 – 310	14	7 – 310	14	7 – 310
	xxxx_Ni	15	10 – 347	15	10 – 347	15	10 – 347
	xxxx_O	14	6 – 301	14	6 – 301	14	6 – 301
	xxxx_S	13	10 – 320	13	10 – 320	13	10 – 320
	xxxx_Si	14	8 – 320	14	8 – 320	14	8 – 320
xxxx_gt50	6	8 – 384	6	8 – 384	6	8 – 384	

Table 2.2.48: PSP_ISOIS-EPIHI_L2-LET2-RATES3600 (contd.). Here, ‘xxxx’ stands for R35C which implies that the values are integrated over ranges R3 – R5.

Side	Species	Count	
		Size (bins)	Energy (MeV/nuc)
C	xxxx_He_BIN xxxx_He_BIN (MASS)	5x16 (5) 16 bins 0 - 15 seg	8 - 32
	xxxx_Ne_BIN xxxx_Ne_BIN (MASS)	6x8 (6) 6 bins 0 - 7 seg	16 - 92

Table 2.2.49: PSP_ISOIS-EPIHI_L2-LET2-RATES3600 (contd.). Here, 'xxxx' stands for R45C and the values presented here are integrated over ranges R4 – R5.

FILE: PSP_ISOIS-EPIHI_L2-LET2-RATES60

This file contains the 60 s cadence measurements of particle Counts, Flux ($\text{cm}^{-2} \text{sr}^{-1} \text{sec}^{-1} \text{MeV}^{-1}$) and Count Rate (counts/s) of Al, Ar, C, Ca, Cr, Fe, H, He, Mg, N, Na, Ne, Ni, O, S and Si coming from sides A and B made by the Low Energy Telescope (LET1). The values of these variables are summarized in Tables 2.2.33 – 2.2.39. The variables are named as: <side>_<species>_<quantity>, where, <side> stands for A or B; <species> stands for the particle species; and <quantity> represents Counts (not used in the variable names, in general), Flux or Rate. Variable names without ranges (e.g. A_C) or with double digit range (e.g. R25) have the values integrated over all the available ranges (e.g. R2 to R5).

Examples: A_C_Flux; PENB_C_Rate; R1A_32to50_Flux.

Side	Species	Counts		Flux		Count Rate	
		Size (bins)	Energy (MeV/nuc)	Size (bins)	Energy (MeV/nuc)	Size (bins)	Energy (MeV/nuc)
C	Al	27	1 - 99	27	1 - 99	27	1 - 99
	Ar	28	1 - 118	28	1 - 118	28	1 - 118
	C	25	1 - 70	25	1 - 70	25	1 - 70
	Ca	30	1 - 140	30	1 - 140	30	1 - 140
	Cr	31	1 - 140	31	1 - 140	31	1 - 140
	Fe	31	1 - 140	31	1 - 140	31	1 - 140
	H	24	1 - 35	24	1 - 35	24	1 - 35
	He	25	1 - 42	25	1 - 42	25	1 - 42
	Mg	27	1 - 99	27	1 - 99	27	1 - 99
	N	25	1 - 70	25	1 - 70	25	1 - 70
	Na	27	1 - 99	27	1 - 99	27	1 - 99
	Ne	27	1 - 99	27	1 - 99	27	1 - 99
	Ni	32	1 - 167	32	1 - 167	32	1 - 167
	O	26	1 - 83	26	2 - 83	26	1 - 83
	S	28	1 - 118	28	1 - 118	28	1 - 118
	Si	28	1 - 118	28	1 - 118	28	1 - 118

Table 2.2.50: PSP_ISOIS-EPIHI_L2-LET2-RATES60. The 60 s cadence measurements of the single-sided (side C) telescope LET2 for different particle species.

Side	Species	Counts		Count Rate	
		Size (bins)	Energy (MeV/nuc)	Size (bins)	Energy (MeV/nuc)
C	PENx_C	11	23 – 364	11	23 – 364
	PENx_Fe	11	45 – 471	11	45 – 471
	PENx_He	11	11 – 310	11	11 – 310
	PENx_Mg	10	38 – 408	10	38 – 408
	PENx_N	11	23 – 364	11	23 – 364
	PENx_Ne	11	27 – 384	11	27 – 384
	PENx_O	11	27 – 384	11	27 – 384
	PENx_Si	10	38 – 408	11	38 – 408

Table 2.2.51: PSP_ISOIS-EPIHI_L2-LET2-RATES60 (contd.). Here ‘x’ stands for side C.

Side	Species	Count			Flux			Count Rate		
		Size (bins)	Range SECT (bins)	Energy (MeV/nuc)	Size (bins)	Range SECT (bins)	Energy (MeV/nuc)	Size (bins)	Range SECT (bins)	Energy (MeV/nuc)
C	xxx_29to32	7	29 – 32	0 – 264	7	29 – 32	0 – 264	7	29 – 32	0 – 264
	xxx_32to50	7	32 – 50	0 – 264	7	32 – 50	0 – 264	7	32 – 50	0 – 264
	xxx_Al	14	–	1 – 260	14	–	1 – 260	14	–	1 – 260
	xxx_Ar	15	–	1 – 261	15	–	1 – 261	15	–	1 – 261
	xxx_C	12	–	1 – 259	12	–	1 – 259	12	–	1 – 259
	xxx_Ca	16	–	1 – 261	16	–	1 – 262	16	–	1 – 261
	xxx_Cr	17	–	1 – 261	17	–	1 – 261	17	–	1 – 261
	xxx_Fe	17	–	1 – 261	17	–	1 – 261	17	–	1 – 261
	xxx_H	12	–	0 – 258	12	–	0 – 258	12	–	0 – 258
	xxx_H_SECT	1x9 (1 bin)	R1 0 – 8 (9)	2 – 2	1x9 (1 bin)	R1 0 – 8 (9)	2 – 2	1x9 (1 bin)	R1 0 – 8 (9)	2 – 2
	xxx_He	12	–	0 – 258	12	–	0 – 258	12	–	0 – 258
	xxx_He_SECT	1x9 (1 bin)	R1 0 – 8 (9)	2 – 2	1x9 (1 bin)	R1 0 – 8 (9)	2 – 2	1x9 (1 bin)	R1 0 – 8 (9)	2 – 2
	xxx_Mg	14	–	1 – 260	14	–	1 – 260	14	–	1 – 260
	xxx_N	12	–	1 – 259	12	–	1 – 259	12	–	1 – 259
	xxx_Na	13	–	1 – 259	13	–	1 – 259	12	–	1 – 259
	xxx_Ne	13	–	1 – 259	13	–	1 – 259	13	–	1 – 259
	xxx_Ni	17	–	1 – 261	17	–	1 – 261	17	–	1 – 261
	xxx_O	13	–	1 – 259	13	–	1 – 259	13	–	1 – 259
	xxx_S	15	–	1 – 261	15	–	1 – 261	15	–	1 – 261
	xxx_Si	14	–	1 – 260	14	–	1 – 260	14	–	1 – 260
	xxx_gt50	7	–	0 – 264	7	–	0 – 264	7	–	0 – 264
R1 ENA_SECT - measured quantity is Counts; Size 8 x 9; E-bins: 8; E-range: 1 - 3 (MeV/nuc); Sectors: 0 - 8 (9).										

Table 2.2.52: PSP_ISOIS-EPIHI_L2-LET2-RATES60 (contd.). Here, ‘xxx’ stands for R1C.

Side	Species	Count			Flux			Count Rate		
		Size (bins)	Range SECT (bins)	Energy (MeV/nuc)	Size (bins)	Range SECT (bins)	Energy (MeV/nuc)	Size (bins)	Range SECT (bins)	Energy (MeV/nuc)
C	xxxx_H_SECT	3x25 (3 bins)	R26 0 – 24 (25)	3 – 12	3x25 (3 bins)	R26 0 – 24 (25)	3 – 12	3x25 (3 bins)	R26 0 – 24 (25)	3 – 12
	xxxx_He_SECT	3x25 (3 bins)	R26 0 – 24 (25)	3 – 12	3x25 (3 bins)	R26 0 – 24 (25)	3 – 12	3x25 (3 bins)	R26 0 – 24 (25)	3 – 12
	xxxx_ENA_SECT	8x25 (8 bins)	R26 0 – 24 (25)	2 – 12	–	–	–	–	–	–

Table 2.2.53: PSP_ISOIS-EPIHI_L2-LET2-RATES60 (contd.). Here, ‘xxxx’ stands for R25C which implies that the values are integrated over ranges R2 – R5.

Side	Species	Count		Flux		Count Rate	
		Size (bins)	Energy (MeV/nuc)	Size (bins)	Energy (MeV/nuc)	Size (bins)	Energy (MeV/nuc)
A/B	xxx_29to32	8	1 – 320	8	1 – 320	8	1 – 320
	xxx_32to50	8	1 – 320	8	1 – 320	8	1 – 320
	xxx_Al	18	2 – 279	18	2 – 279	18	2 – 279
	xxx_Ar	20	2 – 288	20	2 – 288	20	2 – 288
	xxx_C	18	1 – 272	18	1 – 272	18	1 – 272
	xxx_Ca	20	2 – 288	20	2 – 288	20	2 – 288
	xxx_Cr	20	2 – 288	20	2 – 288	20	2 – 288
	xxx_Fe	20	2 – 288	20	2 – 288	20	2 – 288
	xxx_H	17	1 – 264	17	1 – 264	17	1 – 264
	xxx_He	17	1 – 266	17	1 – 266	17	1 – 266
	xxx_Mg	18	2 – 279	18	2 – 279	18	2 – 279
	xxx_N	18	1 – 272	18	1 – 272	18	1 – 272
	xxx_Na	18	1 – 275	18	1 – 275	18	1 – 275
	xxx_Ne	18	1 – 275	18	1 – 275	18	1 – 275
	xxx_Ni	21	2 – 294	21	2 – 294	21	2 – 294
	xxx_O	17	1 – 272	17	1 – 272	17	1 – 272
	xxx_S	20	2 – 288	20	2 – 288	20	2 – 288
xxx_Si	18	2 – 279	18	2 – 279	18	2 – 279	
xxx_gt50	8	1 – 320	8	1 – 320	8	1 – 320	

Table 2.2.54: PSP_ISOIS-EPIHI_L2-LET2-RATES60 (contd.). Here, ‘xxx’ stands for R2C.

Side	Species	Count		Count Rate	
		Size (bins)	Energy (MeV/nuc)	Size (bins)	Energy (MeV/nuc)
C	Electrons_R3C	15	0 – 6	15	0 – 6
	R3C_He_BIN	5x16 (5)	8 – 32	–	–
	R3C_He_BIN (MASS)	16 bins	–	–	–
		0 – 15 seg	–	–	–
	R3C_Ne_BIN	6x8 (6)	16 – 92	–	–
	R3C_Ne_BIN (MASS)	8 bins	–	–	–
		0 – 7 seg	–	–	–
	Electrons_R4C	16	0 – 7	16	0 – 7
	Electrons_R5C	15	1 – 7	15	1 – 7

Table 2.2.55: PSP_ISOIS-EPIHI_L2-LET2-RATES60 (contd.). LET2 electron measurements for ranges R3, R4 and R5.

Side	Species	Count		Flux		Count Rate	
		Size (bins)	Energy (MeV/nuc)	Size (bins)	Energy (MeV/nuc)	Size (bins)	Energy (MeV/nuc)
C	xxxx_29to32	6	8 – 384	6	8 – 384	6	8 – 384
	xxxx_32to50	6	8 – 384	6	8 – 384	6	8 – 384
	xxxx_Al	13	8 – 310	13	8 – 310	13	8 – 310
	xxxx_Ar	13	10 – 320	13	10 – 320	13	10 – 320
	xxxx_C	14	5 – 294	14	5 – 294	14	5 – 294
	xxxx_Ca	14	10 – 332	14	10 – 332	14	10 – 332
	xxxx_Cr	14	10 – 332	14	10 – 332	14	10 – 332
	xxxx_Fe	14	10 – 332	14	10 – 332	14	10 – 332
	xxxx_H	13	3 – 275	13	3 – 275	13	3 – 275
	xxxx_He	14	3 – 279	14	3 – 279	14	3 – 279
	xxxx_Mg	13	8 – 310	13	8 – 310	13	8 – 310
	xxxx_N	14	5 – 294	14	5 – 294	14	5 – 294
	xxxx_Na	14	7 – 310	14	7 – 310	14	7 – 310
	xxxx_Ne	14	7 – 310	14	7 – 310	14	7 – 310
	xxxx_Ni	15	10 – 347	15	10 – 347	15	10 – 347
	xxxx_O	14	6 – 301	14	6 – 301	14	6 – 301
	xxxx_S	13	10 – 320	13	10 – 320	13	10 – 320
	xxxx_Si	14	8 – 320	14	8 – 320	14	8 – 320
	xxxx_gt50	6	8 – 384	6	8 – 384	6	8 – 384

Table 2.2.56: PSP_ISOIS-EPIHI_L2-LET2-RATES60 (contd.). Here, ‘xxxx’ stands for R35C which implies that the values are integrated over ranges R3 – R5.

FILE: PSP_ISOIS-EPIHI_L2-SECOND-RATES

This file contains the 1 s cadence measurements of particle Counts, Flux ($\text{cm}^{-2} \text{sr}^{-1} \text{sec}^{-1} \text{MeV}^{-1}$) and Count Rate (counts/s) of Electrons and H for sides A and B for the double-sided High Energy Telescope (HET) and the Low Energy Telescopes (LET1), and the single-sided Low Energy Telescope (LET2). The values of these variables are summarized in Table 2.2.57. The variables are named as: <tel>_<side>_<species>_<quantity>, where, <tel> stands for HET, LET1 or LET2; <side> stands for A, B or C; <species> stands for the particle species; and <quantity> represents Counts (not used in variable names, in general), Flux or Rate.

Examples: HET_A_Electrons_Flux; LET1_B_H_Rate; LET2_C_H.

Side	Range	Quantity	Electrons		H	
			E-bins	E-range (MeV/nuc) (bins)	E-bins	E-range (MeV/nuc) (bins)
C	HET_A	Count	3	1 – 3	2	13 – 24
		Flux	3	1 – 3	2	13 – 24
		Count Rate	3	1 – 3	2	13 – 24
	HET_B	Count	3	1 – 3	2	13 – 24
		Flux	3	1 – 3	2	13 – 24
		Count Rate	3	1 – 3	2	13 – 24
	LET1_A	Count	2	1 – 2	3	2 – 11
		Flux	2	1 – 2	3	2 – 11
		Count Rate	2	1 – 2	3	2 – 11
	LET1_B	Count	2	1 – 2	3	2 – 11
		Flux	2	1 – 2	3	2 – 11
		Count Rate	2	1 – 2	3	2 – 11
	LET2_C	Count	2	1 – 2	3	2 – 11
		Flux	2	1 – 2	3	2 – 11
		Count Rate	2	1 – 2	3	2 – 11

Table 2.2.57: PSP_ISOIS-EPIHI_L2-SECOND-RATES. The EPI-Hi 1 s data of Electrons and H for HET, LET1 and LET2.

GENERAL LIST OF VARIABLES

PSP_ISOIS-EPIHI_L2-HET-RATES10

A_Electrons_Rate
A_H_Flux
A_H_Rate
A_He_Flux
A_He_Rate
B_Electrons_Rate
B_H_Flux
B_H_Rate
B_He_Flux
B_He_Rate
HCI_Lat
HCI_Lon
HCI_R
HET_A_HCI
HET_A_PA
HET_A_RTN
HET_A_SA
HET_B_HCI
HET_B_PA
HET_B_RTN
HET_B_SA
HGC_Lat
HGC_Lon
HGC_R

PSP_ISOIS-EPIHI_L2-HET-RATES300

A_CNO_SECT_Rate
A_FeGroup_SECT_Rate
A_NetoSi_SECT_Rate
B_CNO_SECT_Rate
B_FeGroup_SECT_Rate
B_NetoSi_SECT_Rate
HCI_Lat
HCI_Lon
HCI_R
HET_A_HCI
HET_A_PA
HET_A_R17_SECT_HCI
HET_A_R17_SECT_PA

HET_A_R17_SECT_RTN
HET_A_R17_SECT_SA
HET_A_RTN
HET_A_SA
HET_B_HCI
HET_B_PA
HET_B_R17_SECT_HCI
HET_B_R17_SECT_PA
HET_B_R17_SECT_RTN
HET_B_R17_SECT_SA
HET_B_RTN
HET_B_SA
HGC_Lat
HGC_Lon
HGC_R

PSP_ISOIS-EPIHI_L2-HET-RATES3600

A_Al_Rate
A_Ar_Rate
A_CNO_SECT_Rate
A_C_Rate
A_Ca_Rate
A_Cr_Rate
A_Electrons_Rate
A_Electrons_SECT_Rate
A_FeGroup_SECT_Rate
A_Fe_Rate
A_H_Flux
A_H_Rate
A_H_SECT_Flux
A_H_SECT_Rate
A_He_Flux
A_He_Rate
A_He_SECT_Flux
A_He_SECT_Rate
A_Mg_Rate
A_N_Rate
A_Na_Rate
A_Ne_Rate
A_NetoSi_SECT_Rate
A_Ni_Rate
A_O_Rate
A_S_Rate

A_Si_Rate
B_Al_Rate
B_Ar_Rate
B_CNO_SECT_Rate
B_C_Rate
B_Ca_Rate
B_Cr_Rate
B_Electrons_Rate
B_Electrons_SECT_Rate
B_FeGroup_SECT_Rate
B_Fe_Rate
B_H_Flux
B_H_Rate
B_H_SECT_Flux
B_H_SECT_Rate
B_He_Flux
B_He_Rate
B_He_SECT_Flux
B_He_SECT_Rate
B_Mg_Rate
B_N_Rate
B_Na_Rate
B_Ne_Rate
B_NetoSi_SECT_Rate
B_Ni_Rate
B_O_Rate
B_S_Rate
B_Si_Rate
HCI_Lat
HCI_Lon
HCI_R
HET_A_HCI
HET_A_PA
HET_A_R17_SECT_HCI
HET_A_R17_SECT_PA
HET_A_R17_SECT_RTN
HET_A_R17_SECT_SA
HET_A_RTN
HET_A_SA
HET_B_HCI
HET_B_PA
HET_B_R17_SECT_HCI
HET_B_R17_SECT_PA
HET_B_R17_SECT_RTN
HET_B_R17_SECT_SA

HET_B_RTN
HET_B_SA
HGC_Lat
HGC_Lon
HGC_R
R1A_He_BIN
R1A_Ne_BIN
R1B_He_BIN
R1B_Ne_BIN
R2A_He_BIN
R2A_Ne_BIN
R2B_He_BIN
R2B_Ne_BIN
R3A_He_BIN
R3A_Ne_BIN
R3B_He_BIN
R3B_Ne_BIN
R4A_He_BIN
R4A_Ne_BIN
R4B_He_BIN
R4B_Ne_BIN
R5A_He_BIN
R5A_Ne_BIN
R5B_He_BIN
R5B_Ne_BIN
R6A_He_BIN
R6A_Ne_BIN
R6B_He_BIN
R6B_Ne_BIN
R7A_He_BIN
R7A_Ne_BIN
R7B_He_BIN
R7B_Ne_BIN

PSP_ISOIS-EPIHI_L2-HET-RATES60

A_Al_Rate
A_Ar_Rate
A_C_Rate
A_Ca_Rate
A_Cr_Rate
A_Electrons_Rate
A_Electrons_SECT_Rate
A_Fe_Rate

A_H_Flux
A_H_Rate
A_H_SECT_Flux
A_H_SECT_Rate
A_He_Flux
A_He_Rate
A_He_SECT_Flux
A_He_SECT_Rate
A_Mg_Rate
A_N_Rate
A_Na_Rate
A_Ne_Rate
A_Ni_Rate
A_O_Rate
A_S_Rate
A_Si_Rate
B_Al_Rate
B_Ar_Rate
B_C_Rate
B_Ca_Rate
B_Cr_Rate
B_Electrons_Rate
B_Electrons_SECT_Rate
B_Fe_Rate
B_H_Flux
B_H_Rate
B_H_SECT_Flux
B_H_SECT_Rate
B_He_Flux
B_He_Rate
B_He_SECT_Flux
B_He_SECT_Rate
B_Mg_Rate
B_N_Rate
B_Na_Rate
B_Ne_Rate
B_Ni_Rate
B_O_Rate
B_S_Rate
B_Si_Rate
HCI_Lat
HCI_Lon
HCI_R
HET_A_HCI
HET_A_PA

HET_A_R17_SECT_HCI
HET_A_R17_SECT_PA
HET_A_R17_SECT_RTN
HET_A_R17_SECT_SA
HET_A_RTN
HET_A_SA
HET_B_HCI
HET_B_PA
HET_B_R17_SECT_HCI
HET_B_R17_SECT_PA
HET_B_R17_SECT_RTN
HET_B_R17_SECT_SA
HET_B_RTN
HET_B_SA
HGC_Lat
HGC_Lon
HGC_R

PSP_ISOIS-EPIHI_L2-LET1-RATES10

A_H_Flux
A_H_Rate
A_He_Flux
A_He_Rate
B_H_Flux
B_H_Rate
B_He_Flux
B_He_Rate
HCI_Lat
HCI_Lon
HCI_R
HGC_Lat
HGC_Lon
HGC_R
LET1_A_HCI
LET1_A_PA
LET1_A_RTN
LET1_A_SA
LET1_B_HCI
LET1_B_PA
LET1_B_RTN
LET1_B_SA

PSP_ISOIS-EPIHI_L2-LET1-RATES300

HCI_Lat
HCI_Lon
HCI_R
HGC_Lat
HGC_Lon
HGC_R
LET1_A_HCI
LET1_A_PA
LET1_A_R1_SECT_HCI
LET1_A_R1_SECT_PA
LET1_A_R1_SECT_RTN
LET1_A_R1_SECT_SA
LET1_A_R26_SECT_HCI
LET1_A_R26_SECT_PA
LET1_A_R26_SECT_RTN
LET1_A_R26_SECT_SA
LET1_A_RTN
LET1_A_SA
LET1_B_HCI
LET1_B_PA
LET1_B_R1_SECT_HCI
LET1_B_R1_SECT_PA
LET1_B_R1_SECT_RTN
LET1_B_R1_SECT_SA
LET1_B_R26_SECT_HCI
LET1_B_R26_SECT_PA
LET1_B_R26_SECT_RTN
LET1_B_R26_SECT_SA
LET1_B_RTN
LET1_B_SA
R1A_CNO_SECT_Rate
R1A_FeGroup_SECT_Rate
R1A_NetoSi_SECT_Rate
R1B_CNO_SECT_Rate
R1B_FeGroup_SECT_Rate
R1B_NetoSi_SECT_Rate
R26A_CNO_SECT_Rate
R26A_FeGroup_SECT_Rate
R26A_NetoSi_SECT_Rate
R26B_CNO_SECT_Rate
R26B_FeGroup_SECT_Rate
R26B_NetoSi_SECT_Rate

PSP_ISOIS-EPIHI_L2-LET1-RATES3600

A_Al_Rate
A_Ar_Rate
A_C_Rate
A_Ca_Rate
A_Cr_Rate
A_Fe_Rate
A_H_Flux
A_H_Rate
A_He_Flux
A_He_Rate
A_Mg_Rate
A_N_Rate
A_Na_Rate
A_Ne_Rate
A_Ni_Rate
A_O_Rate
A_S_Rate
A_Si_Rate
B_Al_Rate
B_Ar_Rate
B_C_Rate
B_Ca_Rate
B_Cr_Rate
B_Fe_Rate
B_H_Flux
B_H_Rate
B_He_Flux
B_He_Rate
B_Mg_Rate
B_N_Rate
B_Na_Rate
B_Ne_Rate
B_Ni_Rate
B_O_Rate
B_S_Rate
B_Si_Rate
HCI_Lat
HCI_Lon
HCI_R
HGC_Lat
HGC_Lon
HGC_R
LET1_A_HCI

LET1_A_PA
LET1_A_R1_SECT_HCI
LET1_A_R1_SECT_PA
LET1_A_R1_SECT_RTN
LET1_A_R1_SECT_SA
LET1_A_R26_SECT_HCI
LET1_A_R26_SECT_PA
LET1_A_R26_SECT_RTN
LET1_A_R26_SECT_SA
LET1_A_RTN
LET1_A_SA
LET1_B_HCI
LET1_B_PA
LET1_B_R1_SECT_HCI
LET1_B_R1_SECT_PA
LET1_B_R1_SECT_RTN
LET1_B_R1_SECT_SA
LET1_B_R26_SECT_HCI
LET1_B_R26_SECT_PA
LET1_B_R26_SECT_RTN
LET1_B_R26_SECT_SA
LET1_B_RTN
LET1_B_SA
R1A_CNO_SECT_Rate
R1A_FeGroup_SECT_Rate
R1A_H_SECT_Flux
R1A_H_SECT_Rate
R1A_He_BIN
R1A_He_SECT_Flux
R1A_He_SECT_Rate
R1A_Ne_BIN
R1A_NetoSi_SECT_Rate
R1B_CNO_SECT_Rate
R1B_FeGroup_SECT_Rate
R1B_H_SECT_Flux
R1B_H_SECT_Rate
R1B_He_BIN
R1B_He_SECT_Flux
R1B_He_SECT_Rate
R1B_Ne_BIN
R1B_NetoSi_SECT_Rate
R26A_CNO_SECT_Rate
R26A_FeGroup_SECT_Rate
R26A_H_SECT_Flux
R26A_H_SECT_Rate

R26A_He_SECT_Flux
R26A_He_SECT_Rate
R26A_NetoSi_SECT_Rate
R26B_CNO_SECT_Rate
R26B_FeGroup_SECT_Rate
R26B_H_SECT_Flux
R26B_H_SECT_Rate
R26B_He_SECT_Flux
R26B_He_SECT_Rate
R26B_NetoSi_SECT_Rate
R2A_He_BIN
R2A_Ne_BIN
R2B_He_BIN
R2B_Ne_BIN
R3A_He_BIN
R3A_Ne_BIN
R3B_He_BIN
R3B_Ne_BIN
R45A_He_BIN
R45A_Ne_BIN
R45B_He_BIN
R45B_Ne_BIN
R6A_He_BIN
R6A_Ne_BIN
R6B_He_BIN
R6B_Ne_BIN

PSP_ISOIS-EPIHI_L2-LET1-RATES60

A_Al_Rate
A_Ar_Rate
A_C_Rate
A_Ca_Rate
A_Cr_Rate
A_Fe_Rate
A_H_Flux
A_H_Rate
A_He_Flux
A_He_Rate
A_Mg_Rate
A_N_Rate
A_Na_Rate
A_Ne_Rate
A_Ni_Rate

A_O_Rate
A_S_Rate
A_Si_Rate
B_Al_Rate
B_Ar_Rate
B_C_Rate
B_Ca_Rate
B_Cr_Rate
B_Fe_Rate
B_H_Flux
B_H_Rate
B_He_Flux
B_He_Rate
B_Mg_Rate
B_N_Rate
B_Na_Rate
B_Ne_Rate
B_Ni_Rate
B_O_Rate
B_S_Rate
B_Si_Rate
HCI_Lat
HCI_Lon
HCI_R
HGC_Lat
HGC_Lon
HGC_R
LET1_A_HCI
LET1_A_PA
LET1_A_R1_SECT_HCI
LET1_A_R1_SECT_PA
LET1_A_R1_SECT_RTN
LET1_A_R1_SECT_SA
LET1_A_R26_SECT_HCI
LET1_A_R26_SECT_PA
LET1_A_R26_SECT_RTN
LET1_A_R26_SECT_SA
LET1_A_RTN
LET1_A_SA
LET1_B_HCI
LET1_B_PA
LET1_B_R1_SECT_HCI
LET1_B_R1_SECT_PA
LET1_B_R1_SECT_RTN
LET1_B_R1_SECT_SA

LET1_B_R26_SECT_HCI
LET1_B_R26_SECT_PA
LET1_B_R26_SECT_RTN
LET1_B_R26_SECT_SA
LET1_B_RTN
LET1_B_SA
R1A_H_SECT_Flux
R1A_H_SECT_Rate
R1A_He_SECT_Flux
R1A_He_SECT_Rate
R1B_H_SECT_Flux
R1B_H_SECT_Rate
R1B_He_SECT_Flux
R1B_He_SECT_Rate
R26A_H_SECT_Flux
R26A_H_SECT_Rate
R26A_He_SECT_Flux
R26A_He_SECT_Rate
R26B_H_SECT_Flux
R26B_H_SECT_Rate
R26B_He_SECT_Flux
R26B_He_SECT_Rate

PSP_ISOIS-EPIHI_L2-LET2-RATES10

C_H_Flux
C_H_Rate
C_He_Flux
C_He_Rate
HCI_Lat
HCI_Lon
HCI_R
HGC_Lat
HGC_Lon
HGC_R
LET2_C_HCI
LET2_C_PA
LET2_C_RTN
LET2_C_SA

PSP_ISOIS-EPIHI_L2-LET2-RATES300

HCI_Lat
HCI_Lon
HCI_R
HGC_Lat
HGC_Lon
HGC_R
LET2_C_HCI
LET2_C_PA
LET2_C_R1_SECT_HCI
LET2_C_R1_SECT_PA
LET2_C_R1_SECT_RTN
LET2_C_R1_SECT_SA
LET2_C_R25_SECT_HCI
LET2_C_R25_SECT_PA
LET2_C_R25_SECT_RTN
LET2_C_R25_SECT_SA
LET2_C_RTN
LET2_C_SA
R1C_CNO_SECT_Rate
R1C_FeGroup_SECT_Rate
R1C_NetoSi_SECT_Rate
R25C_CNO_SECT_Rate
R25C_FeGroup_SECT_Rate
R25C_NetoSi_SECT_Rate

PSP_ISOIS-EPIHI_L2-LET2-RATES3600

C_Al_Rate
C_Ar_Rate
C_C_Rate
C_Ca_Rate
C_Cr_Rate
C_Fe_Rate
C_H_Flux
C_H_Rate
C_He_Flux
C_He_Rate
C_Mg_Rate
C_N_Rate
C_Na_Rate
C_Ne_Rate
C_Ni_Rate

C_O_Rate
C_S_Rate
C_Si_Rate
HCI_Lat
HCI_Lon
HCI_R
HGC_Lat
HGC_Lon
HGC_R
LET2_C_HCI
LET2_C_PA
LET2_C_R1_SECT_HCI
LET2_C_R1_SECT_PA
LET2_C_R1_SECT_RTN
LET2_C_R1_SECT_SA
LET2_C_R25_SECT_HCI
LET2_C_R25_SECT_PA
LET2_C_R25_SECT_RTN
LET2_C_R25_SECT_SA
LET2_C_RTN
LET2_C_SA
R1C_CNO_SECT_Rate
R1C_FeGroup_SECT_Rate
R1C_H_SECT_Flux
R1C_H_SECT_Rate
R1C_He_BIN
R1C_He_SECT_Flux
R1C_He_SECT_Rate
R1C_Ne_BIN
R1C_NetoSi_SECT_Rate
R25C_CNO_SECT_Rate
R25C_FeGroup_SECT_Rate
R25C_H_SECT_Flux
R25C_H_SECT_Rate
R25C_He_SECT_Flux
R25C_He_SECT_Rate
R25C_NetoSi_SECT_Rate
R2C_He_BIN
R2C_Ne_BIN
R3C_He_BIN
R3C_Ne_BIN
R45C_He_BIN
R45C_Ne_BIN

PSP_ISOIS-EPIHI_L2-LET2-RATES60

C_Al_Rate
C_Ar_Rate
C_C_Rate
C_Ca_Rate
C_Cr_Rate
C_Fe_Rate
C_H_Flux
C_H_Rate
C_He_Flux
C_He_Rate
C_Mg_Rate
C_N_Rate
C_Na_Rate
C_Ne_Rate
C_Ni_Rate
C_O_Rate
C_S_Rate
C_Si_Rate
HCI_Lat
HCI_Lon
HCI_R
HGC_Lat
HGC_Lon
HGC_R
LET2_C_HCI
LET2_C_PA
LET2_C_R1_SECT_HCI
LET2_C_R1_SECT_PA
LET2_C_R1_SECT_RTN
LET2_C_R1_SECT_SA
LET2_C_R25_SECT_HCI
LET2_C_R25_SECT_PA
LET2_C_R25_SECT_RTN
LET2_C_R25_SECT_SA
LET2_C_RTN
LET2_C_SA
R1C_H_SECT_Flux
R1C_H_SECT_Rate
R1C_He_SECT_Flux
R1C_He_SECT_Rate
R25C_H_SECT_Flux
R25C_H_SECT_Rate
R25C_He_SECT_Flux

R25C_He_SECT_Rate

PSP_ISOIS-EPIHI_L2-SECOND-RATES

HCI_Lat

HCI_Lon

HCI_R

HET_A_Electrons_Rate

HET_A_HCI

HET_A_H_Rate

HET_A_PA

HET_A_RTN

HET_A_SA

HET_B_Electrons_Rate

HET_B_HCI

HET_B_H_Rate

HET_B_PA

HET_B_RTN

HET_B_SA

HGC_Lat

HGC_Lon

HGC_R

LET1_A_Electrons_Rate

LET1_A_HCI

LET1_A_H_Rate

LET1_A_PA

LET1_A_RTN

LET1_A_SA

LET1_B_Electrons_Rate

LET1_B_HCI

LET1_B_H_Rate

LET1_B_PA

LET1_B_RTN

LET1_B_SA

LET2_C_Electrons_Rate

LET2_C_HCI

LET2_C_H_Rate

LET2_C_PA

LET2_C_RTN

LET2_C_SA

PSP_ISOIS-EPILO_L2-IC

C_CountRate_ChanD
Fe_CountRate_ChanC
HCI_ChanC
HCI_ChanD
HCI_ChanP
HCI_ChanR
HCI_ChanT
HCI_Lat_ChanC
HCI_Lat_ChanD
HCI_Lat_ChanP
HCI_Lat_ChanR
HCI_Lat_ChanT
HCI_Lon_ChanC
HCI_Lon_ChanD
HCI_Lon_ChanP
HCI_Lon_ChanR
HCI_Lon_ChanT
HCI_R_ChanC
HCI_R_ChanD
HCI_R_ChanP
HCI_R_ChanR
HCI_R_ChanT
HGC_Lat_ChanC
HGC_Lat_ChanD
HGC_Lat_ChanP
HGC_Lat_ChanR
HGC_Lat_ChanT
HGC_Lon_ChanC
HGC_Lon_ChanD
HGC_Lon_ChanP
HGC_Lon_ChanR
HGC_Lon_ChanT
HGC_R_ChanC
HGC_R_ChanD
HGC_R_ChanP
HGC_R_ChanR
HGC_R_ChanT
H_CountRate_ChanP
H_CountRate_ChanR
H_CountRate_ChanT
H_Flux_ChanP
H_Flux_ChanR
H_Flux_ChanT

He3_CountRate_ChanC
He4_CountRate_ChanC
He4_Flux_ChanC
Look_Direction_80_DELTAMINUS
Look_Direction_80_DELTAPLUS
Mg_CountRate_ChanD
O_CountRate_ChanC
PA_ChanC
PA_ChanD
PA_ChanP
PA_ChanR
PA_ChanT
RTN_ChanC
RTN_ChanD
RTN_ChanP
RTN_ChanR
RTN_ChanT
SA_ChanC
SA_ChanD
SA_ChanP
SA_ChanR
SA_ChanT
Si_CountRate_ChanD

PSP_ISOIS-EPILO_L2-PE

Electron_CountRate_ChanE
Electron_CountRate_ChanF
Electron_CountRate_ChanG
HCI_ChanE
HCI_ChanF
HCI_ChanG
HCI_Lat_ChanE
HCI_Lat_ChanF
HCI_Lat_ChanG
HCI_Lon_ChanE
HCI_Lon_ChanF
HCI_Lon_ChanG
HCI_R_ChanE
HCI_R_ChanF
HCI_R_ChanG
HGC_Lat_ChanE
HGC_Lat_ChanF
HGC_Lat_ChanG

HGC_Lon_ChanE
HGC_Lon_ChanF
HGC_Lon_ChanG
HGC_R_ChanE
HGC_R_ChanF
HGC_R_ChanG
H_CountRate_ChanE
H_CountRate_ChanF
H_CountRate_ChanG
Look_Direction_08_DELTAMINUS
Look_Direction_08_DELTAPLUS
Look_Direction_80_DELTAMINUS
Look_Direction_80_DELTAPLUS
PA_ChanE
PA_ChanF
PA_ChanG
RTN_ChanE
RTN_ChanF
RTN_ChanG
SA_ChanE
SA_ChanF
SA_ChanG

PSP_ISOIS_L2-SUMMARY

A_H_Rate_TS
A_Heavy_Rate_TS
Electron_CountRate_ChanE
HET_A_Electrons_Rate_TS
HET_A_H_Rate_TS
H_CountRate_ChanT_SP

CDF CONTENTS

PSP_ISOIS_L2-SUMMARY

ISOIS>Integrated Science Investigation of the Sun

L2-Summary>level 2 summary

EPI-Hi HET 3600 second rates cdf. Time tags indicate midpoint of integration.

Instrument paper: Integrated Science Investigation of the Sun (ISIS): Design of the Energetic Particle Investigation. McComas, D. J. et al (2016). Space Sci. Rev., doi:10.1007/s11214-014-0059-1

EPI-Hi 3600 seconds rates cdf. Time tags indicate midpoint of integration.

EPI-Lo, Ion Composition mode.

EPI-Lo, Particle Energy mode.

1 minute to 1 hour

Cite McComas et al (2016), doi:10.1007/s11214-014-0059-1

PRIMARY VARIABLES

OTHER DATA

4.1.2.1 A_H_Rate_TS H count rate side A 2-10MeV (counts s⁻¹)

time-varying

particle_flux>differential_directional_number_rate

4.1.2.2 A_Heavy_Rate_TS Heavy (6<=z<=28) ion count rate side A 4-40 MeV/nuc (counts s⁻¹)

time-varying

particle_flux>differential_directional_number_rate

4.1.2.3 Electron_CountRate_ChanE Electron count rate channel E (HiResElectrons) (counts/sec)

Size: 48 time-varying

particle_flux>differential_directional_number_rate

Particle Energy mode. Corrected for deadtime. May contain substantial non-electron background.

Electron_ChanE_Energy 12 – 9065 keV (32 bins)

4.1.2.4 HET_A_Electrons_Rate_TS HET Electrons count rate side A 1-5MeV (counts s⁻¹)

time-varying

particle_flux>differential_directional_number_rate

4.1.2.5 HET_A_H_Rate_TS HET H count rate side A 10-50MeV (counts s⁻¹)
time-varying
particle_flux>differential_directional_number_rate

4.1.2.6 H_CountRate_ChanT_SP H count rate channel T (IonTOF) (counts/sec)
Size: 47 time-varying
particle_flux>differential_directional_number_rate
Ion Composition mode. Corrected for deadtime. All species; calibrated for H. Look L31, L34, L35 eliminated due to potential photon contamination; see Hill, M.E. et al., 2020, ApJS, doi:10.3847/1538-4365/ab643d .
H_ChanT_Energy 23 – 34454 keV/nuc (31 bins)

OTHER SUPPORT

PSP_ISOIS-EPILO_L2-IC

ISOIS-EPILO>Integrated Science Investigation of the Sun, Energetic Particle Instrument Lo
L2-ic>Level 2 ic
EPI-Lo, Ion Composition mode.
Instrument paper: Integrated Science Investigation of the Sun (ISIS): Design of the Energetic Particle Investigation. McComas, D. J. et al (2016). Space Sci. Rev., doi:10.1007/s11214-014-0059-1
1 minute to 1 hour
Cite McComas et al (2016), doi:10.1007/s11214-014-0059-1

PRIMARY VARIABLES

4.2.1.1 H_Flux_ChanP H flux channel P (HiResProtons) (cm⁻²sr⁻¹sec⁻¹keV⁻¹)
Size: 80 × 48 time-varying
particle_flux>differential_directional_number
Ion Composition mode.
Look_Direction_80 0 – 79 (80 bins)
H_ChanP_Energy 61 – 8290 keV (41 bins)

4.2.1.2 H_Flux_ChanR H flux channel R (HiTimeResProtons) (cm⁻²sr⁻¹sec⁻¹keV⁻¹)
Size: 80 × 48 time-varying
particle_flux>differential_directional_number
Ion Composition mode.
Look_Direction_80 0 – 79 (80 bins)
H_ChanR_Energy 70 – 8290 keV (15 bins)

4.2.1.3 H_Flux_ChanT H flux channel T (IonTOF) ($\text{cm}^{-2}\text{sr}^{-1}\text{sec}^{-1}(\text{keV}/\text{nuc})^{-1}$)

Size: 80×47 time-varying

particle_flux>differential_directional_number

Ion Composition mode. May contain significant photon counts, particularly directions L31, L34, L35. See Hill, M.E. et al., 2020, ApJS, doi:10.3847/1538-4365/ab643d .

Look_Direction_80 0 – 79 (80 bins)

H_ChanT_Energy 20 – 34454 keV/nuc (31 bins)

4.2.1.4 He4_Flux_ChanC He4 flux channel C (Ions1) ($\text{cm}^{-2}\text{sr}^{-1}\text{sec}^{-1}\text{keV}^{-1}$)

Size: 80×48 time-varying

particle_flux>differential_directional_number

Ion Composition mode.

Look_Direction_80 0 – 79 (80 bins)

He4_ChanC_Energy 73 – 18468 keV (46 bins)

OTHER DATA

4.2.2.1 C_CountRate_ChanD C count rate channel D (Ions2) (counts/sec)

Size: 80×48 time-varying

particle_flux>differential_directional_number_rate

Ion Composition mode. Corrected for deadtime.

Look_Direction_80 0 – 79 (80 bins)

C_ChanD_Energy 206 – 17518 keV (21 bins)

4.2.2.2 Fe_CountRate_ChanC Fe count rate channel C (Ions1) (counts/sec)

Size: 80×48 time-varying

particle_flux>differential_directional_number_rate

Ion Composition mode. Corrected for deadtime.

Look_Direction_80 0 – 79 (80 bins)

Fe_ChanC_Energy 440 – 20657 keV (42 bins)

4.2.2.3 HCI_ChanC HCI flow direction ChanC

Size: 80×3 time-varying

position>direction

Unit vector, after Fraenz and Harper, PSS, 2002. ChanC timebase.

Look_Direction_80 0 – 79 (80 bins)

4.2.2.4 HCI_ChanD HCI flow direction ChanD

Size: 80×3 time-varying

position>direction

Unit vector, after Fraenz and Harper, PSS, 2002. ChanD timebase.

Look_Direction_80 0 – 79 (80 bins)

4.2.2.5 HCI_ChanP HCI flow direction ChanP

Size: 80×3 time-varying

position>direction

Unit vector, after Fraenz and Harper, PSS, 2002. ChanP timebase.

Look_Direction_80 0 – 79 (80 bins)

4.2.2.6 HCI_ChanR HCI flow direction ChanR

Size: 80×3 time-varying

position>direction

Unit vector, after Fraenz and Harper, PSS, 2002. ChanR timebase.

Look_Direction_80 0 – 79 (80 bins)

4.2.2.7 HCI_ChanT HCI flow direction ChanT

Size: 80×3 time-varying

position>direction

Unit vector, after Fraenz and Harper, PSS, 2002. ChanT timebase.

Look_Direction_80 0 – 79 (80 bins)

4.2.2.8 HCI_Lat_ChanC HCI latitude ChanC (degrees)

time-varying

position>latitude

At timestamp. After Fraenz and Harper, PSS, 2002. ChanC timebase.

4.2.2.9 HCI_Lat_ChanD HCI latitude ChanD (degrees)

time-varying

position>latitude

At timestamp. After Fraenz and Harper, PSS, 2002. ChanD timebase.

4.2.2.10 HCI_Lat_ChanP HCI latitude ChanP (degrees)

time-varying

position>latitude

At timestamp. After Fraenz and Harper, PSS, 2002. ChanP timebase.

4.2.2.11 HCI_Lat_ChanR HCI latitude ChanR (degrees)

time-varying

position>latitude

At timestamp. After Fraenz and Harper, PSS, 2002. ChanR timebase.

4.2.2.12 HCI_Lat_ChanT HCI latitude ChanT (degrees)

time-varying

position>latitude

At timestamp. After Fraenz and Harper, PSS, 2002. ChanT timebase.

4.2.2.13 HCI_Lon_ChanC HCI longitude ChanC (degrees)

time-varying

position>longitude

At timestamp. After Fraenz and Harper, PSS, 2002. ChanC timebase.

4.2.2.14 HCI_Lon_ChanD HCI longitude ChanD (degrees)

time-varying

position>longitude

At timestamp. After Fraenz and Harper, PSS, 2002. ChanD timebase.

4.2.2.15 HCI_Lon_ChanP HCI longitude ChanP (degrees)

time-varying

position>longitude

At timestamp. After Fraenz and Harper, PSS, 2002. ChanP timebase.

4.2.2.16 HCI_Lon_ChanR HCI longitude ChanR (degrees)

time-varying

position>longitude

At timestamp. After Fraenz and Harper, PSS, 2002. ChanR timebase.

4.2.2.17 HCI_Lon_ChanT HCI longitude ChanT (degrees)

time-varying

position>longitude

At timestamp. After Fraenz and Harper, PSS, 2002. ChanT timebase.

4.2.2.18 HCI_R_ChanC Heliocentric distance ChanC (AU)

time-varying

position>radial

At timestamp. After Fraenz and Harper, PSS, 2002. ChanC timebase.

4.2.2.19 HCI_R_ChanD Heliocentric distance ChanD (AU)

time-varying

position>radial

At timestamp. After Fraenz and Harper, PSS, 2002. ChanD timebase.

4.2.2.20 HCI_R_ChanP Heliocentric distance ChanP (AU)

time-varying

position>radial

At timestamp. After Fraenz and Harper, PSS, 2002. ChanP timebase.

4.2.2.21 HCI_R_ChanR Heliocentric distance ChanR (AU)

time-varying

position>radial

At timestamp. After Fraenz and Harper, PSS, 2002. ChanR timebase.

4.2.2.22 HCI_R_ChanT Heliocentric distance ChanT (AU)

time-varying

position>radial

At timestamp. After Fraenz and Harper, PSS, 2002. ChanT timebase.

4.2.2.23 HGC_Lat_ChanC HGC latitude ChanC (degrees)

time-varying

position>latitude

At timestamp. After Fraenz and Harper, PSS, 2002. ChanC timebase.

4.2.2.24 HGC_Lat_ChanD HGC latitude ChanD (degrees)
time-varying
position>latitude
At timestamp. After Fraenz and Harper, PSS, 2002. ChanD timebase.

4.2.2.25 HGC_Lat_ChanP HGC latitude ChanP (degrees)
time-varying
position>latitude
At timestamp. After Fraenz and Harper, PSS, 2002. ChanP timebase.

4.2.2.26 HGC_Lat_ChanR HGC latitude ChanR (degrees)
time-varying
position>latitude
At timestamp. After Fraenz and Harper, PSS, 2002. ChanR timebase.

4.2.2.27 HGC_Lat_ChanT HGC latitude ChanT (degrees)
time-varying
position>latitude
At timestamp. After Fraenz and Harper, PSS, 2002. ChanT timebase.

4.2.2.28 HGC_Lon_ChanC HGC longitude ChanC (degrees)
time-varying
position>longitude
At timestamp. After Fraenz and Harper, PSS, 2002. ChanC timebase.

4.2.2.29 HGC_Lon_ChanD HGC longitude ChanD (degrees)
time-varying
position>longitude
At timestamp. After Fraenz and Harper, PSS, 2002. ChanD timebase.

4.2.2.30 HGC_Lon_ChanP HGC longitude ChanP (degrees)
time-varying
position>longitude
At timestamp. After Fraenz and Harper, PSS, 2002. ChanP timebase.

4.2.2.31 HGC_Lon_ChanR HGC longitude ChanR (degrees)
time-varying
position>longitude
At timestamp. After Fraenz and Harper, PSS, 2002. ChanR timebase.

4.2.2.32 HGC_Lon_ChanT HGC longitude ChanT (degrees)
time-varying
position>longitude
At timestamp. After Fraenz and Harper, PSS, 2002. ChanT timebase.

4.2.2.33 HGC_R_ChanC Heliocentric distance ChanC (AU)
time-varying
position>radial
At timestamp. After Fraenz and Harper, PSS, 2002. ChanC timebase.

4.2.2.34 HGC_R_ChanD Heliocentric distance ChanD (AU)
time-varying
position>radial
At timestamp. After Fraenz and Harper, PSS, 2002. ChanD timebase.

4.2.2.35 HGC_R_ChanP Heliocentric distance ChanP (AU)
time-varying
position>radial
At timestamp. After Fraenz and Harper, PSS, 2002. ChanP timebase.

4.2.2.36 HGC_R_ChanR Heliocentric distance ChanR (AU)
time-varying
position>radial
At timestamp. After Fraenz and Harper, PSS, 2002. ChanR timebase.

4.2.2.37 HGC_R_ChanT Heliocentric distance ChanT (AU)
time-varying
position>radial
At timestamp. After Fraenz and Harper, PSS, 2002. ChanT timebase.

4.2.2.38 H_CountRate_ChanP H count rate channel P (HiResProtons) (counts/sec)

Size: 80 \times 48 time-varying

particle_flux>differential_directional_number_rate

Ion Composition mode. Corrected for deadtime.

Look_Direction_80 0 – 79 (80 bins)

H_ChanP_Energy 61 – 8290 keV (41 bins)

4.2.2.39 H_CountRate_ChanR H count rate channel R (HiTimeResProtons) (counts/sec)

Size: 80 \times 48 time-varying

particle_flux>differential_directional_number_rate

Ion Composition mode. Corrected for deadtime.

Look_Direction_80 0 – 79 (80 bins)

H_ChanR_Energy 70 – 8290 keV (15 bins)

4.2.2.40 H_CountRate_ChanT H count rate channel T (IonTOF) (counts/sec)

Size: 80 \times 47 time-varying

particle_flux>differential_directional_number_rate

Ion Composition mode. Corrected for deadtime. May contain significant photon counts, particularly directions L31, L34, L35. See Hill, M.E. et al., 2020, ApJS, doi:10.3847/1538-4365/ab643d .

Look_Direction_80 0 – 79 (80 bins)

H_ChanT_Energy 20 – 34454 keV/nuc (31 bins)

4.2.2.41 He3_CountRate_ChanC He3 count rate channel C (Ions1) (counts/sec)

Size: 80 \times 48 time-varying

particle_flux>differential_directional_number_rate

Ion Composition mode. Corrected for deadtime.

Look_Direction_80 0 – 79 (80 bins)

He3_ChanC_Energy 86 – 18464 keV (46 bins)

4.2.2.42 He4_CountRate_ChanC He4 count rate channel C (Ions1) (counts/sec)

Size: 80 \times 48 time-varying

particle_flux>differential_directional_number_rate

Ion Composition mode. Corrected for deadtime.

Look_Direction_80 0 – 79 (80 bins)

He4_ChanC_Energy 73 – 18468 keV (46 bins)

4.2.2.43 Mg_CountRate_ChanD Mg count rate channel D (Ions2) (counts/sec)

Size: 80 × 48 time-varying

particle_flux>differential_directional_number_rate

Ion Composition mode. Corrected for deadtime.

Look_Direction_80 0 – 79 (80 bins)

Mg_ChanD_Energy

4.2.2.44 O_CountRate_ChanC O count rate channel C (Ions1) (counts/sec)

Size: 80 × 48 time-varying

particle_flux>differential_directional_number_rate

Ion Composition mode. Corrected for deadtime.

Look_Direction_80 0 – 79 (80 bins)

O_ChanC_Energy 232 – 19066 keV (41 bins)

4.2.2.45 PA_ChanC Pitch angle ChanC (degree)

Size: 80 time-varying

position>angle

Look_Direction_80 0 – 79 (80 bins)

4.2.2.46 PA_ChanD Pitch angle ChanD (degree)

Size: 80 time-varying

position>angle

Look_Direction_80 0 – 79 (80 bins)

4.2.2.47 PA_ChanP Pitch angle ChanP (degree)

Size: 80 time-varying

position>angle

Look_Direction_80 0 – 79 (80 bins)

4.2.2.48 PA_ChanR Pitch angle ChanR (degree)

Size: 80 time-varying

position>angle

Look_Direction_80 0 – 79 (80 bins)

4.2.2.49 PA_ChanT Pitch angle ChanT (degree)

Size: 80 time-varying

position>angle
Look_Direction_80 0 – 79 (80 bins)

4.2.2.50 RTN_ChanC RTN flow direction ChanC

Size: 80×3 time-varying

position>direction

Unit vector, after Fraenz and Harper, PSS, 2002. ChanC timebase.

Look_Direction_80 0 – 79 (80 bins)

4.2.2.51 RTN_ChanD RTN flow direction ChanD

Size: 80×3 time-varying

position>direction

Unit vector, after Fraenz and Harper, PSS, 2002. ChanD timebase.

Look_Direction_80 0 – 79 (80 bins)

4.2.2.52 RTN_ChanP RTN flow direction ChanP

Size: 80×3 time-varying

position>direction

Unit vector, after Fraenz and Harper, PSS, 2002. ChanP timebase.

Look_Direction_80 0 – 79 (80 bins)

4.2.2.53 RTN_ChanR RTN flow direction ChanR

Size: 80×3 time-varying

position>direction

Unit vector, after Fraenz and Harper, PSS, 2002. ChanR timebase.

Look_Direction_80 0 – 79 (80 bins)

4.2.2.54 RTN_ChanT RTN flow direction ChanT

Size: 80×3 time-varying

position>direction

Unit vector, after Fraenz and Harper, PSS, 2002. ChanT timebase.

Look_Direction_80 0 – 79 (80 bins)

4.2.2.55 SA_ChanC Nominal Parker Spiral angle ChanC (degree)

Size: 80 time-varying

position>angle

Angle between particle direction and nominal outward Parker Spiral, based on 400km/s solar wind and corotation breakdown at 10Rs.

Look_Direction_80 0 – 79 (80 bins)

4.2.2.56 SA_ChanD Nominal Parker Spiral angle ChanD (degree)

Size: 80 time-varying

position>angle

Angle between particle direction and nominal outward Parker Spiral, based on 400km/s solar wind and corotation breakdown at 10Rs.

Look_Direction_80 0 – 79 (80 bins)

4.2.2.57 SA_ChanP Nominal Parker Spiral angle ChanP (degree)

Size: 80 time-varying

position>angle

Angle between particle direction and nominal outward Parker Spiral, based on 400km/s solar wind and corotation breakdown at 10Rs.

Look_Direction_80 0 – 79 (80 bins)

4.2.2.58 SA_ChanR Nominal Parker Spiral angle ChanR (degree)

Size: 80 time-varying

position>angle

Angle between particle direction and nominal outward Parker Spiral, based on 400km/s solar wind and corotation breakdown at 10Rs.

Look_Direction_80 0 – 79 (80 bins)

4.2.2.59 SA_ChanT Nominal Parker Spiral angle ChanT (degree)

Size: 80 time-varying

position>angle

Angle between particle direction and nominal outward Parker Spiral, based on 400km/s solar wind and corotation breakdown at 10Rs.

Look_Direction_80 0 – 79 (80 bins)

4.2.2.60 Si_CountRate_ChanD Si count rate channel D (Ions2) (counts/sec)

Size: 80 × 48 time-varying

particle_flux>differential_directional_number_rate

Ion Composition mode. Corrected for deadtime.

Look_Direction_80 0 – 79 (80 bins)

Si_ChanD_Energy 593 – 18610 keV (15 bins)

OTHER SUPPORT

4.2.3.1 Look_Direction_80_DELTAMINUS Size: 80 constant number

4.2.3.2 Look_Direction_80_DELTAPLUS Size: 80 constant number

PSP_ISOIS-EPILO_L2-PE

ISOIS-EPILO>Integrated Science Investigation of the Sun, Energetic Particle Instrument Lo L2-pe>Level 2 pe
EPI-Lo, Particle Energy mode.

Instrument paper: Integrated Science Investigation of the Sun (ISIS): Design of the Energetic Particle Investigation. McComas, D. J. et al (2016). Space Sci. Rev., doi:10.1007/s11214-014-0059-1

1 minute to 1 hour

Cite McComas et al (2016), doi:10.1007/s11214-014-0059-1

PRIMARY VARIABLES

OTHER DATA

4.3.2.1 Electron_CountRate_ChanE Electron count rate channel E (HiResElectrons) (counts/sec)

Size: 8×48 time-varying

particle_flux>differential_directional_number_rate

Particle Energy mode. Corrected for deadtime.

Look_Direction_08 0 – 7 (8 bins)

Electron_ChanE_Energy 12 – 9065 keV (32 bins)

4.3.2.2 Electron_CountRate_ChanF Electron count rate channel F (HiTimeResElectrons) (counts/sec)

Size: 8×48 time-varying

particle_flux>differential_directional_number_rate

Particle Energy mode. Corrected for deadtime.

Look_Direction_08 0 – 7 (8 bins)

Electron_ChanF_Energy 19 – 6607 keV (12 bins)

4.3.2.3 Electron_CountRate_ChanG Electron count rate channel G (HiLookResElectrons)
(counts/sec)

Size: 80×48 time-varying

particle_flux>differential_directional_number_rate

Particle Energy mode. Corrected for deadtime.

Look_Direction_80 0 – 79 (80 bins)

Electron_ChanG_Energy 12 – 9065 keV (32 bins)

4.3.2.4 HCI_ChanE HCI flow direction ChanE

Size: 8×3 time-varying

position>direction

Unit vector, after Fraenz and Harper, PSS, 2002. ChanE timebase.

Look_Direction_08 0 – 7 (8 bins)

4.3.2.5 HCI_ChanF HCI flow direction ChanF

Size: 8×3 time-varying

position>direction

Unit vector, after Fraenz and Harper, PSS, 2002. ChanF timebase.

Look_Direction_08 0 – 7 (8 bins)

4.3.2.6 HCI_ChanG HCI flow direction ChanG

Size: 80×3 time-varying

position>direction

Unit vector, after Fraenz and Harper, PSS, 2002. ChanG timebase.

Look_Direction_80 0 – 79 (80 bins)

4.3.2.7 HCI_Lat_ChanE HCI latitude ChanE (degrees)

time-varying

position>latitude

At timestamp. After Fraenz and Harper, PSS, 2002. ChanE timebase.

4.3.2.8 HCI_Lat_ChanF HCI latitude ChanF (degrees)

time-varying

position>latitude

At timestamp. After Fraenz and Harper, PSS, 2002. ChanF timebase.

4.3.2.9 HCI_Lat_ChanG HCI latitude ChanG (degrees)
time-varying
position>latitude
At timestamp. After Fraenz and Harper, PSS, 2002. ChanG timebase.

4.3.2.10 HCI_Lon_ChanE HCI longitude ChanE (degrees)
time-varying
position>longitude
At timestamp. After Fraenz and Harper, PSS, 2002. ChanE timebase.

4.3.2.11 HCI_Lon_ChanF HCI longitude ChanF (degrees)
time-varying
position>longitude
At timestamp. After Fraenz and Harper, PSS, 2002. ChanF timebase.

4.3.2.12 HCI_Lon_ChanG HCI longitude ChanG (degrees)
time-varying
position>longitude
At timestamp. After Fraenz and Harper, PSS, 2002. ChanG timebase.

4.3.2.13 HCI_R_ChanE Heliocentric distance ChanE (AU)
time-varying
position>radial
At timestamp. After Fraenz and Harper, PSS, 2002. ChanE timebase.

4.3.2.14 HCI_R_ChanF Heliocentric distance ChanF (AU)
time-varying
position>radial
At timestamp. After Fraenz and Harper, PSS, 2002. ChanF timebase.

4.3.2.15 HCI_R_ChanG Heliocentric distance ChanG (AU)
time-varying
position>radial
At timestamp. After Fraenz and Harper, PSS, 2002. ChanG timebase.

4.3.2.16 HGC_Lat_ChanE HGC latitude ChanE (degrees)
time-varying
position>latitude
At timestamp. After Fraenz and Harper, PSS, 2002. ChanE timebase.

4.3.2.17 HGC_Lat_ChanF HGC latitude ChanF (degrees)
time-varying
position>latitude
At timestamp. After Fraenz and Harper, PSS, 2002. ChanF timebase.

4.3.2.18 HGC_Lat_ChanG HGC latitude ChanG (degrees)
time-varying
position>latitude
At timestamp. After Fraenz and Harper, PSS, 2002. ChanG timebase.

4.3.2.19 HGC_Lon_ChanE HGC longitude ChanE (degrees)
time-varying
position>longitude
At timestamp. After Fraenz and Harper, PSS, 2002. ChanE timebase.

4.3.2.20 HGC_Lon_ChanF HGC longitude ChanF (degrees)
time-varying
position>longitude
At timestamp. After Fraenz and Harper, PSS, 2002. ChanF timebase.

4.3.2.21 HGC_Lon_ChanG HGC longitude ChanG (degrees)
time-varying
position>longitude
At timestamp. After Fraenz and Harper, PSS, 2002. ChanG timebase.

4.3.2.22 HGC_R_ChanE Heliocentric distance ChanE (AU)
time-varying
position>radial
At timestamp. After Fraenz and Harper, PSS, 2002. ChanE timebase.

4.3.2.23 HGC_R_ChanF Heliocentric distance ChanF (AU)

time-varying

position>radial

At timestamp. After Fraenz and Harper, PSS, 2002. ChanF timebase.

4.3.2.24 HGC_R_ChanG Heliocentric distance ChanG (AU)

time-varying

position>radial

At timestamp. After Fraenz and Harper, PSS, 2002. ChanG timebase.

4.3.2.25 H_CountRate_ChanE H count rate channel E (HiResElectrons) (counts/sec)

Size: 8×48 time-varying

particle_flux>differential_directional_number_rate

Particle Energy mode. Corrected for deadtime.

Look_Direction_08 0 – 7 (8 bins)

H_ChanE_Energy

4.3.2.26 H_CountRate_ChanF H count rate channel F (HiTimeResElectrons) (counts/sec)

Size: 8×48 time-varying

particle_flux>differential_directional_number_rate

Particle Energy mode. Corrected for deadtime.

Look_Direction_08 0 – 7 (8 bins)

H_ChanF_Energy

4.3.2.27 H_CountRate_ChanG H count rate channel G (HiLookResElectrons) (counts/sec)

Size: 80×48 time-varying

particle_flux>differential_directional_number_rate

Particle Energy mode. Corrected for deadtime.

Look_Direction_80 0 – 79 (80 bins)

H_ChanG_Energy

4.3.2.28 PA_ChanE Pitch angle ChanE (degree)

Size: 8 time-varying

position>angle

Look_Direction_08 0 – 7 (8 bins)

4.3.2.29 PA_ChanF Pitch angle ChanF (degree)

Size: 8 time-varying

position>angle

Look_Direction_08 0 – 7 (8 bins)

4.3.2.30 PA_ChanG Pitch angle ChanG (degree)

Size: 80 time-varying

position>angle

Look_Direction_80 0 – 79 (80 bins)

4.3.2.31 RTN_ChanE RTN flow direction ChanE

Size: 8×3 time-varying

position>direction

Unit vector, after Fraenz and Harper, PSS, 2002. ChanE timebase.

Look_Direction_08 0 – 7 (8 bins)

4.3.2.32 RTN_ChanF RTN flow direction ChanF

Size: 8×3 time-varying

position>direction

Unit vector, after Fraenz and Harper, PSS, 2002. ChanF timebase.

Look_Direction_08 0 – 7 (8 bins)

4.3.2.33 RTN_ChanG RTN flow direction ChanG

Size: 80×3 time-varying

position>direction

Unit vector, after Fraenz and Harper, PSS, 2002. ChanG timebase.

Look_Direction_80 0 – 79 (80 bins)

4.3.2.34 SA_ChanE Nominal Parker Spiral angle ChanE (degree)

Size: 8 time-varying

position>angle

Angle between particle direction and nominal outward Parker Spiral, based on 400km/s solar wind and corotation breakdown at 10Rs.

Look_Direction_08 0 – 7 (8 bins)

4.3.2.35 SA_ChanF Nominal Parker Spiral angle ChanF (degree)

Size: 8 time-varying

position>angle

Angle between particle direction and nominal outward Parker Spiral, based on 400km/s solar wind and corotation breakdown at 10Rs.

Look_Direction_08 0 – 7 (8 bins)

4.3.2.36 SA_ChanG Nominal Parker Spiral angle ChanG (degree)

Size: 80 time-varying

position>angle

Angle between particle direction and nominal outward Parker Spiral, based on 400km/s solar wind and corotation breakdown at 10Rs.

Look_Direction_80 0 – 79 (80 bins)

OTHER SUPPORT

4.3.3.1 Look_Direction_08_DELTAMINUS Size: 8 constant number

4.3.3.2 Look_Direction_08_DELTAPLUS Size: 8 constant number

4.3.3.3 Look_Direction_80_DELTAMINUS Size: 80 constant number

4.3.3.4 Look_Direction_80_DELTAPLUS Size: 80 constant number

PSP_ISOIS-EPIHI_L2-HET-RATES10

ISOIS-EPIHI>Integrated Science Investigation of the Sun, Energetic Particle Instrument Hi L2-HET-rates10>Level 2 HET 10-second rates

EPI-Hi 10 second rates cdf. Time tags indicate midpoint of integration.

Instrument paper: Integrated Science Investigation of the Sun (ISIS): Design of the Energetic Particle Investigation. McComas, D. J. et al (2016). Space Sci. Rev., doi:10.1007/s11214-014-0059-1

1 minute to 1 hour

Cite McComas et al (2016), doi:10.1007/s11214-014-0059-1

PRIMARY VARIABLES

4.4.1.1 A_H_Flux H flux side A ($\text{cm}^{-2}\text{sr}^{-1}\text{sec}^{-1}\text{MeV}^{-1}$)

Size: 13 time-varying

particle_flux>differential_directional_number

Energy Bins for H 9 – 70 MeV (13 bins)

4.4.1.2 A_He_Flux He flux side A ($\text{cm}^{-2}\text{sr}^{-1}\text{sec}^{-1}(\text{MeV}/\text{nuc})^{-1}$)

Size: 14 time-varying

particle_flux>differential_directional_number

Energy Bins for He 9 – 83 MeV/nuc (14 bins)

4.4.1.3 B_H_Flux H flux side B ($\text{cm}^{-2}\text{sr}^{-1}\text{sec}^{-1}\text{MeV}^{-1}$)

Size: 13 time-varying

particle_flux>differential_directional_number

Energy Bins for H 9 – 70 MeV (13 bins)

4.4.1.4 B_He_Flux He flux side B ($\text{cm}^{-2}\text{sr}^{-1}\text{sec}^{-1}(\text{MeV}/\text{nuc})^{-1}$)

Size: 14 time-varying

particle_flux>differential_directional_number

Energy Bins for He 9 – 83 MeV/nuc (14 bins)

OTHER DATA

4.4.2.1 A_Electrons_Rate Electrons count rate side A (counts s^{-1})

Size: 18 time-varying

particle_flux>differential_directional_number_rate

Energy Bins for Electrons 1 – 10 MeV (18 bins)

4.4.2.2 A_H_Rate H count rate side A (counts s^{-1})

Size: 13 time-varying

particle_flux>differential_directional_number_rate

Energy Bins for H 9 – 70 MeV (13 bins)

4.4.2.3 A_He_Rate He count rate side A (counts s⁻¹)

Size: 14 time-varying

particle_flux>differential_directional_number_rate

Energy Bins for He 9 – 83 MeV/nuc (14 bins)

4.4.2.4 B_Electrons_Rate Electrons count rate side B (counts s⁻¹)

Size: 18 time-varying

particle_flux>differential_directional_number_rate

Energy Bins for Electrons 1 – 10 MeV (18 bins)

4.4.2.5 B_H_Rate H count rate side B (counts s⁻¹)

Size: 13 time-varying

particle_flux>differential_directional_number_rate

Energy Bins for H 9 – 70 MeV (13 bins)

4.4.2.6 B_He_Rate He count rate side B (counts s⁻¹)

Size: 14 time-varying

particle_flux>differential_directional_number_rate

Energy Bins for He 9 – 83 MeV/nuc (14 bins)

4.4.2.7 HCI_Lat HCI latitude (degrees)

time-varying

position>latitude

At timestamp. After Fraenz and Harper, PSS, 2002.

4.4.2.8 HCI_Lon HCI longitude (degrees)

time-varying

position>longitude

At timestamp. After Fraenz and Harper, PSS, 2002.

4.4.2.9 HCI_R Heliocentric distance (AU)

time-varying

position>radial

At timestamp. After Fraenz and Harper, PSS, 2002.

4.4.2.10 HET_A_HCI HCI flow direction HETA

Size: 3 time-varying

position>direction

Unit vector, after Fraenz and Harper, PSS, 2002.

4.4.2.11 HET_A_PA Pitch angle HETA (degree)

time-varying

position>angle

4.4.2.12 HET_A_RTN RTN flow direction HETA

Size: 3 time-varying

position>direction

Unit vector, after Fraenz and Harper, PSS, 2002.

4.4.2.13 HET_A_SA Nominal Parker Spiral angle HETA (degree)

time-varying

position>angle

Angle between particle direction and nominal outward Parker Spiral, based on 400km/s solar wind and corotation breakdown at 10Rs.

4.4.2.14 HET_B_HCI HCI flow direction HETB

Size: 3 time-varying

position>direction

Unit vector, after Fraenz and Harper, PSS, 2002.

4.4.2.15 HET_B_PA Pitch angle HETB (degree)

time-varying

position>angle

4.4.2.16 HET_B_RTN RTN flow direction HETB

Size: 3 time-varying

position>direction

Unit vector, after Fraenz and Harper, PSS, 2002.

4.4.2.17 HET_B_SA Nominal Parker Spiral angle HETB (degree)

time-varying

position>angle

Angle between particle direction and nominal outward Parker Spiral, based on 400km/s solar wind and corotation breakdown at 10Rs.

4.4.2.18 HGC_Lat HGC latitude (degrees)

time-varying

position>latitude

At timestamp. After Fraenz and Harper, PSS, 2002.

4.4.2.19 HGC_Lon HGC longitude (degrees)

time-varying

position>longitude

At timestamp. After Fraenz and Harper, PSS, 2002.

4.4.2.20 HGC_R Heliocentric distance (AU)

time-varying

position>radial

At timestamp. After Fraenz and Harper, PSS, 2002.

OTHER SUPPORT

PSP_ISOIS-EPIHI_L2-HET-RATES300

ISOIS-EPIHI>Integrated Science Investigation of the Sun, Energetic Particle Instrument Hi

L2-HET-rates300>Level 2 HET 5-minute rates

EPI-Hi HET 300 second rates cdf. Time tags indicate midpoint of integration.

Instrument paper: Integrated Science Investigation of the Sun (ISIS): Design of the Energetic Particle Investigation. McComas, D. J. et al (2016). Space Sci. Rev., doi:10.1007/s11214-014-0059-1

1 minute to 1 hour

Cite McComas et al (2016), doi:10.1007/s11214-014-0059-1

PRIMARY VARIABLES

OTHER DATA

4.5.2.1 A_CNO_SECT_Rate CNO sector count rate side A (counts s⁻¹)

Size: 2 × 25 time-varying

particle_flux>differential_directional_number_rate
Energy Bins for CNO SECT 35 – 64 MeV/nuc (2 bins)
HET_R17_SECTORS 0 – 24 (25 bins)

4.5.2.2 A_FeGroup_SECT_Rate FeGroup sectored count rate side A (counts s⁻¹)

Size: 1 × 25 time-varying

particle_flux>differential_directional_number_rate
Energy Bins for FeGroup SECT 76 – 76 MeV/nuc (1 bins)
HET_R17_SECTORS 0 – 24 (25 bins)

4.5.2.3 A_NetoSi_SECT_Rate NetoSi sectored count rate side A (counts s⁻¹)

Size: 1 × 25 time-varying

particle_flux>differential_directional_number_rate
Energy Bins for NetoSi SECT 54 – 54 MeV/nuc (1 bins)
HET_R17_SECTORS 0 – 24 (25 bins)

4.5.2.4 B_CNO_SECT_Rate CNO sectored count rate side B (counts s⁻¹)

Size: 2 × 25 time-varying

particle_flux>differential_directional_number_rate
Energy Bins for CNO SECT 35 – 64 MeV/nuc (2 bins)
HET_R17_SECTORS 0 – 24 (25 bins)

4.5.2.5 B_FeGroup_SECT_Rate FeGroup sectored count rate side B (counts s⁻¹)

Size: 1 × 25 time-varying

particle_flux>differential_directional_number_rate
Energy Bins for FeGroup SECT 76 – 76 MeV/nuc (1 bins)
HET_R17_SECTORS 0 – 24 (25 bins)

4.5.2.6 B_NetoSi_SECT_Rate NetoSi sectored count rate side B (counts s⁻¹)

Size: 1 × 25 time-varying

particle_flux>differential_directional_number_rate
Energy Bins for NetoSi SECT 54 – 54 MeV/nuc (1 bins)
HET_R17_SECTORS 0 – 24 (25 bins)

4.5.2.7 HCI_Lat HCI latitude (degrees)

time-varying

position>latitude

At timestamp. After Fraenz and Harper, PSS, 2002.

4.5.2.8 HCI_Lon HCI longitude (degrees)

time-varying

position>longitude

At timestamp. After Fraenz and Harper, PSS, 2002.

4.5.2.9 HCI_R Heliocentric distance (AU)

time-varying

position>radial

At timestamp. After Fraenz and Harper, PSS, 2002.

4.5.2.10 HET_A_HCI HCI flow direction HETA

Size: 3 time-varying

position>direction

Unit vector, after Fraenz and Harper, PSS, 2002.

4.5.2.11 HET_A_PA Pitch angle HETA (degree)

time-varying

position>angle

4.5.2.12 HET_A_R17_SECT_HCI HCI flow direction HETAR17SECT

Size: 25 × 3 time-varying

position>direction

Unit vector, after Fraenz and Harper, PSS, 2002.

HET_R17_SECTORS 0 – 24 (25 bins)

4.5.2.13 HET_A_R17_SECT_PA Pitch angle HETAR17SECT (degree)

Size: 25 time-varying

position>angle

HET_R17_SECTORS 0 – 24 (25 bins)

4.5.2.14 HET_A_R17_SECT_RTN RTN flow direction HETAR17SECT

Size: 25 × 3 time-varying

position>direction

Unit vector, after Fraenz and Harper, PSS, 2002.

HET_R17_SECTORS 0 – 24 (25 bins)

4.5.2.15 HET_A_R17_SECT_SA Nominal Parker Spiral angle HETAR17SECT (degree)

Size: 25 time-varying

position>angle

Angle between particle direction and nominal outward Parker Spiral, based on 400km/s solar wind and corotation breakdown at 10Rs.

HET_R17_SECTORS 0 – 24 (25 bins)

4.5.2.16 HET_A_RTN RTN flow direction HETA

Size: 3 time-varying

position>direction

Unit vector, after Fraenz and Harper, PSS, 2002.

4.5.2.17 HET_A_SA Nominal Parker Spiral angle HETA (degree)

time-varying

position>angle

Angle between particle direction and nominal outward Parker Spiral, based on 400km/s solar wind and corotation breakdown at 10Rs.

4.5.2.18 HET_B_HCI HCI flow direction HETB

Size: 3 time-varying

position>direction

Unit vector, after Fraenz and Harper, PSS, 2002.

4.5.2.19 HET_B_PA Pitch angle HETB (degree)

time-varying

position>angle

4.5.2.20 HET_B_R17_SECT_HCI HCI flow direction HETBR17SECT

Size: 25 × 3 time-varying

position>direction

Unit vector, after Fraenz and Harper, PSS, 2002.
HET_R17_SECTORS 0 – 24 (25 bins)

4.5.2.21 HET_B_R17_SECT_PA Pitch angle HETBR17SECT (degree)
Size: 25 time-varying
position>angle
HET_R17_SECTORS 0 – 24 (25 bins)

4.5.2.22 HET_B_R17_SECT_RTN RTN flow direction HETBR17SECT
Size: 25 × 3 time-varying
position>direction
Unit vector, after Fraenz and Harper, PSS, 2002.
HET_R17_SECTORS 0 – 24 (25 bins)

4.5.2.23 HET_B_R17_SECT_SA Nominal Parker Spiral angle HETBR17SECT (degree)
Size: 25 time-varying
position>angle
Angle between particle direction and nominal outward Parker Spiral, based on 400km/s solar wind and corotation breakdown at 10Rs.
HET_R17_SECTORS 0 – 24 (25 bins)

4.5.2.24 HET_B_RTN RTN flow direction HETB
Size: 3 time-varying
position>direction
Unit vector, after Fraenz and Harper, PSS, 2002.

4.5.2.25 HET_B_SA Nominal Parker Spiral angle HETB (degree)
time-varying
position>angle
Angle between particle direction and nominal outward Parker Spiral, based on 400km/s solar wind and corotation breakdown at 10Rs.

4.5.2.26 HGC_Lat HGC latitude (degrees)
time-varying
position>latitude

At timestamp. After Fraenz and Harper, PSS, 2002.

4.5.2.27 HGC_Lon HGC longitude (degrees)

time-varying

position>longitude

At timestamp. After Fraenz and Harper, PSS, 2002.

4.5.2.28 HGC_R Heliocentric distance (AU)

time-varying

position>radial

At timestamp. After Fraenz and Harper, PSS, 2002.

OTHER SUPPORT

PSP_ISOIS-EPIHI_L2-HET-RATES3600

ISOIS-EPIHI>Integrated Science Investigation of the Sun, Energetic Particle Instrument Hi

L2-HET-rates3600>Level 2 HET hourly rates

EPI-Hi HET 3600 second rates cdf. Time tags indicate midpoint of integration.

Instrument paper: Integrated Science Investigation of the Sun (ISIS): Design of the Energetic Particle Investigation. McComas, D. J. et al (2016). Space Sci. Rev., doi:10.1007/s11214-014-0059-1

1 minute to 1 hour

Cite McComas et al (2016), doi:10.1007/s11214-014-0059-1

PRIMARY VARIABLES

4.6.1.1 A_H_Flux H flux side A ($\text{cm}^{-2}\text{sr}^{-1}\text{sec}^{-1}\text{MeV}^{-1}$)

Size: 15 time-varying

particle_flux>differential_directional_number

Energy Bins for H 7 – 83 MeV (15 bins)

4.6.1.2 A_H_SECT_Flux H sectored flux side A ($\text{cm}^{-2}\text{sr}^{-1}\text{sec}^{-1}\text{MeV}^{-1}$)

Size: 2×25 time-varying

particle_flux>differential_directional_number

Energy Bins for H SECT 17 – 32 MeV (2 bins)

HET_R17_SECTORS 0 – 24 (25 bins)

4.6.1.3 A_He_Flux He flux side A ($\text{cm}^{-2}\text{sr}^{-1}\text{sec}^{-1}(\text{MeV}/\text{nuc})^{-1}$)

Size: 16 time-varying

particle_flux>differential_directional_number

Energy Bins for He 7 – 99 MeV/nuc (16 bins)

4.6.1.4 A_He_SECT_Flux He sectored flux side A ($\text{cm}^{-2}\text{sr}^{-1}\text{sec}^{-1}(\text{MeV}/\text{nuc})^{-1}$)

Size: 2×25 time-varying

particle_flux>differential_directional_number

Energy Bins for He SECT 17 – 32 MeV/nuc (2 bins)

HET_R17_SECTORS 0 – 24 (25 bins)

4.6.1.5 B_H_Flux H flux side B ($\text{cm}^{-2}\text{sr}^{-1}\text{sec}^{-1}\text{MeV}^{-1}$)

Size: 15 time-varying

particle_flux>differential_directional_number

Energy Bins for H 7 – 83 MeV (15 bins)

4.6.1.6 B_H_SECT_Flux H sectored flux side B ($\text{cm}^{-2}\text{sr}^{-1}\text{sec}^{-1}\text{MeV}^{-1}$)

Size: 2×25 time-varying

particle_flux>differential_directional_number

Energy Bins for H SECT 17 – 32 MeV (2 bins)

HET_R17_SECTORS 0 – 24 (25 bins)

4.6.1.7 B_He_Flux He flux side B ($\text{cm}^{-2}\text{sr}^{-1}\text{sec}^{-1}(\text{MeV}/\text{nuc})^{-1}$)

Size: 16 time-varying

particle_flux>differential_directional_number

Energy Bins for He 7 – 99 MeV/nuc (16 bins)

4.6.1.8 B_He_SECT_Flux He sectored flux side B ($\text{cm}^{-2}\text{sr}^{-1}\text{sec}^{-1}(\text{MeV}/\text{nuc})^{-1}$)

Size: 2×25 time-varying

particle_flux>differential_directional_number

Energy Bins for He SECT 17 – 32 MeV/nuc (2 bins)

HET_R17_SECTORS 0 – 24 (25 bins)

OTHER DATA

4.6.2.1 A_Al_Rate Al count rate side A (counts s^{-1})

Size: 15 time-varying

particle_flux>differential_directional_number_rate
Energy Bins for Al 21 – 235 MeV/nuc (15 bins)

4.6.2.2 A_Ar_Rate Ar count rate side A (counts s⁻¹)

Size: 15 time-varying

particle_flux>differential_directional_number_rate
Energy Bins for Ar 25 – 279 MeV/nuc (15 bins)

4.6.2.3 A_CNO_SECT_Rate CNO sectored count rate side A (counts s⁻¹)

Size: 2 × 25 time-varying

particle_flux>differential_directional_number_rate
Energy Bins for CNO SECT 35 – 64 MeV/nuc (2 bins)
HET_R17_SECTORS 0 – 24 (25 bins)

4.6.2.4 A_C_Rate C count rate side A (counts s⁻¹)

Size: 15 time-varying

particle_flux>differential_directional_number_rate
Energy Bins for C 12 – 140 MeV/nuc (15 bins)

4.6.2.5 A_Ca_Rate Ca count rate side A (counts s⁻¹)

Size: 15 time-varying

particle_flux>differential_directional_number_rate
Energy Bins for Ca 25 – 279 MeV/nuc (15 bins)

4.6.2.6 A_Cr_Rate Cr count rate side A (counts s⁻¹)

Size: 16 time-varying

particle_flux>differential_directional_number_rate
Energy Bins for Cr 25 – 332 MeV/nuc (16 bins)

4.6.2.7 A_Electrons_Rate Electrons count rate side A (counts s⁻¹)

Size: 19 time-varying

particle_flux>differential_directional_number_rate
Energy Bins for Electrons 0 – 10 MeV (19 bins)

4.6.2.8 A_Electrons_SECT_Rate Electrons sectored count rate side A (counts s⁻¹)

Size: 2 × 25 time-varying

particle_flux>differential_directional_number_rate

Energy Bins for Electrons SECT 1 – 3 MeV (2 bins)

HET_R17_SECTORS 0 – 24 (25 bins)

4.6.2.9 A_FeGroup_SECT_Rate FeGroup sectored count rate side A (counts s⁻¹)

Size: 1 × 25 time-varying

particle_flux>differential_directional_number_rate

Energy Bins for FeGroup SECT 76 – 76 MeV/nuc (1 bins)

HET_R17_SECTORS 0 – 24 (25 bins)

4.6.2.10 A_Fe_Rate Fe count rate side A (counts s⁻¹)

Size: 15 time-varying

particle_flux>differential_directional_number_rate

Energy Bins for Fe 29 – 332 MeV/nuc (15 bins)

4.6.2.11 A_H_Rate H count rate side A (counts s⁻¹)

Size: 15 time-varying

particle_flux>differential_directional_number_rate

Energy Bins for H 7 – 83 MeV (15 bins)

4.6.2.12 A_H_SECT_Rate H sectored count rate side A (counts s⁻¹)

Size: 2 × 25 time-varying

particle_flux>differential_directional_number_rate

Energy Bins for H SECT 17 – 32 MeV (2 bins)

HET_R17_SECTORS 0 – 24 (25 bins)

4.6.2.13 A_He_Rate He count rate side A (counts s⁻¹)

Size: 16 time-varying

particle_flux>differential_directional_number_rate

Energy Bins for He 7 – 99 MeV/nuc (16 bins)

4.6.2.14 A_He_SECT_Rate He sectored count rate side A (counts s⁻¹)

Size: 2 × 25 time-varying

particle_flux>differential_directional_number_rate

Energy Bins for He SECT 17 – 32 MeV/nuc (2 bins)
HET_R17_SECTORS 0 – 24 (25 bins)

4.6.2.15 A_Mg_Rate Mg count rate side A (counts s⁻¹)
Size: 15 time-varying
particle_flux>differential_directional_number_rate
Energy Bins for Mg 21 – 235 MeV/nuc (15 bins)

4.6.2.16 A_N_Rate N count rate side A (counts s⁻¹)
Size: 15 time-varying
particle_flux>differential_directional_number_rate
Energy Bins for N 12 – 140 MeV/nuc (15 bins)

4.6.2.17 A_Na_Rate Na count rate side A (counts s⁻¹)
Size: 15 time-varying
particle_flux>differential_directional_number_rate
Energy Bins for Na 17 – 197 MeV/nuc (15 bins)

4.6.2.18 A_Ne_Rate Ne count rate side A (counts s⁻¹)
Size: 15 time-varying
particle_flux>differential_directional_number_rate
Energy Bins for Ne 17 – 197 MeV/nuc (15 bins)

4.6.2.19 A_NetoSi_SECT_Rate NetoS_i sectored count rate side A (counts s⁻¹)
Size: 1 × 25 time-varying
particle_flux>differential_directional_number_rate
Energy Bins for NetoS_i SECT 54 – 54 MeV/nuc (1 bins)
HET_R17_SECTORS 0 – 24 (25 bins)

4.6.2.20 A_Ni_Rate Ni count rate side A (counts s⁻¹)
Size: 15 time-varying
particle_flux>differential_directional_number_rate
Energy Bins for Ni 29 – 332 MeV/nuc (15 bins)

4.6.2.21 A_O_Rate O count rate side A (counts s⁻¹)

Size: 15 time-varying

particle_flux>differential_directional_number_rate

Energy Bins for O 15 – 166 MeV/nuc (15 bins)

4.6.2.22 A_S_Rate S count rate side A (counts s⁻¹)

Size: 16 time-varying

particle_flux>differential_directional_number_rate

Energy Bins for S 21 – 279 MeV/nuc (16 bins)

4.6.2.23 A_Si_Rate Si count rate side A (counts s⁻¹)

Size: 15 time-varying

particle_flux>differential_directional_number_rate

Energy Bins for Si 21 – 235 MeV/nuc (15 bins)

4.6.2.24 B_Al_Rate Al count rate side B (counts s⁻¹)

Size: 15 time-varying

particle_flux>differential_directional_number_rate

Energy Bins for Al 21 – 235 MeV/nuc (15 bins)

4.6.2.25 B_Ar_Rate Ar count rate side B (counts s⁻¹)

Size: 15 time-varying

particle_flux>differential_directional_number_rate

Energy Bins for Ar 25 – 279 MeV/nuc (15 bins)

4.6.2.26 B_CNO_SECT_Rate CNO sectored count rate side B (counts s⁻¹)

Size: 2 × 25 time-varying

particle_flux>differential_directional_number_rate

Energy Bins for CNO SECT 35 – 64 MeV/nuc (2 bins)

HET_R17_SECTORS 0 – 24 (25 bins)

4.6.2.27 B_C_Rate C count rate side B (counts s⁻¹)

Size: 15 time-varying

particle_flux>differential_directional_number_rate

Energy Bins for C 12 – 140 MeV/nuc (15 bins)

4.6.2.28 B_Ca_Rate Ca count rate side B (counts s⁻¹)

Size: 15 time-varying

particle_flux>differential_directional_number_rate

Energy Bins for Ca 25 – 279 MeV/nuc (15 bins)

4.6.2.29 B_Cr_Rate Cr count rate side B (counts s⁻¹)

Size: 16 time-varying

particle_flux>differential_directional_number_rate

Energy Bins for Cr 25 – 332 MeV/nuc (16 bins)

4.6.2.30 B_Electrons_Rate Electrons count rate side B (counts s⁻¹)

Size: 19 time-varying

particle_flux>differential_directional_number_rate

Energy Bins for Electrons 0 – 10 MeV (19 bins)

4.6.2.31 B_Electrons_SECT_Rate Electrons sectored count rate side B (counts s⁻¹)

Size: 2 × 25 time-varying

particle_flux>differential_directional_number_rate

Energy Bins for Electrons SECT 1 – 3 MeV (2 bins)

HET_R17_SECTORS 0 – 24 (25 bins)

4.6.2.32 B_FeGroup_SECT_Rate FeGroup sectored count rate side B (counts s⁻¹)

Size: 1 × 25 time-varying

particle_flux>differential_directional_number_rate

Energy Bins for FeGroup SECT 76 – 76 MeV/nuc (1 bins)

HET_R17_SECTORS 0 – 24 (25 bins)

4.6.2.33 B_Fe_Rate Fe count rate side B (counts s⁻¹)

Size: 15 time-varying

particle_flux>differential_directional_number_rate

Energy Bins for Fe 29 – 332 MeV/nuc (15 bins)

4.6.2.34 B_H_Rate H count rate side B (counts s⁻¹)

Size: 15 time-varying

particle_flux>differential_directional_number_rate

Energy Bins for H 7 – 83 MeV (15 bins)

4.6.2.35 B_H_SECT_Rate H sectored count rate side B (counts s⁻¹)

Size: 2 × 25 time-varying

particle_flux>differential_directional_number_rate

Energy Bins for H SECT 17 – 32 MeV (2 bins)

HET_R17_SECTORS 0 – 24 (25 bins)

4.6.2.36 B_He_Rate He count rate side B (counts s⁻¹)

Size: 16 time-varying

particle_flux>differential_directional_number_rate

Energy Bins for He 7 – 99 MeV/nuc (16 bins)

4.6.2.37 B_He_SECT_Rate He sectored count rate side B (counts s⁻¹)

Size: 2 × 25 time-varying

particle_flux>differential_directional_number_rate

Energy Bins for He SECT 17 – 32 MeV/nuc (2 bins)

HET_R17_SECTORS 0 – 24 (25 bins)

4.6.2.38 B_Mg_Rate Mg count rate side B (counts s⁻¹)

Size: 15 time-varying

particle_flux>differential_directional_number_rate

Energy Bins for Mg 21 – 235 MeV/nuc (15 bins)

4.6.2.39 B_N_Rate N count rate side B (counts s⁻¹)

Size: 15 time-varying

particle_flux>differential_directional_number_rate

Energy Bins for N 12 – 140 MeV/nuc (15 bins)

4.6.2.40 B_Na_Rate Na count rate side B (counts s⁻¹)

Size: 15 time-varying

particle_flux>differential_directional_number_rate

Energy Bins for Na 17 – 197 MeV/nuc (15 bins)

4.6.2.41 B_Ne_Rate Ne count rate side B (counts s⁻¹)

Size: 15 time-varying

particle_flux>differential_directional_number_rate

Energy Bins for Ne 17 – 197 MeV/nuc (15 bins)

4.6.2.42 B_NetoSi_SECT_Rate NetoSi sectored count rate side B (counts s⁻¹)

Size: 1 × 25 time-varying

particle_flux>differential_directional_number_rate

Energy Bins for NetoSi SECT 54 – 54 MeV/nuc (1 bins)

HET_R17_SECTORS 0 – 24 (25 bins)

4.6.2.43 B_Ni_Rate Ni count rate side B (counts s⁻¹)

Size: 15 time-varying

particle_flux>differential_directional_number_rate

Energy Bins for Ni 29 – 332 MeV/nuc (15 bins)

4.6.2.44 B_O_Rate O count rate side B (counts s⁻¹)

Size: 15 time-varying

particle_flux>differential_directional_number_rate

Energy Bins for O 15 – 166 MeV/nuc (15 bins)

4.6.2.45 B_S_Rate S count rate side B (counts s⁻¹)

Size: 16 time-varying

particle_flux>differential_directional_number_rate

Energy Bins for S 21 – 279 MeV/nuc (16 bins)

4.6.2.46 B_Si_Rate Si count rate side B (counts s⁻¹)

Size: 15 time-varying

particle_flux>differential_directional_number_rate

Energy Bins for Si 21 – 235 MeV/nuc (15 bins)

4.6.2.47 HCI_Lat HCI latitude (degrees)

time-varying

position>latitude

At timestamp. After Fraenz and Harper, PSS, 2002.

4.6.2.48 HCI_Lon HCI longitude (degrees)
time-varying
position>longitude
At timestamp. After Fraenz and Harper, PSS, 2002.

4.6.2.49 HCI_R Heliocentric distance (AU)
time-varying
position>radial
At timestamp. After Fraenz and Harper, PSS, 2002.

4.6.2.50 HET_A_HCI HCI flow direction HETA
Size: 3 time-varying
position>direction
Unit vector, after Fraenz and Harper, PSS, 2002.

4.6.2.51 HET_A_PA Pitch angle HETA (degree)
time-varying
position>angle

4.6.2.52 HET_A_R17_SECT_HCI HCI flow direction HETAR17SECT
Size: 25 × 3 time-varying
position>direction
Unit vector, after Fraenz and Harper, PSS, 2002.
HET_R17_SECTORS 0 – 24 (25 bins)

4.6.2.53 HET_A_R17_SECT_PA Pitch angle HETAR17SECT (degree)
Size: 25 time-varying
position>angle
HET_R17_SECTORS 0 – 24 (25 bins)

4.6.2.54 HET_A_R17_SECT_RTN RTN flow direction HETAR17SECT
Size: 25 × 3 time-varying
position>direction
Unit vector, after Fraenz and Harper, PSS, 2002.
HET_R17_SECTORS 0 – 24 (25 bins)

4.6.2.55 HET_A_R17_SECT_SA Nominal Parker Spiral angle HETAR17SECT (degree)

Size: 25 time-varying

position>angle

Angle between particle direction and nominal outward Parker Spiral, based on 400km/s solar wind and corotation breakdown at 10Rs.

HET_R17_SECTORS 0 – 24 (25 bins)

4.6.2.56 HET_A_RTN RTN flow direction HETA

Size: 3 time-varying

position>direction

Unit vector, after Fraenz and Harper, PSS, 2002.

4.6.2.57 HET_A_SA Nominal Parker Spiral angle HETA (degree)

time-varying

position>angle

Angle between particle direction and nominal outward Parker Spiral, based on 400km/s solar wind and corotation breakdown at 10Rs.

4.6.2.58 HET_B_HCI HCI flow direction HETB

Size: 3 time-varying

position>direction

Unit vector, after Fraenz and Harper, PSS, 2002.

4.6.2.59 HET_B_PA Pitch angle HETB (degree)

time-varying

position>angle

4.6.2.60 HET_B_R17_SECT_HCI HCI flow direction HETBR17SECT

Size: 25 × 3 time-varying

position>direction

Unit vector, after Fraenz and Harper, PSS, 2002.

HET_R17_SECTORS 0 – 24 (25 bins)

4.6.2.61 HET_B_R17_SECT_PA Pitch angle HETBR17SECT (degree)

Size: 25 time-varying

position>angle

HET_R17_SECTORS 0 – 24 (25 bins)

4.6.2.62 HET_B_R17_SECT_RTN RTN flow direction HETBR17SECT

Size: 25 × 3 time-varying

position>direction

Unit vector, after Fraenz and Harper, PSS, 2002.

HET_R17_SECTORS 0 – 24 (25 bins)

4.6.2.63 HET_B_R17_SECT_SA Nominal Parker Spiral angle HETBR17SECT (degree)

Size: 25 time-varying

position>angle

Angle between particle direction and nominal outward Parker Spiral, based on 400km/s solar wind and corotation breakdown at 10Rs.

HET_R17_SECTORS 0 – 24 (25 bins)

4.6.2.64 HET_B_RTN RTN flow direction HETB

Size: 3 time-varying

position>direction

Unit vector, after Fraenz and Harper, PSS, 2002.

4.6.2.65 HET_B_SA Nominal Parker Spiral angle HETB (degree)

time-varying

position>angle

Angle between particle direction and nominal outward Parker Spiral, based on 400km/s solar wind and corotation breakdown at 10Rs.

4.6.2.66 HGC_Lat HGC latitude (degrees)

time-varying

position>latitude

At timestamp. After Fraenz and Harper, PSS, 2002.

4.6.2.67 HGC_Lon HGC longitude (degrees)

time-varying

position>longitude

At timestamp. After Fraenz and Harper, PSS, 2002.

4.6.2.68 HGC_R Heliocentric distance (AU)

time-varying

position>radial

At timestamp. After Fraenz and Harper, PSS, 2002.

4.6.2.69 R1A_He_BIN R1A He Rates (counts)

Size: 5×16 time-varying

particle_flux>differential_directional_number_rate

Energy Bins for R1 He BIN 9 – 32 MeV/nuc (5 bins)

R1A_He_BIN_MASS_BIN 0 – 15 segment (16 bins)

4.6.2.70 R1A_Ne_BIN R1A Ne Rates (counts)

Size: 4×8 time-varying

particle_flux>differential_directional_number_rate

Energy Bins for R1 Ne BIN 23 – 64 MeV/nuc (4 bins)

R1A_Ne_BIN_MASS_BIN 0 – 7 segment (8 bins)

4.6.2.71 R1B_He_BIN R1B He Rates (counts)

Size: 5×16 time-varying

particle_flux>differential_directional_number_rate

Energy Bins for R1 He BIN 9 – 32 MeV/nuc (5 bins)

R1B_He_BIN_MASS_BIN 0 – 15 segment (16 bins)

4.6.2.72 R1B_Ne_BIN R1B Ne Rates (counts)

Size: 4×8 time-varying

particle_flux>differential_directional_number_rate

Energy Bins for R1 Ne BIN 23 – 64 MeV/nuc (4 bins)

R1B_Ne_BIN_MASS_BIN 0 – 7 segment (8 bins)

4.6.2.73 R2A_He_BIN R2A He Rates (counts)

Size: 4×16 time-varying

particle_flux>differential_directional_number_rate

Energy Bins for R2 He BIN 16 – 45 MeV/nuc (4 bins)

R2A_He_BIN_MASS_BIN 0 – 15 segment (16 bins)

4.6.2.74 R2A_Ne_BIN R2A Ne Rates (counts)

Size: 4×8 time-varying

particle_flux>differential_directional_number_rate

Energy Bins for R2 Ne BIN 32 – 91 MeV/nuc (4 bins)

R2A_Ne_BIN_MASS_BIN 0 – 7 segment (8 bins)

4.6.2.75 R2B_He_BIN R2B He Rates (counts)

Size: 4×16 time-varying

particle_flux>differential_directional_number_rate

Energy Bins for R2 He BIN 16 – 45 MeV/nuc (4 bins)

R2B_He_BIN_MASS_BIN 0 – 15 segment (16 bins)

4.6.2.76 R2B_Ne_BIN R2B Ne Rates (counts)

Size: 4×8 time-varying

particle_flux>differential_directional_number_rate

Energy Bins for R2 Ne BIN 32 – 91 MeV/nuc (4 bins)

R2B_Ne_BIN_MASS_BIN 0 – 7 segment (8 bins)

4.6.2.77 R3A_He_BIN R3A He Rates (counts)

Size: 4×16 time-varying

particle_flux>differential_directional_number_rate

Energy Bins for R3 He BIN 23 – 64 MeV/nuc (4 bins)

R3A_He_BIN_MASS_BIN 0 – 15 segment (16 bins)

4.6.2.78 R3A_Ne_BIN R3A Ne Rates (counts)

Size: 4×8 time-varying

particle_flux>differential_directional_number_rate

Energy Bins for R3 Ne BIN 45 – 128 MeV/nuc (4 bins)

R3A_Ne_BIN_MASS_BIN 0 – 7 segment (8 bins)

4.6.2.79 R3B_He_BIN R3B He Rates (counts)

Size: 4×16 time-varying

particle_flux>differential_directional_number_rate

Energy Bins for R3 He BIN 23 – 64 MeV/nuc (4 bins)

R3B_He_BIN_MASS_BIN 0 – 15 segment (16 bins)

4.6.2.80 R3B_Ne_BIN R3B Ne Rates (counts)

Size: 4×8 time-varying

particle_flux>differential_directional_number_rate

Energy Bins for R3 Ne BIN 45 – 128 MeV/nuc (4 bins)

R3B_Ne_BIN_MASS_BIN 0 – 7 segment (8 bins)

4.6.2.81 R4A_He_BIN R4A He Rates (counts)

Size: 3×16 time-varying

particle_flux>differential_directional_number_rate

Energy Bins for R4 He BIN 32 – 64 MeV/nuc (3 bins)

R4A_He_BIN_MASS_BIN 0 – 15 segment (16 bins)

4.6.2.82 R4A_Ne_BIN R4A Ne Rates (counts)

Size: 3×8 time-varying

particle_flux>differential_directional_number_rate

Energy Bins for R4 Ne BIN 64 – 128 MeV/nuc (3 bins)

R4A_Ne_BIN_MASS_BIN 0 – 7 segment (8 bins)

4.6.2.83 R4B_He_BIN R4B He Rates (counts)

Size: 3×16 time-varying

particle_flux>differential_directional_number_rate

Energy Bins for R4 He BIN 32 – 64 MeV/nuc (3 bins)

R4B_He_BIN_MASS_BIN 0 – 15 segment (16 bins)

4.6.2.84 R4B_Ne_BIN R4B Ne Rates (counts)

Size: 3×8 time-varying

particle_flux>differential_directional_number_rate

Energy Bins for R4 Ne BIN 64 – 128 MeV/nuc (3 bins)

R4B_Ne_BIN_MASS_BIN 0 – 7 segment (8 bins)

4.6.2.85 R5A_He_BIN R5A He Rates (counts)

Size: 3×16 time-varying

particle_flux>differential_directional_number_rate

Energy Bins for R5 He BIN 32 – 64 MeV/nuc (3 bins)

R5A_He_BIN_MASS_BIN 0 – 15 segment (16 bins)

4.6.2.86 R5A_Ne_BIN R5A Ne Rates (counts)

Size: 2×8 time-varying

particle_flux>differential_directional_number_rate

Energy Bins for R5 Ne BIN 91 – 128 MeV/nuc (2 bins)

R5A_Ne_BIN_MASS_BIN 0 – 7 segment (8 bins)

4.6.2.87 R5B_He_BIN R5B He Rates (counts)

Size: 3×16 time-varying

particle_flux>differential_directional_number_rate

Energy Bins for R5 He BIN 32 – 64 MeV/nuc (3 bins)

R5B_He_BIN_MASS_BIN 0 – 15 segment (16 bins)

4.6.2.88 R5B_Ne_BIN R5B Ne Rates (counts)

Size: 2×8 time-varying

particle_flux>differential_directional_number_rate

Energy Bins for R5 Ne BIN 91 – 128 MeV/nuc (2 bins)

R5B_Ne_BIN_MASS_BIN 0 – 7 segment (8 bins)

4.6.2.89 R6A_He_BIN R6A He Rates (counts)

Size: 3×16 time-varying

particle_flux>differential_directional_number_rate

Energy Bins for R6 He BIN 32 – 64 MeV/nuc (3 bins)

R6A_He_BIN_MASS_BIN 0 – 15 segment (16 bins)

4.6.2.90 R6A_Ne_BIN R6A Ne Rates (counts)

Size: 3×8 time-varying

particle_flux>differential_directional_number_rate

Energy Bins for R6 Ne BIN 91 – 181 MeV/nuc (3 bins)

R6A_Ne_BIN_MASS_BIN 0 – 7 segment (8 bins)

4.6.2.91 R6B_He_BIN R6B He Rates (counts)

Size: 3×16 time-varying

particle_flux>differential_directional_number_rate

Energy Bins for R6 He BIN 32 – 64 MeV/nuc (3 bins)

R6B_He_BIN_MASS_BIN 0 – 15 segment (16 bins)

4.6.2.92 R6B_Ne_BIN R6B Ne Rates (counts)

Size: 3×8 time-varying

particle_flux>differential_directional_number_rate

Energy Bins for R6 Ne BIN 91 – 181 MeV/nuc (3 bins)

R6B_Ne_BIN_MASS_BIN 0 – 7 segment (8 bins)

4.6.2.93 R7A_He_BIN R7A He Rates (counts)

Size: 2×16 time-varying

particle_flux>differential_directional_number_rate

Energy Bins for R7 He BIN 45 – 64 MeV/nuc (2 bins)

R7A_He_BIN_MASS_BIN 0 – 15 segment (16 bins)

4.6.2.94 R7A_Ne_BIN R7A Ne Rates (counts)

Size: 3×8 time-varying

particle_flux>differential_directional_number_rate

Energy Bins for R7 Ne BIN 91 – 181 MeV/nuc (3 bins)

R7A_Ne_BIN_MASS_BIN 0 – 7 segment (8 bins)

4.6.2.95 R7B_He_BIN R7B He Rates (counts)

Size: 2×16 time-varying

particle_flux>differential_directional_number_rate

Energy Bins for R7 He BIN 45 – 64 MeV/nuc (2 bins)

R7B_He_BIN_MASS_BIN 0 – 15 segment (16 bins)

4.6.2.96 R7B_Ne_BIN R7B Ne Rates (counts)

Size: 3×8 time-varying

particle_flux>differential_directional_number_rate

Energy Bins for R7 Ne BIN 91 – 181 MeV/nuc (3 bins)

R7B_Ne_BIN_MASS_BIN 0 – 7 segment (8 bins)

OTHER SUPPORT

PSP_ISOIS-EPIHI_L2-HET-RATES60

ISOIS-EPIHI>Integrated Science Investigation of the Sun, Energetic Particle Instrument Hi

L2-HET-rates60>Level 2 HET 1-minute rates

EPI-Hi HET 60 second rates cdf. Time tags indicate midpoint of integration.

Instrument paper: Integrated Science Investigation of the Sun (ISIS): Design of the Energetic

Particle Investigation. McComas, D. J. et al (2016). Space Sci. Rev., doi:10.1007/s11214-014-0059-1

1 minute to 1 hour

Cite McComas et al (2016), doi:10.1007/s11214-014-0059-1

PRIMARY VARIABLES

4.7.1.1 A_H_Flux H flux side A ($\text{cm}^{-2}\text{sr}^{-1}\text{sec}^{-1}\text{MeV}^{-1}$)

Size: 15 time-varying

particle_flux>differential_directional_number

Energy Bins for H 7 – 83 MeV (15 bins)

4.7.1.2 A_H_SECT_Flux H sectored flux side A ($\text{cm}^{-2}\text{sr}^{-1}\text{sec}^{-1}\text{MeV}^{-1}$)

Size: 2×25 time-varying

particle_flux>differential_directional_number

Energy Bins for H SECT 17 – 32 MeV (2 bins)

HET_R17_SECTORS 0 – 24 (25 bins)

4.7.1.3 A_He_Flux He flux side A ($\text{cm}^{-2}\text{sr}^{-1}\text{sec}^{-1}(\text{MeV}/\text{nuc})^{-1}$)

Size: 16 time-varying

particle_flux>differential_directional_number

Energy Bins for He 7 – 99 MeV/nuc (16 bins)

4.7.1.4 A_He_SECT_Flux He sectored flux side A ($\text{cm}^{-2}\text{sr}^{-1}\text{sec}^{-1}(\text{MeV}/\text{nuc})^{-1}$)

Size: 2×25 time-varying

particle_flux>differential_directional_number

Energy Bins for He SECT 17 – 32 MeV/nuc (2 bins)

HET_R17_SECTORS 0 – 24 (25 bins)

4.7.1.5 B_H_Flux H flux side B ($\text{cm}^{-2}\text{sr}^{-1}\text{sec}^{-1}\text{MeV}^{-1}$)

Size: 15 time-varying

particle_flux>differential_directional_number

Energy Bins for H 7 – 83 MeV (15 bins)

4.7.1.6 B_H_SECT_Flux H sectored flux side B ($\text{cm}^{-2}\text{sr}^{-1}\text{sec}^{-1}\text{MeV}^{-1}$)

Size: 2×25 time-varying

particle_flux>differential_directional_number

Energy Bins for H SECT 17 – 32 MeV (2 bins)
HET_R17_SECTORS 0 – 24 (25 bins)

4.7.1.7 B_He_Flux He flux side B ($\text{cm}^{-2}\text{sr}^{-1}\text{sec}^{-1}(\text{MeV}/\text{nuc})^{-1}$)
Size: 16 time-varying
particle_flux>differential_directional_number
Energy Bins for He 7 – 99 MeV/nuc (16 bins)

4.7.1.8 B_He_SECT_Flux He sectored flux side B ($\text{cm}^{-2}\text{sr}^{-1}\text{sec}^{-1}(\text{MeV}/\text{nuc})^{-1}$)
Size: 2×25 time-varying
particle_flux>differential_directional_number
Energy Bins for He SECT 17 – 32 MeV/nuc (2 bins)
HET_R17_SECTORS 0 – 24 (25 bins)

OTHER DATA

4.7.2.1 A_Al_Rate Al count rate side A (counts s^{-1})
Size: 15 time-varying
particle_flux>differential_directional_number_rate
Energy Bins for Al 21 – 235 MeV/nuc (15 bins)

4.7.2.2 A_Ar_Rate Ar count rate side A (counts s^{-1})
Size: 15 time-varying
particle_flux>differential_directional_number_rate
Energy Bins for Ar 25 – 279 MeV/nuc (15 bins)

4.7.2.3 A_C_Rate C count rate side A (counts s^{-1})
Size: 15 time-varying
particle_flux>differential_directional_number_rate
Energy Bins for C 12 – 140 MeV/nuc (15 bins)

4.7.2.4 A_Ca_Rate Ca count rate side A (counts s^{-1})
Size: 15 time-varying
particle_flux>differential_directional_number_rate
Energy Bins for Ca 25 – 279 MeV/nuc (15 bins)

4.7.2.5 A_Cr_Rate Cr count rate side A (counts s⁻¹)

Size: 16 time-varying

particle_flux>differential_directional_number_rate

Energy Bins for Cr 25 – 332 MeV/nuc (16 bins)

4.7.2.6 A_Electrons_Rate Electrons count rate side A (counts s⁻¹)

Size: 19 time-varying

particle_flux>differential_directional_number_rate

Energy Bins for Electrons 0 – 10 MeV (19 bins)

4.7.2.7 A_Electrons_SECT_Rate Electrons sectored count rate side A (counts s⁻¹)

Size: 2 × 25 time-varying

particle_flux>differential_directional_number_rate

Energy Bins for Electrons SECT 1 – 3 MeV (2 bins)

HET_R17_SECTORS 0 – 24 (25 bins)

4.7.2.8 A_Fe_Rate Fe count rate side A (counts s⁻¹)

Size: 15 time-varying

particle_flux>differential_directional_number_rate

Energy Bins for Fe 29 – 332 MeV/nuc (15 bins)

4.7.2.9 A_H_Rate H count rate side A (counts s⁻¹)

Size: 15 time-varying

particle_flux>differential_directional_number_rate

Energy Bins for H 7 – 83 MeV (15 bins)

4.7.2.10 A_H_SECT_Rate H sectored count rate side A (counts s⁻¹)

Size: 2 × 25 time-varying

particle_flux>differential_directional_number_rate

Energy Bins for H SECT 17 – 32 MeV (2 bins)

HET_R17_SECTORS 0 – 24 (25 bins)

4.7.2.11 A_He_Rate He count rate side A (counts s⁻¹)

Size: 16 time-varying

particle_flux>differential_directional_number_rate

Energy Bins for He 7 – 99 MeV/nuc (16 bins)

4.7.2.12 A_He_SECT_Rate He sectored count rate side A (counts s⁻¹)

Size: 2 × 25 time-varying

particle_flux>differential_directional_number_rate

Energy Bins for He SECT 17 – 32 MeV/nuc (2 bins)

HET_R17_SECTORS 0 – 24 (25 bins)

4.7.2.13 A_Mg_Rate Mg count rate side A (counts s⁻¹)

Size: 15 time-varying

particle_flux>differential_directional_number_rate

Energy Bins for Mg 21 – 235 MeV/nuc (15 bins)

4.7.2.14 A_N_Rate N count rate side A (counts s⁻¹)

Size: 15 time-varying

particle_flux>differential_directional_number_rate

Energy Bins for N 12 – 140 MeV/nuc (15 bins)

4.7.2.15 A_Na_Rate Na count rate side A (counts s⁻¹)

Size: 15 time-varying

particle_flux>differential_directional_number_rate

Energy Bins for Na 17 – 197 MeV/nuc (15 bins)

4.7.2.16 A_Ne_Rate Ne count rate side A (counts s⁻¹)

Size: 15 time-varying

particle_flux>differential_directional_number_rate

Energy Bins for Ne 17 – 197 MeV/nuc (15 bins)

4.7.2.17 A_Ni_Rate Ni count rate side A (counts s⁻¹)

Size: 15 time-varying

particle_flux>differential_directional_number_rate

Energy Bins for Ni 29 – 332 MeV/nuc (15 bins)

4.7.2.18 A_O_Rate O count rate side A (counts s⁻¹)

Size: 15 time-varying

particle_flux>differential_directional_number_rate

Energy Bins for O 15 – 166 MeV/nuc (15 bins)

4.7.2.19 A_S_Rate S count rate side A (counts s⁻¹)

Size: 16 time-varying

particle_flux>differential_directional_number_rate

Energy Bins for S 21 – 279 MeV/nuc (16 bins)

4.7.2.20 A_Si_Rate Si count rate side A (counts s⁻¹)

Size: 15 time-varying

particle_flux>differential_directional_number_rate

Energy Bins for Si 21 – 235 MeV/nuc (15 bins)

4.7.2.21 B_Al_Rate Al count rate side B (counts s⁻¹)

Size: 15 time-varying

particle_flux>differential_directional_number_rate

Energy Bins for Al 21 – 235 MeV/nuc (15 bins)

4.7.2.22 B_Ar_Rate Ar count rate side B (counts s⁻¹)

Size: 15 time-varying

particle_flux>differential_directional_number_rate

Energy Bins for Ar 25 – 279 MeV/nuc (15 bins)

4.7.2.23 B_C_Rate C count rate side B (counts s⁻¹)

Size: 15 time-varying

particle_flux>differential_directional_number_rate

Energy Bins for C 12 – 140 MeV/nuc (15 bins)

4.7.2.24 B_Ca_Rate Ca count rate side B (counts s⁻¹)

Size: 15 time-varying

particle_flux>differential_directional_number_rate

Energy Bins for Ca 25 – 279 MeV/nuc (15 bins)

4.7.2.25 B_Cr_Rate Cr count rate side B (counts s⁻¹)

Size: 16 time-varying

particle_flux>differential_directional_number_rate

Energy Bins for Cr 25 – 332 MeV/nuc (16 bins)

4.7.2.26 B_Electrons_Rate Electrons count rate side B (counts s⁻¹)

Size: 19 time-varying

particle_flux>differential_directional_number_rate

Energy Bins for Electrons 0 – 10 MeV (19 bins)

4.7.2.27 B_Electrons_SECT_Rate Electrons sectored count rate side B (counts s⁻¹)

Size: 2 × 25 time-varying

particle_flux>differential_directional_number_rate

Energy Bins for Electrons SECT 1 – 3 MeV (2 bins)

HET_R17_SECTORS 0 – 24 (25 bins)

4.7.2.28 B_Fe_Rate Fe count rate side B (counts s⁻¹)

Size: 15 time-varying

particle_flux>differential_directional_number_rate

Energy Bins for Fe 29 – 332 MeV/nuc (15 bins)

4.7.2.29 B_H_Rate H count rate side B (counts s⁻¹)

Size: 15 time-varying

particle_flux>differential_directional_number_rate

Energy Bins for H 7 – 83 MeV (15 bins)

4.7.2.30 B_H_SECT_Rate H sectored count rate side B (counts s⁻¹)

Size: 2 × 25 time-varying

particle_flux>differential_directional_number_rate

Energy Bins for H SECT 17 – 32 MeV (2 bins)

HET_R17_SECTORS 0 – 24 (25 bins)

4.7.2.31 B_He_Rate He count rate side B (counts s⁻¹)

Size: 16 time-varying

particle_flux>differential_directional_number_rate

Energy Bins for He 7 – 99 MeV/nuc (16 bins)

4.7.2.32 B_He_SECT_Rate He sectored count rate side B (counts s⁻¹)

Size: 2 × 25 time-varying

particle_flux>differential_directional_number_rate

Energy Bins for He SECT 17 – 32 MeV/nuc (2 bins)

HET_R17_SECTORS 0 – 24 (25 bins)

4.7.2.33 B_Mg_Rate Mg count rate side B (counts s⁻¹)

Size: 15 time-varying

particle_flux>differential_directional_number_rate

Energy Bins for Mg 21 – 235 MeV/nuc (15 bins)

4.7.2.34 B_N_Rate N count rate side B (counts s⁻¹)

Size: 15 time-varying

particle_flux>differential_directional_number_rate

Energy Bins for N 12 – 140 MeV/nuc (15 bins)

4.7.2.35 B_Na_Rate Na count rate side B (counts s⁻¹)

Size: 15 time-varying

particle_flux>differential_directional_number_rate

Energy Bins for Na 17 – 197 MeV/nuc (15 bins)

4.7.2.36 B_Ne_Rate Ne count rate side B (counts s⁻¹)

Size: 15 time-varying

particle_flux>differential_directional_number_rate

Energy Bins for Ne 17 – 197 MeV/nuc (15 bins)

4.7.2.37 B_Ni_Rate Ni count rate side B (counts s⁻¹)

Size: 15 time-varying

particle_flux>differential_directional_number_rate

Energy Bins for Ni 29 – 332 MeV/nuc (15 bins)

4.7.2.38 B_O_Rate O count rate side B (counts s⁻¹)

Size: 15 time-varying

particle_flux>differential_directional_number_rate

Energy Bins for O 15 – 166 MeV/nuc (15 bins)

4.7.2.39 B_S_Rate S count rate side B (counts s⁻¹)

Size: 16 time-varying

particle_flux>differential_directional_number_rate

Energy Bins for S 21 – 279 MeV/nuc (16 bins)

4.7.2.40 B_Si_Rate Si count rate side B (counts s⁻¹)

Size: 15 time-varying

particle_flux>differential_directional_number_rate

Energy Bins for Si 21 – 235 MeV/nuc (15 bins)

4.7.2.41 HCI_Lat HCI latitude (degrees)

time-varying

position>latitude

At timestamp. After Fraenz and Harper, PSS, 2002.

4.7.2.42 HCI_Lon HCI longitude (degrees)

time-varying

position>longitude

At timestamp. After Fraenz and Harper, PSS, 2002.

4.7.2.43 HCI_R Heliocentric distance (AU)

time-varying

position>radial

At timestamp. After Fraenz and Harper, PSS, 2002.

4.7.2.44 HET_A_HCI HCI flow direction HETA

Size: 3 time-varying

position>direction

Unit vector, after Fraenz and Harper, PSS, 2002.

4.7.2.45 HET_A_PA Pitch angle HETA (degree)

time-varying
position>angle

4.7.2.46 HET_A_R17_SECT_HCI HCI flow direction HETAR17SECT

Size: 25 × 3 time-varying
position>direction
Unit vector, after Fraenz and Harper, PSS, 2002.
HET_R17_SECTORS 0 – 24 (25 bins)

4.7.2.47 HET_A_R17_SECT_PA Pitch angle HETAR17SECT (degree)

Size: 25 time-varying
position>angle
HET_R17_SECTORS 0 – 24 (25 bins)

4.7.2.48 HET_A_R17_SECT_RTN RTN flow direction HETAR17SECT

Size: 25 × 3 time-varying
position>direction
Unit vector, after Fraenz and Harper, PSS, 2002.
HET_R17_SECTORS 0 – 24 (25 bins)

4.7.2.49 HET_A_R17_SECT_SA Nominal Parker Spiral angle HETAR17SECT (degree)

Size: 25 time-varying
position>angle
Angle between particle direction and nominal outward Parker Spiral, based on 400km/s solar wind and corotation breakdown at 10Rs.
HET_R17_SECTORS 0 – 24 (25 bins)

4.7.2.50 HET_A_RTN RTN flow direction HETA

Size: 3 time-varying
position>direction
Unit vector, after Fraenz and Harper, PSS, 2002.

4.7.2.51 HET_A_SA Nominal Parker Spiral angle HETA (degree)

time-varying
position>angle

Angle between particle direction and nominal outward Parker Spiral, based on 400km/s solar wind and corotation breakdown at 10Rs.

4.7.2.52 HET_B_HCI HCI flow direction HETB

Size: 3 time-varying

position>direction

Unit vector, after Fraenz and Harper, PSS, 2002.

4.7.2.53 HET_B_PA Pitch angle HETB (degree)

time-varying

position>angle

4.7.2.54 HET_B_R17_SECT_HCI HCI flow direction HETBR17SECT

Size: 25 \times 3 time-varying

position>direction

Unit vector, after Fraenz and Harper, PSS, 2002.

HET_R17_SECTORS 0 – 24 (25 bins)

4.7.2.55 HET_B_R17_SECT_PA Pitch angle HETBR17SECT (degree)

Size: 25 time-varying

position>angle

HET_R17_SECTORS 0 – 24 (25 bins)

4.7.2.56 HET_B_R17_SECT_RTN RTN flow direction HETBR17SECT

Size: 25 \times 3 time-varying

position>direction

Unit vector, after Fraenz and Harper, PSS, 2002.

HET_R17_SECTORS 0 – 24 (25 bins)

4.7.2.57 HET_B_R17_SECT_SA Nominal Parker Spiral angle HETBR17SECT (degree)

Size: 25 time-varying

position>angle

Angle between particle direction and nominal outward Parker Spiral, based on 400km/s solar wind and corotation breakdown at 10Rs.

HET_R17_SECTORS 0 – 24 (25 bins)

4.7.2.58 HET_B_RTN RTN flow direction HETB

Size: 3 time-varying

position>direction

Unit vector, after Fraenz and Harper, PSS, 2002.

4.7.2.59 HET_B_SA Nominal Parker Spiral angle HETB (degree)

time-varying

position>angle

Angle between particle direction and nominal outward Parker Spiral, based on 400km/s solar wind and corotation breakdown at 10Rs.

4.7.2.60 HGC_Lat HGC latitude (degrees)

time-varying

position>latitude

At timestamp. After Fraenz and Harper, PSS, 2002.

4.7.2.61 HGC_Lon HGC longitude (degrees)

time-varying

position>longitude

At timestamp. After Fraenz and Harper, PSS, 2002.

4.7.2.62 HGC_R Heliocentric distance (AU)

time-varying

position>radial

At timestamp. After Fraenz and Harper, PSS, 2002.

OTHER SUPPORT

PSP_ISOIS-EPIHI_L2-LET1-RATES10

ISOIS-EPIHI>Integrated Science Investigation of the Sun, Energetic Particle Instrument Hi

L2-LET1-rates10>Level 2 LET1 10-second rates

EPI-Hi 10 second rates cdf. Time tags indicate midpoint of integration.

Instrument paper: Integrated Science Investigation of the Sun (ISIS): Design of the Energetic Particle Investigation. McComas, D. J. et al (2016). Space Sci. Rev., doi:10.1007/s11214-014-0059-1

1 minute to 1 hour

Cite McComas et al (2016), doi:10.1007/s11214-014-0059-1

PRIMARY VARIABLES

4.8.1.1 A_H_Flux H flux side A ($\text{cm}^{-2}\text{sr}^{-1}\text{sec}^{-1}\text{MeV}^{-1}$)

Size: 18 time-varying

particle_flux>differential_directional_number

Energy Bins for H 1 – 15 MeV (18 bins)

4.8.1.2 A_He_Flux He flux side A ($\text{cm}^{-2}\text{sr}^{-1}\text{sec}^{-1}(\text{MeV}/\text{nuc})^{-1}$)

Size: 22 time-varying

particle_flux>differential_directional_number

Energy Bins for He 1 – 29 MeV/nuc (22 bins)

4.8.1.3 B_H_Flux H flux side B ($\text{cm}^{-2}\text{sr}^{-1}\text{sec}^{-1}\text{MeV}^{-1}$)

Size: 18 time-varying

particle_flux>differential_directional_number

Energy Bins for H 1 – 15 MeV (18 bins)

4.8.1.4 B_He_Flux He flux side B ($\text{cm}^{-2}\text{sr}^{-1}\text{sec}^{-1}(\text{MeV}/\text{nuc})^{-1}$)

Size: 22 time-varying

particle_flux>differential_directional_number

Energy Bins for He 1 – 29 MeV/nuc (22 bins)

OTHER DATA

4.8.2.1 A_H_Rate H count rate side A (counts s^{-1})

Size: 18 time-varying

particle_flux>differential_directional_number_rate

Energy Bins for H 1 – 15 MeV (18 bins)

4.8.2.2 A_He_Rate He count rate side A (counts s^{-1})

Size: 22 time-varying

particle_flux>differential_directional_number_rate

Energy Bins for He 1 – 29 MeV/nuc (22 bins)

4.8.2.3 B_H_Rate H count rate side B (counts s^{-1})

Size: 18 time-varying

particle_flux>differential_directional_number_rate

Energy Bins for H 1 – 15 MeV (18 bins)

4.8.2.4 B_He_Rate He count rate side B (counts s⁻¹)

Size: 22 time-varying

particle_flux>differential_directional_number_rate

Energy Bins for He 1 – 29 MeV/nuc (22 bins)

4.8.2.5 HCI_Lat HCI latitude (degrees)

time-varying

position>latitude

At timestamp. After Fraenz and Harper, PSS, 2002.

4.8.2.6 HCI_Lon HCI longitude (degrees)

time-varying

position>longitude

At timestamp. After Fraenz and Harper, PSS, 2002.

4.8.2.7 HCI_R Heliocentric distance (AU)

time-varying

position>radial

At timestamp. After Fraenz and Harper, PSS, 2002.

4.8.2.8 HGC_Lat HGC latitude (degrees)

time-varying

position>latitude

At timestamp. After Fraenz and Harper, PSS, 2002.

4.8.2.9 HGC_Lon HGC longitude (degrees)

time-varying

position>longitude

At timestamp. After Fraenz and Harper, PSS, 2002.

4.8.2.10 HGC_R Heliocentric distance (AU)

time-varying

position>radial

At timestamp. After Fraenz and Harper, PSS, 2002.

4.8.2.11 LET1_A_HCI HCI flow direction LET1A

Size: 3 time-varying

position>direction

Unit vector, after Fraenz and Harper, PSS, 2002.

4.8.2.12 LET1_A_PA Pitch angle LET1A (degree)

time-varying

position>angle

4.8.2.13 LET1_A_RTN RTN flow direction LET1A

Size: 3 time-varying

position>direction

Unit vector, after Fraenz and Harper, PSS, 2002.

4.8.2.14 LET1_A_SA Nominal Parker Spiral angle LET1A (degree)

time-varying

position>angle

Angle between particle direction and nominal outward Parker Spiral, based on 400km/s solar wind and corotation breakdown at 10Rs.

4.8.2.15 LET1_B_HCI HCI flow direction LET1B

Size: 3 time-varying

position>direction

Unit vector, after Fraenz and Harper, PSS, 2002.

4.8.2.16 LET1_B_PA Pitch angle LET1B (degree)

time-varying

position>angle

4.8.2.17 LET1_B_RTN RTN flow direction LET1B

Size: 3 time-varying

position>direction

Unit vector, after Fraenz and Harper, PSS, 2002.

4.8.2.18 LET1_B_SA Nominal Parker Spiral angle LET1B (degree)

time-varying

position>angle

Angle between particle direction and nominal outward Parker Spiral, based on 400km/s solar wind and corotation breakdown at 10Rs.

OTHER SUPPORT

PSP_ISOIS-EPIHI_L2-LET1-RATES300

ISOIS-EPIHI>Integrated Science Investigation of the Sun, Energetic Particle Instrument Hi

L2-LET1-rates300>Level 2 LET1 5-minute rates

EPI-Hi LET1 300 second rates cdf. Time tags indicate midpoint of integration.

Instrument paper: Integrated Science Investigation of the Sun (ISIS): Design of the Energetic Particle Investigation. McComas, D. J. et al (2016). Space Sci. Rev., doi:10.1007/s11214-014-0059-1

1 minute to 1 hour

Cite McComas et al (2016), doi:10.1007/s11214-014-0059-1

PRIMARY VARIABLES

OTHER DATA

4.9.2.1 HCI_Lat HCI latitude (degrees)

time-varying

position>latitude

At timestamp. After Fraenz and Harper, PSS, 2002.

4.9.2.2 HCI_Lon HCI longitude (degrees)

time-varying

position>longitude

At timestamp. After Fraenz and Harper, PSS, 2002.

4.9.2.3 HCI_R Heliocentric distance (AU)

time-varying

position>radial

At timestamp. After Fraenz and Harper, PSS, 2002.

4.9.2.4 HGC_Lat HGC latitude (degrees)
time-varying
position>latitude
At timestamp. After Fraenz and Harper, PSS, 2002.

4.9.2.5 HGC_Lon HGC longitude (degrees)
time-varying
position>longitude
At timestamp. After Fraenz and Harper, PSS, 2002.

4.9.2.6 HGC_R Heliocentric distance (AU)
time-varying
position>radial
At timestamp. After Fraenz and Harper, PSS, 2002.

4.9.2.7 LET1_A_HCI HCI flow direction LET1A
Size: 3 time-varying
position>direction
Unit vector, after Fraenz and Harper, PSS, 2002.

4.9.2.8 LET1_A_PA Pitch angle LET1A (degree)
time-varying
position>angle

4.9.2.9 LET1_A_R1_SECT_HCI HCI flow direction LET1AR1SECT
Size: 9×3 time-varying
position>direction
Unit vector, after Fraenz and Harper, PSS, 2002.
LET1_R1_SECTORS 0 – 8 (9 bins)

4.9.2.10 LET1_A_R1_SECT_PA Pitch angle LET1AR1SECT (degree)
Size: 9 time-varying
position>angle
LET1_R1_SECTORS 0 – 8 (9 bins)

4.9.2.11 LET1_A_R1_SECT_RTN RTN flow direction LET1AR1SECT

Size: 9×3 time-varying

position>direction

Unit vector, after Fraenz and Harper, PSS, 2002.

LET1_R1_SECTORS 0 – 8 (9 bins)

4.9.2.12 LET1_A_R1_SECT_SA Nominal Parker Spiral angle LET1AR1SECT (degree)

Size: 9 time-varying

position>angle

Angle between particle direction and nominal outward Parker Spiral, based on 400km/s solar wind and corotation breakdown at 10Rs.

LET1_R1_SECTORS 0 – 8 (9 bins)

4.9.2.13 LET1_A_R26_SECT_HCI HCI flow direction LET1AR26SECT

Size: 25×3 time-varying

position>direction

Unit vector, after Fraenz and Harper, PSS, 2002.

LET1_R26_SECTORS 0 – 24 (25 bins)

4.9.2.14 LET1_A_R26_SECT_PA Pitch angle LET1AR26SECT (degree)

Size: 25 time-varying

position>angle

LET1_R26_SECTORS 0 – 24 (25 bins)

4.9.2.15 LET1_A_R26_SECT_RTN RTN flow direction LET1AR26SECT

Size: 25×3 time-varying

position>direction

Unit vector, after Fraenz and Harper, PSS, 2002.

LET1_R26_SECTORS 0 – 24 (25 bins)

4.9.2.16 LET1_A_R26_SECT_SA Nominal Parker Spiral angle LET1AR26SECT (degree)

Size: 25 time-varying

position>angle

Angle between particle direction and nominal outward Parker Spiral, based on 400km/s solar wind and corotation breakdown at 10Rs.

LET1_R26_SECTORS 0 – 24 (25 bins)

4.9.2.17 LET1_A_RTN RTN flow direction LET1A

Size: 3 time-varying

position>direction

Unit vector, after Fraenz and Harper, PSS, 2002.

4.9.2.18 LET1_A_SA Nominal Parker Spiral angle LET1A (degree)

time-varying

position>angle

Angle between particle direction and nominal outward Parker Spiral, based on 400km/s solar wind and corotation breakdown at 10Rs.

4.9.2.19 LET1_B_HCI HCI flow direction LET1B

Size: 3 time-varying

position>direction

Unit vector, after Fraenz and Harper, PSS, 2002.

4.9.2.20 LET1_B_PA Pitch angle LET1B (degree)

time-varying

position>angle

4.9.2.21 LET1_B_R1_SECT_HCI HCI flow direction LET1BR1SECT

Size: 9×3 time-varying

position>direction

Unit vector, after Fraenz and Harper, PSS, 2002.

LET1_R1_SECTORS 0 – 8 (9 bins)

4.9.2.22 LET1_B_R1_SECT_PA Pitch angle LET1BR1SECT (degree)

Size: 9 time-varying

position>angle

LET1_R1_SECTORS 0 – 8 (9 bins)

4.9.2.23 LET1_B_R1_SECT_RTN RTN flow direction LET1BR1SECT

Size: 9×3 time-varying

position>direction

Unit vector, after Fraenz and Harper, PSS, 2002.

LET1_R1_SECTORS 0 – 8 (9 bins)

4.9.2.24 LET1_B_R1_SECT_SA Nominal Parker Spiral angle LET1BR1SECT (degree)

Size: 9 time-varying

position>angle

Angle between particle direction and nominal outward Parker Spiral, based on 400km/s solar wind and corotation breakdown at 10Rs.

LET1_R1_SECTORS 0 – 8 (9 bins)

4.9.2.25 LET1_B_R26_SECT_HCI HCI flow direction LET1BR26SECT

Size: 25 \times 3 time-varying

position>direction

Unit vector, after Fraenz and Harper, PSS, 2002.

LET1_R26_SECTORS 0 – 24 (25 bins)

4.9.2.26 LET1_B_R26_SECT_PA Pitch angle LET1BR26SECT (degree)

Size: 25 time-varying

position>angle

LET1_R26_SECTORS 0 – 24 (25 bins)

4.9.2.27 LET1_B_R26_SECT_RTN RTN flow direction LET1BR26SECT

Size: 25 \times 3 time-varying

position>direction

Unit vector, after Fraenz and Harper, PSS, 2002.

LET1_R26_SECTORS 0 – 24 (25 bins)

4.9.2.28 LET1_B_R26_SECT_SA Nominal Parker Spiral angle LET1BR26SECT (degree)

Size: 25 time-varying

position>angle

Angle between particle direction and nominal outward Parker Spiral, based on 400km/s solar wind and corotation breakdown at 10Rs.

LET1_R26_SECTORS 0 – 24 (25 bins)

4.9.2.29 LET1_B_RTN RTN flow direction LET1B

Size: 3 time-varying

position>direction

Unit vector, after Fraenz and Harper, PSS, 2002.

4.9.2.30 LET1_B_SA Nominal Parker Spiral angle LET1B (degree)

time-varying

position>angle

Angle between particle direction and nominal outward Parker Spiral, based on 400km/s solar wind and corotation breakdown at 10Rs.

4.9.2.31 R1A_CNO_SECT_Rate CNO sectored count rate R1A (counts s⁻¹)

Size: 1 × 9 time-varying

particle_flux>differential_directional_number_rate

Energy Bins for R1 CNO SECT 3 – 3 MeV/nuc (1 bins)

LET1_R1_SECTORS 0 – 8 (9 bins)

4.9.2.32 R1A_FeGroup_SECT_Rate FeGroup sectored count rate R1A (counts s⁻¹)

Size: 1 × 9 time-varying

particle_flux>differential_directional_number_rate

Energy Bins for R1 FeGroup SECT 3 – 3 MeV/nuc (1 bins)

LET1_R1_SECTORS 0 – 8 (9 bins)

4.9.2.33 R1A_NetoSi_SECT_Rate NetoS_i sectored count rate R1A (counts s⁻¹)

Size: 1 × 9 time-varying

particle_flux>differential_directional_number_rate

Energy Bins for R1 NetoS_i SECT 3 – 3 MeV/nuc (1 bins)

LET1_R1_SECTORS 0 – 8 (9 bins)

4.9.2.34 R1B_CNO_SECT_Rate CNO sectored count rate R1B (counts s⁻¹)

Size: 1 × 9 time-varying

particle_flux>differential_directional_number_rate

Energy Bins for R1 CNO SECT 3 – 3 MeV/nuc (1 bins)

LET1_R1_SECTORS 0 – 8 (9 bins)

4.9.2.35 R1B_FeGroup_SECT_Rate FeGroup sectored count rate R1B (counts s⁻¹)

Size: 1 × 9 time-varying

particle_flux>differential_directional_number_rate

Energy Bins for R1 FeGroup SECT 3 – 3 MeV/nuc (1 bins)

LET1_R1_SECTORS 0 – 8 (9 bins)

4.9.2.36 R1B_NetoSi_SECT_Rate NetoS i sectored count rate R1B (counts s $^{-1}$)

Size: 1 \times 9 time-varying

particle_flux>differential_directional_number_rate

Energy Bins for R1 NetoS i SECT 3 – 3 MeV/nuc (1 bins)

LET1_R1_SECTORS 0 – 8 (9 bins)

4.9.2.37 R26A_CNO_SECT_Rate CNO sectored count rate R26A (counts s $^{-1}$)

Size: 3 \times 25 time-varying

particle_flux>differential_directional_number_rate

Energy Bins for R26 CNO SECT 6 – 23 MeV/nuc (3 bins)

LET1_R26_SECTORS 0 – 24 (25 bins)

4.9.2.38 R26A_FeGroup_SECT_Rate FeGroup sectored count rate R26A (counts s $^{-1}$)

Size: 3 \times 25 time-varying

particle_flux>differential_directional_number_rate

Energy Bins for R26 FeGroup SECT 6 – 23 MeV/nuc (3 bins)

LET1_R26_SECTORS 0 – 24 (25 bins)

4.9.2.39 R26A_NetoSi_SECT_Rate NetoS i sectored count rate R26A (counts s $^{-1}$)

Size: 3 \times 25 time-varying

particle_flux>differential_directional_number_rate

Energy Bins for R26 NetoS i SECT 6 – 23 MeV/nuc (3 bins)

LET1_R26_SECTORS 0 – 24 (25 bins)

4.9.2.40 R26B_CNO_SECT_Rate CNO sectored count rate R26B (counts s $^{-1}$)

Size: 3 \times 25 time-varying

particle_flux>differential_directional_number_rate

Energy Bins for R26 CNO SECT 6 – 23 MeV/nuc (3 bins)

LET1_R26_SECTORS 0 – 24 (25 bins)

4.9.2.41 R26B_FeGroup_SECT_Rate FeGroup sectored count rate R26B (counts s $^{-1}$)

Size: 3 \times 25 time-varying

particle_flux>differential_directional_number_rate

Energy Bins for R26 FeGroup SECT 6 – 23 MeV/nuc (3 bins)

LET1_R26_SECTORS 0 – 24 (25 bins)

4.9.2.42 R26B_NetoSi_SECT_Rate NetoS_i sectored count rate R26B (counts s⁻¹)

Size: 3 × 25 time-varying

particle_flux>differential_directional_number_rate

Energy Bins for R26 NetoS_i SECT 6 – 23 MeV/nuc (3 bins)

LET1_R26_SECTORS 0 – 24 (25 bins)

OTHER SUPPORT

PSP_ISOIS-EPIHI_L2-LET1-RATES3600

ISOIS-EPIHI>Integrated Science Investigation of the Sun, Energetic Particle Instrument Hi

L2-LET1-rates3600>Level 2 LET1 hourly rates

EPI-Hi 3600 seconds rates cdf. Time tags indicate midpoint of integration.

Instrument paper: Integrated Science Investigation of the Sun (ISIS): Design of the Energetic Particle Investigation. McComas, D. J. et al (2016). Space Sci. Rev., doi:10.1007/s11214-014-0059-1

1 minute to 1 hour

Cite McComas et al (2016), doi:10.1007/s11214-014-0059-1

PRIMARY VARIABLES

4.10.1.1 A_H_Flux H flux side A (cm⁻²sr⁻¹sec⁻¹MeV⁻¹)

Size: 25 time-varying

particle_flux>differential_directional_number

Energy Bins for H 1 – 41 MeV (25 bins)

4.10.1.2 A_He_Flux He flux side A (cm⁻²sr⁻¹sec⁻¹(MeV/nuc)⁻¹)

Size: 26 time-varying

particle_flux>differential_directional_number

Energy Bins for He 1 – 49 MeV/nuc (26 bins)

4.10.1.3 B_H_Flux H flux side B (cm⁻²sr⁻¹sec⁻¹MeV⁻¹)

Size: 25 time-varying

particle_flux>differential_directional_number

Energy Bins for H 1 – 41 MeV (25 bins)

4.10.1.4 B_He_Flux He flux side B ($\text{cm}^{-2}\text{sr}^{-1}\text{sec}^{-1}(\text{MeV}/\text{nuc})^{-1}$)

Size: 26 time-varying

particle_flux>differential_directional_number

Energy Bins for He 1 – 49 MeV/nuc (26 bins)

4.10.1.5 R1A_H_SECT_Flux H sectored flux R1A ($\text{cm}^{-2}\text{sr}^{-1}\text{sec}^{-1}\text{MeV}^{-1}$)

Size: 1×9 time-varying

particle_flux>differential_directional_number

Energy Bins for R1 H SECT 1 – 1 MeV (1 bins)

LET1_R1_SECTORS 0 – 8 (9 bins)

4.10.1.6 R1A_He_SECT_Flux He sectored flux R1A ($\text{cm}^{-2}\text{sr}^{-1}\text{sec}^{-1}(\text{MeV}/\text{nuc})^{-1}$)

Size: 1×9 time-varying

particle_flux>differential_directional_number

Energy Bins for R1 He SECT 1 – 1 MeV/nuc (1 bins)

LET1_R1_SECTORS 0 – 8 (9 bins)

4.10.1.7 R1B_H_SECT_Flux H sectored flux R1B ($\text{cm}^{-2}\text{sr}^{-1}\text{sec}^{-1}\text{MeV}^{-1}$)

Size: 1×9 time-varying

particle_flux>differential_directional_number

Energy Bins for R1 H SECT 1 – 1 MeV (1 bins)

LET1_R1_SECTORS 0 – 8 (9 bins)

4.10.1.8 R1B_He_SECT_Flux He sectored flux R1B ($\text{cm}^{-2}\text{sr}^{-1}\text{sec}^{-1}(\text{MeV}/\text{nuc})^{-1}$)

Size: 1×9 time-varying

particle_flux>differential_directional_number

Energy Bins for R1 He SECT 1 – 1 MeV/nuc (1 bins)

LET1_R1_SECTORS 0 – 8 (9 bins)

4.10.1.9 R26A_H_SECT_Flux H sectored flux R26A ($\text{cm}^{-2}\text{sr}^{-1}\text{sec}^{-1}\text{MeV}^{-1}$)

Size: 3×25 time-varying

particle_flux>differential_directional_number

Energy Bins for R26 H SECT 3 – 11 MeV (3 bins)

LET1_R26_SECTORS 0 – 24 (25 bins)

4.10.1.10 R26A_He_SECT_Flux He sectored flux R26A ($\text{cm}^{-2}\text{sr}^{-1}\text{sec}^{-1}(\text{MeV}/\text{nuc})^{-1}$)

Size: 3×25 time-varying

particle_flux>differential_directional_number

Energy Bins for R26 He SECT 3 – 11 MeV/nuc (3 bins)

LET1_R26_SECTORS 0 – 24 (25 bins)

4.10.1.11 R26B_H_SECT_Flux H sectored flux R26B ($\text{cm}^{-2}\text{sr}^{-1}\text{sec}^{-1}\text{MeV}^{-1}$)

Size: 3×25 time-varying

particle_flux>differential_directional_number

Energy Bins for R26 H SECT 3 – 11 MeV (3 bins)

LET1_R26_SECTORS 0 – 24 (25 bins)

4.10.1.12 R26B_He_SECT_Flux He sectored flux R26B ($\text{cm}^{-2}\text{sr}^{-1}\text{sec}^{-1}(\text{MeV}/\text{nuc})^{-1}$)

Size: 3×25 time-varying

particle_flux>differential_directional_number

Energy Bins for R26 He SECT 3 – 11 MeV/nuc (3 bins)

LET1_R26_SECTORS 0 – 24 (25 bins)

OTHER DATA

4.10.2.1 A_Al_Rate Al count rate side A (counts s^{-1})

Size: 28 time-varying

particle_flux>differential_directional_number_rate

Energy Bins for Al 1 – 117 MeV/nuc (28 bins)

4.10.2.2 A_Ar_Rate Ar count rate side A (counts s^{-1})

Size: 29 time-varying

particle_flux>differential_directional_number_rate

Energy Bins for Ar 1 – 140 MeV/nuc (29 bins)

4.10.2.3 A_C_Rate C count rate side A (counts s^{-1})

Size: 27 time-varying

particle_flux>differential_directional_number_rate

Energy Bins for C 1 – 99 MeV/nuc (27 bins)

4.10.2.4 A_Ca_Rate Ca count rate side A (counts s^{-1})

Size: 30 time-varying

particle_flux>differential_directional_number_rate
Energy Bins for Ca 1 – 140 MeV/nuc (30 bins)

4.10.2.5 A_Cr_Rate Cr count rate side A (counts s⁻¹)

Size: 31 time-varying

particle_flux>differential_directional_number_rate
Energy Bins for Cr 1 – 140 MeV/nuc (31 bins)

4.10.2.6 A_Fe_Rate Fe count rate side A (counts s⁻¹)

Size: 32 time-varying

particle_flux>differential_directional_number_rate
Energy Bins for Fe 1 – 166 MeV/nuc (32 bins)

4.10.2.7 A_H_Rate H count rate side A (counts s⁻¹)

Size: 25 time-varying

particle_flux>differential_directional_number_rate
Energy Bins for H 1 – 41 MeV (25 bins)

4.10.2.8 A_He_Rate He count rate side A (counts s⁻¹)

Size: 26 time-varying

particle_flux>differential_directional_number_rate
Energy Bins for He 1 – 49 MeV/nuc (26 bins)

4.10.2.9 A_Mg_Rate Mg count rate side A (counts s⁻¹)

Size: 28 time-varying

particle_flux>differential_directional_number_rate
Energy Bins for Mg 1 – 117 MeV/nuc (28 bins)

4.10.2.10 A_N_Rate N count rate side A (counts s⁻¹)

Size: 27 time-varying

particle_flux>differential_directional_number_rate
Energy Bins for N 1 – 99 MeV/nuc (27 bins)

4.10.2.11 A_Na_Rate Na count rate side A (counts s⁻¹)

Size: 28 time-varying

particle_flux>differential_directional_number_rate

Energy Bins for Na 1 – 117 MeV/nuc (28 bins)

4.10.2.12 A_Ne_Rate Ne count rate side A (counts s⁻¹)

Size: 28 time-varying

particle_flux>differential_directional_number_rate

Energy Bins for Ne 1 – 117 MeV/nuc (28 bins)

4.10.2.13 A_Ni_Rate Ni count rate side A (counts s⁻¹)

Size: 33 time-varying

particle_flux>differential_directional_number_rate

Energy Bins for Ni 1 – 197 MeV/nuc (33 bins)

4.10.2.14 A_O_Rate O count rate side A (counts s⁻¹)

Size: 28 time-varying

particle_flux>differential_directional_number_rate

Energy Bins for O 1 – 117 MeV/nuc (28 bins)

4.10.2.15 A_S_Rate S count rate side A (counts s⁻¹)

Size: 29 time-varying

particle_flux>differential_directional_number_rate

Energy Bins for S 1 – 140 MeV/nuc (29 bins)

4.10.2.16 A_Si_Rate Si count rate side A (counts s⁻¹)

Size: 29 time-varying

particle_flux>differential_directional_number_rate

Energy Bins for Si 1 – 140 MeV/nuc (29 bins)

4.10.2.17 B_Al_Rate Al count rate side B (counts s⁻¹)

Size: 28 time-varying

particle_flux>differential_directional_number_rate

Energy Bins for Al 1 – 117 MeV/nuc (28 bins)

4.10.2.18 B_Ar_Rate Ar count rate side B (counts s⁻¹)

Size: 29 time-varying

particle_flux>differential_directional_number_rate

Energy Bins for Ar 1 – 140 MeV/nuc (29 bins)

4.10.2.19 B_C_Rate C count rate side B (counts s⁻¹)

Size: 27 time-varying

particle_flux>differential_directional_number_rate

Energy Bins for C 1 – 99 MeV/nuc (27 bins)

4.10.2.20 B_Ca_Rate Ca count rate side B (counts s⁻¹)

Size: 30 time-varying

particle_flux>differential_directional_number_rate

Energy Bins for Ca 1 – 140 MeV/nuc (30 bins)

4.10.2.21 B_Cr_Rate Cr count rate side B (counts s⁻¹)

Size: 31 time-varying

particle_flux>differential_directional_number_rate

Energy Bins for Cr 1 – 140 MeV/nuc (31 bins)

4.10.2.22 B_Fe_Rate Fe count rate side B (counts s⁻¹)

Size: 32 time-varying

particle_flux>differential_directional_number_rate

Energy Bins for Fe 1 – 166 MeV/nuc (32 bins)

4.10.2.23 B_H_Rate H count rate side B (counts s⁻¹)

Size: 25 time-varying

particle_flux>differential_directional_number_rate

Energy Bins for H 1 – 41 MeV (25 bins)

4.10.2.24 B_He_Rate He count rate side B (counts s⁻¹)

Size: 26 time-varying

particle_flux>differential_directional_number_rate

Energy Bins for He 1 – 49 MeV/nuc (26 bins)

4.10.2.25 B_Mg_Rate Mg count rate side B (counts s⁻¹)

Size: 28 time-varying

particle_flux>differential_directional_number_rate

Energy Bins for Mg 1 – 117 MeV/nuc (28 bins)

4.10.2.26 B_N_Rate N count rate side B (counts s⁻¹)

Size: 27 time-varying

particle_flux>differential_directional_number_rate

Energy Bins for N 1 – 99 MeV/nuc (27 bins)

4.10.2.27 B_Na_Rate Na count rate side B (counts s⁻¹)

Size: 28 time-varying

particle_flux>differential_directional_number_rate

Energy Bins for Na 1 – 117 MeV/nuc (28 bins)

4.10.2.28 B_Ne_Rate Ne count rate side B (counts s⁻¹)

Size: 28 time-varying

particle_flux>differential_directional_number_rate

Energy Bins for Ne 1 – 117 MeV/nuc (28 bins)

4.10.2.29 B_Ni_Rate Ni count rate side B (counts s⁻¹)

Size: 33 time-varying

particle_flux>differential_directional_number_rate

Energy Bins for Ni 1 – 197 MeV/nuc (33 bins)

4.10.2.30 B_O_Rate O count rate side B (counts s⁻¹)

Size: 28 time-varying

particle_flux>differential_directional_number_rate

Energy Bins for O 1 – 117 MeV/nuc (28 bins)

4.10.2.31 B_S_Rate S count rate side B (counts s⁻¹)

Size: 29 time-varying

particle_flux>differential_directional_number_rate

Energy Bins for S 1 – 140 MeV/nuc (29 bins)

4.10.2.32 B_Si_Rate Si count rate side B (counts s⁻¹)

Size: 29 time-varying

particle_flux>differential_directional_number_rate

Energy Bins for Si 1 – 140 MeV/nuc (29 bins)

4.10.2.33 HCI_Lat HCI latitude (degrees)

time-varying

position>latitude

At timestamp. After Fraenz and Harper, PSS, 2002.

4.10.2.34 HCI_Lon HCI longitude (degrees)

time-varying

position>longitude

At timestamp. After Fraenz and Harper, PSS, 2002.

4.10.2.35 HCI_R Heliocentric distance (AU)

time-varying

position>radial

At timestamp. After Fraenz and Harper, PSS, 2002.

4.10.2.36 HGC_Lat HGC latitude (degrees)

time-varying

position>latitude

At timestamp. After Fraenz and Harper, PSS, 2002.

4.10.2.37 HGC_Lon HGC longitude (degrees)

time-varying

position>longitude

At timestamp. After Fraenz and Harper, PSS, 2002.

4.10.2.38 HGC_R Heliocentric distance (AU)

time-varying

position>radial

At timestamp. After Fraenz and Harper, PSS, 2002.

4.10.2.39 LET1_A_HCI HCI flow direction LET1A

Size: 3 time-varying

position>direction

Unit vector, after Fraenz and Harper, PSS, 2002.

4.10.2.40 LET1_A_PA Pitch angle LET1A (degree)

time-varying

position>angle

4.10.2.41 LET1_A_R1_SECT_HCI HCI flow direction LET1AR1SECT

Size: 9×3 time-varying

position>direction

Unit vector, after Fraenz and Harper, PSS, 2002.

LET1_R1_SECTORS 0 – 8 (9 bins)

4.10.2.42 LET1_A_R1_SECT_PA Pitch angle LET1AR1SECT (degree)

Size: 9 time-varying

position>angle

LET1_R1_SECTORS 0 – 8 (9 bins)

4.10.2.43 LET1_A_R1_SECT_RTN RTN flow direction LET1AR1SECT

Size: 9×3 time-varying

position>direction

Unit vector, after Fraenz and Harper, PSS, 2002.

LET1_R1_SECTORS 0 – 8 (9 bins)

4.10.2.44 LET1_A_R1_SECT_SA Nominal Parker Spiral angle LET1AR1SECT (degree)

Size: 9 time-varying

position>angle

Angle between particle direction and nominal outward Parker Spiral, based on 400km/s solar wind and corotation breakdown at 10Rs.

LET1_R1_SECTORS 0 – 8 (9 bins)

4.10.2.45 LET1_A_R26_SECT_HCI HCI flow direction LET1AR26SECT

Size: 25×3 time-varying

position>direction

Unit vector, after Fraenz and Harper, PSS, 2002.
LET1_R26_SECTORS 0 – 24 (25 bins)

4.10.2.46 LET1_A_R26_SECT_PA Pitch angle LET1AR26SECT (degree)
Size: 25 time-varying
position>angle
LET1_R26_SECTORS 0 – 24 (25 bins)

4.10.2.47 LET1_A_R26_SECT_RTN RTN flow direction LET1AR26SECT
Size: 25 × 3 time-varying
position>direction
Unit vector, after Fraenz and Harper, PSS, 2002.
LET1_R26_SECTORS 0 – 24 (25 bins)

4.10.2.48 LET1_A_R26_SECT_SA Nominal Parker Spiral angle LET1AR26SECT (degree)
Size: 25 time-varying
position>angle
Angle between particle direction and nominal outward Parker Spiral, based on 400km/s solar wind and corotation breakdown at 10Rs.
LET1_R26_SECTORS 0 – 24 (25 bins)

4.10.2.49 LET1_A_RTN RTN flow direction LET1A
Size: 3 time-varying
position>direction
Unit vector, after Fraenz and Harper, PSS, 2002.

4.10.2.50 LET1_A_SA Nominal Parker Spiral angle LET1A (degree)
time-varying
position>angle
Angle between particle direction and nominal outward Parker Spiral, based on 400km/s solar wind and corotation breakdown at 10Rs.

4.10.2.51 LET1_B_HCI HCI flow direction LET1B
Size: 3 time-varying
position>direction

Unit vector, after Fraenz and Harper, PSS, 2002.

4.10.2.52 LET1_B_PA Pitch angle LET1B (degree)

time-varying

position>angle

4.10.2.53 LET1_B_R1_SECT_HCI HCI flow direction LET1BR1SECT

Size: 9×3 time-varying

position>direction

Unit vector, after Fraenz and Harper, PSS, 2002.

LET1_R1_SECTORS 0 – 8 (9 bins)

4.10.2.54 LET1_B_R1_SECT_PA Pitch angle LET1BR1SECT (degree)

Size: 9 time-varying

position>angle

LET1_R1_SECTORS 0 – 8 (9 bins)

4.10.2.55 LET1_B_R1_SECT_RTN RTN flow direction LET1BR1SECT

Size: 9×3 time-varying

position>direction

Unit vector, after Fraenz and Harper, PSS, 2002.

LET1_R1_SECTORS 0 – 8 (9 bins)

4.10.2.56 LET1_B_R1_SECT_SA Nominal Parker Spiral angle LET1BR1SECT (degree)

Size: 9 time-varying

position>angle

Angle between particle direction and nominal outward Parker Spiral, based on 400km/s solar wind and corotation breakdown at 10Rs.

LET1_R1_SECTORS 0 – 8 (9 bins)

4.10.2.57 LET1_B_R26_SECT_HCI HCI flow direction LET1BR26SECT

Size: 25×3 time-varying

position>direction

Unit vector, after Fraenz and Harper, PSS, 2002.

LET1_R26_SECTORS 0 – 24 (25 bins)

4.10.2.58 LET1_B_R26_SECT_PA Pitch angle LET1BR26SECT (degree)

Size: 25 time-varying

position>angle

LET1_R26_SECTORS 0 – 24 (25 bins)

4.10.2.59 LET1_B_R26_SECT_RTN RTN flow direction LET1BR26SECT

Size: 25 × 3 time-varying

position>direction

Unit vector, after Fraenz and Harper, PSS, 2002.

LET1_R26_SECTORS 0 – 24 (25 bins)

4.10.2.60 LET1_B_R26_SECT_SA Nominal Parker Spiral angle LET1BR26SECT (degree)

Size: 25 time-varying

position>angle

Angle between particle direction and nominal outward Parker Spiral, based on 400km/s solar wind and corotation breakdown at 10Rs.

LET1_R26_SECTORS 0 – 24 (25 bins)

4.10.2.61 LET1_B_RTN RTN flow direction LET1B

Size: 3 time-varying

position>direction

Unit vector, after Fraenz and Harper, PSS, 2002.

4.10.2.62 LET1_B_SA Nominal Parker Spiral angle LET1B (degree)

time-varying

position>angle

Angle between particle direction and nominal outward Parker Spiral, based on 400km/s solar wind and corotation breakdown at 10Rs.

4.10.2.63 R1A_CNO_SECT_Rate CNO sectored count rate R1A (counts s⁻¹)

Size: 1 × 9 time-varying

particle_flux>differential_directional_number_rate

Energy Bins for R1 CNO SECT 3 – 3 MeV/nuc (1 bins)

LET1_R1_SECTORS 0 – 8 (9 bins)

4.10.2.64 R1A_FeGroup_SECT_Rate FeGroup sectored count rate R1A (counts s⁻¹)

Size: 1 × 9 time-varying

particle_flux>differential_directional_number_rate

Energy Bins for R1 FeGroup SECT 3 – 3 MeV/nuc (1 bins)

LET1_R1_SECTORS 0 – 8 (9 bins)

4.10.2.65 R1A_H_SECT_Rate H sectored count rate R1A (counts s⁻¹)

Size: 1 × 9 time-varying

particle_flux>differential_directional_number_rate

Energy Bins for R1 H SECT 1 – 1 MeV (1 bins)

LET1_R1_SECTORS 0 – 8 (9 bins)

4.10.2.66 R1A_He_BIN R1A He Rates (counts)

Size: 5 × 16 time-varying

particle_flux>differential_directional_number_rate

Energy Bins for R1 He BIN 1 – 3 MeV/nuc (5 bins)

R1A_He_BIN_MASS_BIN 0 – 15 segment (16 bins)

4.10.2.67 R1A_He_SECT_Rate He sectored count rate R1A (counts s⁻¹)

Size: 1 × 9 time-varying

particle_flux>differential_directional_number_rate

Energy Bins for R1 He SECT 1 – 1 MeV/nuc (1 bins)

LET1_R1_SECTORS 0 – 8 (9 bins)

4.10.2.68 R1A_Ne_BIN R1A Ne Rates (counts)

Size: 5 × 8 time-varying

particle_flux>differential_directional_number_rate

Energy Bins for R1 Ne BIN 1 – 6 MeV/nuc (5 bins)

R1A_Ne_BIN_MASS_BIN 0 – 7 segment (8 bins)

4.10.2.69 R1A_NetoSi_SECT_Rate NetoS_i sectored count rate R1A (counts s⁻¹)

Size: 1 × 9 time-varying

particle_flux>differential_directional_number_rate

Energy Bins for R1 NetoS_i SECT 3 – 3 MeV/nuc (1 bins)

LET1_R1_SECTORS 0 – 8 (9 bins)

4.10.2.70 R1B_CNO_SECT_Rate CNO sectored count rate R1B (counts s⁻¹)

Size: 1 × 9 time-varying

particle_flux>differential_directional_number_rate

Energy Bins for R1 CNO SECT 3 – 3 MeV/nuc (1 bins)

LET1_R1_SECTORS 0 – 8 (9 bins)

4.10.2.71 R1B_FeGroup_SECT_Rate FeGroup sectored count rate R1B (counts s⁻¹)

Size: 1 × 9 time-varying

particle_flux>differential_directional_number_rate

Energy Bins for R1 FeGroup SECT 3 – 3 MeV/nuc (1 bins)

LET1_R1_SECTORS 0 – 8 (9 bins)

4.10.2.72 R1B_H_SECT_Rate H sectored count rate R1B (counts s⁻¹)

Size: 1 × 9 time-varying

particle_flux>differential_directional_number_rate

Energy Bins for R1 H SECT 1 – 1 MeV (1 bins)

LET1_R1_SECTORS 0 – 8 (9 bins)

4.10.2.73 R1B_He_BIN R1B He Rates (counts)

Size: 5 × 16 time-varying

particle_flux>differential_directional_number_rate

Energy Bins for R1 He BIN 1 – 3 MeV/nuc (5 bins)

R1B_He_BIN_MASS_BIN 0 – 15 segment (16 bins)

4.10.2.74 R1B_He_SECT_Rate He sectored count rate R1B (counts s⁻¹)

Size: 1 × 9 time-varying

particle_flux>differential_directional_number_rate

Energy Bins for R1 He SECT 1 – 1 MeV/nuc (1 bins)

LET1_R1_SECTORS 0 – 8 (9 bins)

4.10.2.75 R1B_Ne_BIN R1B Ne Rates (counts)

Size: 5 × 8 time-varying

particle_flux>differential_directional_number_rate

Energy Bins for R1 Ne BIN 1 – 6 MeV/nuc (5 bins)

R1B_Ne_BIN_MASS_BIN 0 – 7 segment (8 bins)

4.10.2.76 R1B_NetoSi_SECT_Rate NetoS $\dot{\text{i}}$ sectored count rate R1B (counts s $^{-1}$)

Size: 1 \times 9 time-varying

particle_flux>differential_directional_number_rate

Energy Bins for R1 NetoS $\dot{\text{i}}$ SECT 3 – 3 MeV/nuc (1 bins)

LET1_R1_SECTORS 0 – 8 (9 bins)

4.10.2.77 R26A_CNO_SECT_Rate CNO sectored count rate R26A (counts s $^{-1}$)

Size: 3 \times 25 time-varying

particle_flux>differential_directional_number_rate

Energy Bins for R26 CNO SECT 6 – 23 MeV/nuc (3 bins)

LET1_R26_SECTORS 0 – 24 (25 bins)

4.10.2.78 R26A_FeGroup_SECT_Rate FeGroup sectored count rate R26A (counts s $^{-1}$)

Size: 3 \times 25 time-varying

particle_flux>differential_directional_number_rate

Energy Bins for R26 FeGroup SECT 6 – 23 MeV/nuc (3 bins)

LET1_R26_SECTORS 0 – 24 (25 bins)

4.10.2.79 R26A_H_SECT_Rate H sectored count rate R26A (counts s $^{-1}$)

Size: 3 \times 25 time-varying

particle_flux>differential_directional_number_rate

Energy Bins for R26 H SECT 3 – 11 MeV (3 bins)

LET1_R26_SECTORS 0 – 24 (25 bins)

4.10.2.80 R26A_He_SECT_Rate He sectored count rate R26A (counts s $^{-1}$)

Size: 3 \times 25 time-varying

particle_flux>differential_directional_number_rate

Energy Bins for R26 He SECT 3 – 11 MeV/nuc (3 bins)

LET1_R26_SECTORS 0 – 24 (25 bins)

4.10.2.81 R26A_NetoSi_SECT_Rate NetoS $\dot{\text{i}}$ sectored count rate R26A (counts s $^{-1}$)

Size: 3 \times 25 time-varying

particle_flux>differential_directional_number_rate

Energy Bins for R26 NetoS $\dot{\text{i}}$ SECT 6 – 23 MeV/nuc (3 bins)

LET1_R26_SECTORS 0 – 24 (25 bins)

4.10.2.82 R26B_CNO_SECT_Rate CNO sectored count rate R26B (counts s⁻¹)

Size: 3 × 25 time-varying

particle_flux>differential_directional_number_rate

Energy Bins for R26 CNO SECT 6 – 23 MeV/nuc (3 bins)

LET1_R26_SECTORS 0 – 24 (25 bins)

4.10.2.83 R26B_FeGroup_SECT_Rate FeGroup sectored count rate R26B (counts s⁻¹)

Size: 3 × 25 time-varying

particle_flux>differential_directional_number_rate

Energy Bins for R26 FeGroup SECT 6 – 23 MeV/nuc (3 bins)

LET1_R26_SECTORS 0 – 24 (25 bins)

4.10.2.84 R26B_H_SECT_Rate H sectored count rate R26B (counts s⁻¹)

Size: 3 × 25 time-varying

particle_flux>differential_directional_number_rate

Energy Bins for R26 H SECT 3 – 11 MeV (3 bins)

LET1_R26_SECTORS 0 – 24 (25 bins)

4.10.2.85 R26B_He_SECT_Rate He sectored count rate R26B (counts s⁻¹)

Size: 3 × 25 time-varying

particle_flux>differential_directional_number_rate

Energy Bins for R26 He SECT 3 – 11 MeV/nuc (3 bins)

LET1_R26_SECTORS 0 – 24 (25 bins)

4.10.2.86 R26B_NetoSi_SECT_Rate NetoS_i sectored count rate R26B (counts s⁻¹)

Size: 3 × 25 time-varying

particle_flux>differential_directional_number_rate

Energy Bins for R26 NetoS_i SECT 6 – 23 MeV/nuc (3 bins)

LET1_R26_SECTORS 0 – 24 (25 bins)

4.10.2.87 R2A_He_BIN R2A He Rates (counts)

Size: 7 × 16 time-varying

particle_flux>differential_directional_number_rate

Energy Bins for R2 He BIN 2 – 16 MeV/nuc (7 bins)

R2A_He_BIN_MASS_BIN 0 – 15 segment (16 bins)

4.10.2.88 R2A_Ne_BIN R2A Ne Rates (counts)

Size: 8×8 time-varying

particle_flux>differential_directional_number_rate

Energy Bins for R2 Ne BIN 3 – 32 MeV/nuc (8 bins)

R2A_Ne_BIN_MASS_BIN 0 – 7 segment (8 bins)

4.10.2.89 R2B_He_BIN R2B He Rates (counts)

Size: 7×16 time-varying

particle_flux>differential_directional_number_rate

Energy Bins for R2 He BIN 2 – 16 MeV/nuc (7 bins)

R2B_He_BIN_MASS_BIN 0 – 15 segment (16 bins)

4.10.2.90 R2B_Ne_BIN R2B Ne Rates (counts)

Size: 8×8 time-varying

particle_flux>differential_directional_number_rate

Energy Bins for R2 Ne BIN 3 – 32 MeV/nuc (8 bins)

R2B_Ne_BIN_MASS_BIN 0 – 7 segment (8 bins)

4.10.2.91 R3A_He_BIN R3A He Rates (counts)

Size: 5×16 time-varying

particle_flux>differential_directional_number_rate

Energy Bins for R3 He BIN 8 – 32 MeV/nuc (5 bins)

R3A_He_BIN_MASS_BIN 0 – 15 segment (16 bins)

4.10.2.92 R3A_Ne_BIN R3A Ne Rates (counts)

Size: 6×8 time-varying

particle_flux>differential_directional_number_rate

Energy Bins for R3 Ne BIN 16 – 91 MeV/nuc (6 bins)

R3A_Ne_BIN_MASS_BIN 0 – 7 segment (8 bins)

4.10.2.93 R3B_He_BIN R3B He Rates (counts)

Size: 5×16 time-varying

particle_flux>differential_directional_number_rate

Energy Bins for R3 He BIN 8 – 32 MeV/nuc (5 bins)

R3B_He_BIN_MASS_BIN 0 – 15 segment (16 bins)

4.10.2.94 R3B_Ne_BIN R3B Ne Rates (counts)

Size: 6×8 time-varying

particle_flux>differential_directional_number_rate

Energy Bins for R3 Ne BIN 16 – 91 MeV/nuc (6 bins)

R3B_Ne_BIN_MASS_BIN 0 – 7 segment (8 bins)

4.10.2.95 R45A_He_BIN R45A He Rates (counts)

Size: 5×16 time-varying

particle_flux>differential_directional_number_rate

Energy Bins for R45 He BIN 8 – 32 MeV/nuc (5 bins)

R45A_He_BIN_MASS_BIN 0 – 15 segment (16 bins)

4.10.2.96 R45A_Ne_BIN R45A Ne Rates (counts)

Size: 6×8 time-varying

particle_flux>differential_directional_number_rate

Energy Bins for R45 Ne BIN 16 – 91 MeV/nuc (6 bins)

R45A_Ne_BIN_MASS_BIN 0 – 7 segment (8 bins)

4.10.2.97 R45B_He_BIN R45B He Rates (counts)

Size: 5×16 time-varying

particle_flux>differential_directional_number_rate

Energy Bins for R45 He BIN 8 – 32 MeV/nuc (5 bins)

R45B_He_BIN_MASS_BIN 0 – 15 segment (16 bins)

4.10.2.98 R45B_Ne_BIN R45B Ne Rates (counts)

Size: 6×8 time-varying

particle_flux>differential_directional_number_rate

Energy Bins for R45 Ne BIN 16 – 91 MeV/nuc (6 bins)

R45B_Ne_BIN_MASS_BIN 0 – 7 segment (8 bins)

4.10.2.99 R6A_He_BIN R6A He Rates (counts)

Size: 3×16 time-varying

particle_flux>differential_directional_number_rate

Energy Bins for R6 He BIN 23 – 45 MeV/nuc (3 bins)

R6A_He_BIN_MASS_BIN 0 – 15 segment (16 bins)

4.10.2.100 R6A_Ne_BIN R6A Ne Rates (counts)

Size: 3×8 time-varying

particle_flux>differential_directional_number_rate

Energy Bins for R6 Ne BIN 45 – 91 MeV/nuc (3 bins)

R6A_Ne_BIN_MASS_BIN 0 – 7 segment (8 bins)

4.10.2.101 R6B_He_BIN R6B He Rates (counts)

Size: 3×16 time-varying

particle_flux>differential_directional_number_rate

Energy Bins for R6 He BIN 23 – 45 MeV/nuc (3 bins)

R6B_He_BIN_MASS_BIN 0 – 15 segment (16 bins)

4.10.2.102 R6B_Ne_BIN R6B Ne Rates (counts)

Size: 3×8 time-varying

particle_flux>differential_directional_number_rate

Energy Bins for R6 Ne BIN 45 – 91 MeV/nuc (3 bins)

R6B_Ne_BIN_MASS_BIN 0 – 7 segment (8 bins)

OTHER SUPPORT

PSP_ISOIS-EPIHI_L2-LET1-RATES60

ISOIS-EPIHI>Integrated Science Investigation of the Sun, Energetic Particle Instrument Hi

L2-LET1-rates60>Level 2 LET1 1-minute rates

EPI-Hi LET1 60 second rates cdf. Time tags indicate midpoint of integration.

Instrument paper: Integrated Science Investigation of the Sun (ISIS): Design of the Energetic Particle Investigation. McComas, D. J. et al (2016). Space Sci. Rev., doi:10.1007/s11214-014-0059-1

1 minute to 1 hour

Cite McComas et al (2016), doi:10.1007/s11214-014-0059-1

PRIMARY VARIABLES

4.11.1.1 A_H_Flux H flux side A ($\text{cm}^{-2}\text{sr}^{-1}\text{sec}^{-1}\text{MeV}^{-1}$)

Size: 25 time-varying

particle_flux>differential_directional_number

Energy Bins for H 1 – 41 MeV (25 bins)

4.11.1.2 A_He_Flux He flux side A ($\text{cm}^{-2}\text{sr}^{-1}\text{sec}^{-1}(\text{MeV/nuc})^{-1}$)

Size: 26 time-varying

particle_flux>differential_directional_number
Energy Bins for He 1 – 49 MeV/nuc (26 bins)

4.11.1.3 B_H_Flux H flux side B ($\text{cm}^{-2}\text{sr}^{-1}\text{sec}^{-1}\text{MeV}^{-1}$)
Size: 25 time-varying

particle_flux>differential_directional_number
Energy Bins for H 1 – 41 MeV (25 bins)

4.11.1.4 B_He_Flux He flux side B ($\text{cm}^{-2}\text{sr}^{-1}\text{sec}^{-1}(\text{MeV}/\text{nuc})^{-1}$)
Size: 26 time-varying

particle_flux>differential_directional_number
Energy Bins for He 1 – 49 MeV/nuc (26 bins)

4.11.1.5 R1A_H_SECT_Flux H sectored flux R1A ($\text{cm}^{-2}\text{sr}^{-1}\text{sec}^{-1}\text{MeV}^{-1}$)
Size: 1×9 time-varying

particle_flux>differential_directional_number
Energy Bins for R1 H SECT 1 – 1 MeV (1 bins)
LET1_R1_SECTORS 0 – 8 (9 bins)

4.11.1.6 R1A_He_SECT_Flux He sectored flux R1A ($\text{cm}^{-2}\text{sr}^{-1}\text{sec}^{-1}(\text{MeV}/\text{nuc})^{-1}$)
Size: 1×9 time-varying

particle_flux>differential_directional_number
Energy Bins for R1 He SECT 1 – 1 MeV/nuc (1 bins)
LET1_R1_SECTORS 0 – 8 (9 bins)

4.11.1.7 R1B_H_SECT_Flux H sectored flux R1B ($\text{cm}^{-2}\text{sr}^{-1}\text{sec}^{-1}\text{MeV}^{-1}$)
Size: 1×9 time-varying

particle_flux>differential_directional_number
Energy Bins for R1 H SECT 1 – 1 MeV (1 bins)
LET1_R1_SECTORS 0 – 8 (9 bins)

4.11.1.8 R1B_He_SECT_Flux He sectored flux R1B ($\text{cm}^{-2}\text{sr}^{-1}\text{sec}^{-1}(\text{MeV}/\text{nuc})^{-1}$)
Size: 1×9 time-varying

particle_flux>differential_directional_number
Energy Bins for R1 He SECT 1 – 1 MeV/nuc (1 bins)

LET1_R1_SECTORS 0 – 8 (9 bins)

4.11.1.9 R26A_H_SECT_Flux H sectored flux R26A ($\text{cm}^{-2}\text{sr}^{-1}\text{sec}^{-1}\text{MeV}^{-1}$)

Size: 3×25 time-varying

particle_flux>differential_directional_number

Energy Bins for R26 H SECT 3 – 11 MeV (3 bins)

LET1_R26_SECTORS 0 – 24 (25 bins)

4.11.1.10 R26A_He_SECT_Flux He sectored flux R26A ($\text{cm}^{-2}\text{sr}^{-1}\text{sec}^{-1}(\text{MeV}/\text{nuc})^{-1}$)

Size: 3×25 time-varying

particle_flux>differential_directional_number

Energy Bins for R26 He SECT 3 – 11 MeV/nuc (3 bins)

LET1_R26_SECTORS 0 – 24 (25 bins)

4.11.1.11 R26B_H_SECT_Flux H sectored flux R26B ($\text{cm}^{-2}\text{sr}^{-1}\text{sec}^{-1}\text{MeV}^{-1}$)

Size: 3×25 time-varying

particle_flux>differential_directional_number

Energy Bins for R26 H SECT 3 – 11 MeV (3 bins)

LET1_R26_SECTORS 0 – 24 (25 bins)

4.11.1.12 R26B_He_SECT_Flux He sectored flux R26B ($\text{cm}^{-2}\text{sr}^{-1}\text{sec}^{-1}(\text{MeV}/\text{nuc})^{-1}$)

Size: 3×25 time-varying

particle_flux>differential_directional_number

Energy Bins for R26 He SECT 3 – 11 MeV/nuc (3 bins)

LET1_R26_SECTORS 0 – 24 (25 bins)

OTHER DATA

4.11.2.1 A_Al_Rate Al count rate side A (counts s^{-1})

Size: 28 time-varying

particle_flux>differential_directional_number_rate

Energy Bins for Al 1 – 117 MeV/nuc (28 bins)

4.11.2.2 A_Ar_Rate Ar count rate side A (counts s^{-1})

Size: 29 time-varying

particle_flux>differential_directional_number_rate

Energy Bins for Ar 1 – 140 MeV/nuc (29 bins)

4.11.2.3 A_C_Rate C count rate side A (counts s⁻¹)

Size: 27 time-varying

particle_flux>differential_directional_number_rate

Energy Bins for C 1 – 99 MeV/nuc (27 bins)

4.11.2.4 A_Ca_Rate Ca count rate side A (counts s⁻¹)

Size: 30 time-varying

particle_flux>differential_directional_number_rate

Energy Bins for Ca 1 – 140 MeV/nuc (30 bins)

4.11.2.5 A_Cr_Rate Cr count rate side A (counts s⁻¹)

Size: 31 time-varying

particle_flux>differential_directional_number_rate

Energy Bins for Cr 1 – 140 MeV/nuc (31 bins)

4.11.2.6 A_Fe_Rate Fe count rate side A (counts s⁻¹)

Size: 32 time-varying

particle_flux>differential_directional_number_rate

Energy Bins for Fe 1 – 166 MeV/nuc (32 bins)

4.11.2.7 A_H_Rate H count rate side A (counts s⁻¹)

Size: 25 time-varying

particle_flux>differential_directional_number_rate

Energy Bins for H 1 – 41 MeV (25 bins)

4.11.2.8 A_He_Rate He count rate side A (counts s⁻¹)

Size: 26 time-varying

particle_flux>differential_directional_number_rate

Energy Bins for He 1 – 49 MeV/nuc (26 bins)

4.11.2.9 A_Mg_Rate Mg count rate side A (counts s⁻¹)

Size: 28 time-varying

particle_flux>differential_directional_number_rate
Energy Bins for Mg 1 – 117 MeV/nuc (28 bins)

4.11.2.10 A_N_Rate N count rate side A (counts s⁻¹)

Size: 27 time-varying

particle_flux>differential_directional_number_rate
Energy Bins for N 1 – 99 MeV/nuc (27 bins)

4.11.2.11 A_Na_Rate Na count rate side A (counts s⁻¹)

Size: 28 time-varying

particle_flux>differential_directional_number_rate
Energy Bins for Na 1 – 117 MeV/nuc (28 bins)

4.11.2.12 A_Ne_Rate Ne count rate side A (counts s⁻¹)

Size: 28 time-varying

particle_flux>differential_directional_number_rate
Energy Bins for Ne 1 – 117 MeV/nuc (28 bins)

4.11.2.13 A_Ni_Rate Ni count rate side A (counts s⁻¹)

Size: 33 time-varying

particle_flux>differential_directional_number_rate
Energy Bins for Ni 1 – 197 MeV/nuc (33 bins)

4.11.2.14 A_O_Rate O count rate side A (counts s⁻¹)

Size: 28 time-varying

particle_flux>differential_directional_number_rate
Energy Bins for O 1 – 117 MeV/nuc (28 bins)

4.11.2.15 A_S_Rate S count rate side A (counts s⁻¹)

Size: 29 time-varying

particle_flux>differential_directional_number_rate
Energy Bins for S 1 – 140 MeV/nuc (29 bins)

4.11.2.16 A_Si_Rate Si count rate side A (counts s⁻¹)

Size: 29 time-varying

particle_flux>differential_directional_number_rate

Energy Bins for Si 1 – 140 MeV/nuc (29 bins)

4.11.2.17 B_Al_Rate Al count rate side B (counts s⁻¹)

Size: 28 time-varying

particle_flux>differential_directional_number_rate

Energy Bins for Al 1 – 117 MeV/nuc (28 bins)

4.11.2.18 B_Ar_Rate Ar count rate side B (counts s⁻¹)

Size: 29 time-varying

particle_flux>differential_directional_number_rate

Energy Bins for Ar 1 – 140 MeV/nuc (29 bins)

4.11.2.19 B_C_Rate C count rate side B (counts s⁻¹)

Size: 27 time-varying

particle_flux>differential_directional_number_rate

Energy Bins for C 1 – 99 MeV/nuc (27 bins)

4.11.2.20 B_Ca_Rate Ca count rate side B (counts s⁻¹)

Size: 30 time-varying

particle_flux>differential_directional_number_rate

Energy Bins for Ca 1 – 140 MeV/nuc (30 bins)

4.11.2.21 B_Cr_Rate Cr count rate side B (counts s⁻¹)

Size: 31 time-varying

particle_flux>differential_directional_number_rate

Energy Bins for Cr 1 – 140 MeV/nuc (31 bins)

4.11.2.22 B_Fe_Rate Fe count rate side B (counts s⁻¹)

Size: 32 time-varying

particle_flux>differential_directional_number_rate

Energy Bins for Fe 1 – 166 MeV/nuc (32 bins)

4.11.2.23 B_H_Rate H count rate side B (counts s⁻¹)

Size: 25 time-varying

particle_flux>differential_directional_number_rate

Energy Bins for H 1 – 41 MeV (25 bins)

4.11.2.24 B_He_Rate He count rate side B (counts s⁻¹)

Size: 26 time-varying

particle_flux>differential_directional_number_rate

Energy Bins for He 1 – 49 MeV/nuc (26 bins)

4.11.2.25 B_Mg_Rate Mg count rate side B (counts s⁻¹)

Size: 28 time-varying

particle_flux>differential_directional_number_rate

Energy Bins for Mg 1 – 117 MeV/nuc (28 bins)

4.11.2.26 B_N_Rate N count rate side B (counts s⁻¹)

Size: 27 time-varying

particle_flux>differential_directional_number_rate

Energy Bins for N 1 – 99 MeV/nuc (27 bins)

4.11.2.27 B_Na_Rate Na count rate side B (counts s⁻¹)

Size: 28 time-varying

particle_flux>differential_directional_number_rate

Energy Bins for Na 1 – 117 MeV/nuc (28 bins)

4.11.2.28 B_Ne_Rate Ne count rate side B (counts s⁻¹)

Size: 28 time-varying

particle_flux>differential_directional_number_rate

Energy Bins for Ne 1 – 117 MeV/nuc (28 bins)

4.11.2.29 B_Ni_Rate Ni count rate side B (counts s⁻¹)

Size: 33 time-varying

particle_flux>differential_directional_number_rate

Energy Bins for Ni 1 – 197 MeV/nuc (33 bins)

4.11.2.30 B_O_Rate O count rate side B (counts s⁻¹)

Size: 28 time-varying

particle_flux>differential_directional_number_rate

Energy Bins for O 1 – 117 MeV/nuc (28 bins)

4.11.2.31 B_S_Rate S count rate side B (counts s⁻¹)

Size: 29 time-varying

particle_flux>differential_directional_number_rate

Energy Bins for S 1 – 140 MeV/nuc (29 bins)

4.11.2.32 B_Si_Rate Si count rate side B (counts s⁻¹)

Size: 29 time-varying

particle_flux>differential_directional_number_rate

Energy Bins for Si 1 – 140 MeV/nuc (29 bins)

4.11.2.33 HCI_Lat HCI latitude (degrees)

time-varying

position>latitude

At timestamp. After Fraenz and Harper, PSS, 2002.

4.11.2.34 HCI_Lon HCI longitude (degrees)

time-varying

position>longitude

At timestamp. After Fraenz and Harper, PSS, 2002.

4.11.2.35 HCI_R Heliocentric distance (AU)

time-varying

position>radial

At timestamp. After Fraenz and Harper, PSS, 2002.

4.11.2.36 HGC_Lat HGC latitude (degrees)

time-varying

position>latitude

At timestamp. After Fraenz and Harper, PSS, 2002.

4.11.2.37 HGC_Lon HGC longitude (degrees)

time-varying

position>longitude

At timestamp. After Fraenz and Harper, PSS, 2002.

4.11.2.38 HGC_R Heliocentric distance (AU)

time-varying

position>radial

At timestamp. After Fraenz and Harper, PSS, 2002.

4.11.2.39 LET1_A_HCI HCI flow direction LET1A

Size: 3 time-varying

position>direction

Unit vector, after Fraenz and Harper, PSS, 2002.

4.11.2.40 LET1_A_PA Pitch angle LET1A (degree)

time-varying

position>angle

4.11.2.41 LET1_A_R1_SECT_HCI HCI flow direction LET1AR1SECT

Size: 9×3 time-varying

position>direction

Unit vector, after Fraenz and Harper, PSS, 2002.

LET1_R1_SECTORS 0 – 8 (9 bins)

4.11.2.42 LET1_A_R1_SECT_PA Pitch angle LET1AR1SECT (degree)

Size: 9 time-varying

position>angle

LET1_R1_SECTORS 0 – 8 (9 bins)

4.11.2.43 LET1_A_R1_SECT_RTN RTN flow direction LET1AR1SECT

Size: 9×3 time-varying

position>direction

Unit vector, after Fraenz and Harper, PSS, 2002.

LET1_R1_SECTORS 0 – 8 (9 bins)

4.11.2.44 LET1_A_R1_SECT_SA Nominal Parker Spiral angle LET1AR1SECT (degree)

Size: 9 time-varying

position>angle

Angle between particle direction and nominal outward Parker Spiral, based on 400km/s solar wind and corotation breakdown at 10Rs.

LET1_R1_SECTORS 0 – 8 (9 bins)

4.11.2.45 LET1_A_R26_SECT_HCI HCI flow direction LET1AR26SECT

Size: 25 × 3 time-varying

position>direction

Unit vector, after Fraenz and Harper, PSS, 2002.

LET1_R26_SECTORS 0 – 24 (25 bins)

4.11.2.46 LET1_A_R26_SECT_PA Pitch angle LET1AR26SECT (degree)

Size: 25 time-varying

position>angle

LET1_R26_SECTORS 0 – 24 (25 bins)

4.11.2.47 LET1_A_R26_SECT_RTN RTN flow direction LET1AR26SECT

Size: 25 × 3 time-varying

position>direction

Unit vector, after Fraenz and Harper, PSS, 2002.

LET1_R26_SECTORS 0 – 24 (25 bins)

4.11.2.48 LET1_A_R26_SECT_SA Nominal Parker Spiral angle LET1AR26SECT (degree)

Size: 25 time-varying

position>angle

Angle between particle direction and nominal outward Parker Spiral, based on 400km/s solar wind and corotation breakdown at 10Rs.

LET1_R26_SECTORS 0 – 24 (25 bins)

4.11.2.49 LET1_A_RTN RTN flow direction LET1A

Size: 3 time-varying

position>direction

Unit vector, after Fraenz and Harper, PSS, 2002.

4.11.2.50 LET1_A_SA Nominal Parker Spiral angle LET1A (degree)

time-varying

position>angle

Angle between particle direction and nominal outward Parker Spiral, based on 400km/s solar wind and corotation breakdown at 10Rs.

4.11.2.51 LET1_B_HCI HCI flow direction LET1B

Size: 3 time-varying

position>direction

Unit vector, after Fraenz and Harper, PSS, 2002.

4.11.2.52 LET1_B_PA Pitch angle LET1B (degree)

time-varying

position>angle

4.11.2.53 LET1_B_R1_SECT_HCI HCI flow direction LET1BR1SECT

Size: 9 × 3 time-varying

position>direction

Unit vector, after Fraenz and Harper, PSS, 2002.

LET1_R1_SECTORS 0 – 8 (9 bins)

4.11.2.54 LET1_B_R1_SECT_PA Pitch angle LET1BR1SECT (degree)

Size: 9 time-varying

position>angle

LET1_R1_SECTORS 0 – 8 (9 bins)

4.11.2.55 LET1_B_R1_SECT_RTN RTN flow direction LET1BR1SECT

Size: 9 × 3 time-varying

position>direction

Unit vector, after Fraenz and Harper, PSS, 2002.

LET1_R1_SECTORS 0 – 8 (9 bins)

4.11.2.56 LET1_B_R1_SECT_SA Nominal Parker Spiral angle LET1BR1SECT (degree)

Size: 9 time-varying

position>angle

Angle between particle direction and nominal outward Parker Spiral, based on 400km/s solar wind

and corotation breakdown at 10Rs.
LET1_R1_SECTORS 0 – 8 (9 bins)

4.11.2.57 LET1_B_R26_SECT_HCI HCI flow direction LET1BR26SECT
Size: 25 × 3 time-varying
position>direction
Unit vector, after Fraenz and Harper, PSS, 2002.
LET1_R26_SECTORS 0 – 24 (25 bins)

4.11.2.58 LET1_B_R26_SECT_PA Pitch angle LET1BR26SECT (degree)
Size: 25 time-varying
position>angle
LET1_R26_SECTORS 0 – 24 (25 bins)

4.11.2.59 LET1_B_R26_SECT_RTN RTN flow direction LET1BR26SECT
Size: 25 × 3 time-varying
position>direction
Unit vector, after Fraenz and Harper, PSS, 2002.
LET1_R26_SECTORS 0 – 24 (25 bins)

4.11.2.60 LET1_B_R26_SECT_SA Nominal Parker Spiral angle LET1BR26SECT (degree)
Size: 25 time-varying
position>angle
Angle between particle direction and nominal outward Parker Spiral, based on 400km/s solar wind and corotation breakdown at 10Rs.
LET1_R26_SECTORS 0 – 24 (25 bins)

4.11.2.61 LET1_B_RTN RTN flow direction LET1B
Size: 3 time-varying
position>direction
Unit vector, after Fraenz and Harper, PSS, 2002.

4.11.2.62 LET1_B_SA Nominal Parker Spiral angle LET1B (degree)
time-varying
position>angle
Angle between particle direction and nominal outward Parker Spiral, based on 400km/s solar wind

and corotation breakdown at 10Rs.

4.11.2.63 R1A_H_SECT_Rate H sectored count rate R1A (counts s⁻¹)

Size: 1 × 9 time-varying

particle_flux>differential_directional_number_rate

Energy Bins for R1 H SECT 1 – 1 MeV (1 bins)

LET1_R1_SECTORS 0 – 8 (9 bins)

4.11.2.64 R1A_He_SECT_Rate He sectored count rate R1A (counts s⁻¹)

Size: 1 × 9 time-varying

particle_flux>differential_directional_number_rate

Energy Bins for R1 He SECT 1 – 1 MeV/nuc (1 bins)

LET1_R1_SECTORS 0 – 8 (9 bins)

4.11.2.65 R1B_H_SECT_Rate H sectored count rate R1B (counts s⁻¹)

Size: 1 × 9 time-varying

particle_flux>differential_directional_number_rate

Energy Bins for R1 H SECT 1 – 1 MeV (1 bins)

LET1_R1_SECTORS 0 – 8 (9 bins)

4.11.2.66 R1B_He_SECT_Rate He sectored count rate R1B (counts s⁻¹)

Size: 1 × 9 time-varying

particle_flux>differential_directional_number_rate

Energy Bins for R1 He SECT 1 – 1 MeV/nuc (1 bins)

LET1_R1_SECTORS 0 – 8 (9 bins)

4.11.2.67 R26A_H_SECT_Rate H sectored count rate R26A (counts s⁻¹)

Size: 3 × 25 time-varying

particle_flux>differential_directional_number_rate

Energy Bins for R26 H SECT 3 – 11 MeV (3 bins)

LET1_R26_SECTORS 0 – 24 (25 bins)

4.11.2.68 R26A_He_SECT_Rate He sectored count rate R26A (counts s⁻¹)

Size: 3 × 25 time-varying

particle_flux>differential_directional_number_rate

Energy Bins for R26 He SECT 3 – 11 MeV/nuc (3 bins)

LET1_R26_SECTORS 0 – 24 (25 bins)

4.11.2.69 R26B_H_SECT_Rate H sectored count rate R26B (counts s⁻¹)

Size: 3 × 25 time-varying

particle_flux>differential_directional_number_rate

Energy Bins for R26 H SECT 3 – 11 MeV (3 bins)

LET1_R26_SECTORS 0 – 24 (25 bins)

4.11.2.70 R26B_He_SECT_Rate He sectored count rate R26B (counts s⁻¹)

Size: 3 × 25 time-varying

particle_flux>differential_directional_number_rate

Energy Bins for R26 He SECT 3 – 11 MeV/nuc (3 bins)

LET1_R26_SECTORS 0 – 24 (25 bins)

OTHER SUPPORT

PSP_ISOIS-EPIHI_L2-LET2-RATES10

ISOIS-EPIHI>Integrated Science Investigation of the Sun, Energetic Particle Instrument Hi

L2-LET2-rates10>Level 2 LET2 10-second rates

EPI-Hi 10 second rates cdf. Time tags indicate midpoint of integration.

Instrument paper: Integrated Science Investigation of the Sun (ISIS): Design of the Energetic Particle Investigation. McComas, D. J. et al (2016). Space Sci. Rev., doi:10.1007/s11214-014-0059-1

1 minute to 1 hour

Cite McComas et al (2016), doi:10.1007/s11214-014-0059-1

PRIMARY VARIABLES

4.12.1.1 C_H_Flux H flux side C (cm⁻²sr⁻¹sec⁻¹MeV⁻¹)

Size: 18 time-varying

particle_flux>differential_directional_number

Energy Bins for H 1 – 15 MeV (18 bins)

4.12.1.2 C_He_Flux He flux side C (cm⁻²sr⁻¹sec⁻¹(MeV/nuc)⁻¹)

Size: 22 time-varying

particle_flux>differential_directional_number

Energy Bins for He 1 – 29 MeV/nuc (22 bins)

OTHER DATA

4.12.2.1 C_H_Rate H count rate side C (counts s⁻¹)

Size: 18 time-varying

particle_flux>differential_directional_number_rate

Energy Bins for H 1 – 15 MeV (18 bins)

4.12.2.2 C_He_Rate He count rate side C (counts s⁻¹)

Size: 22 time-varying

particle_flux>differential_directional_number_rate

Energy Bins for He 1 – 29 MeV/nuc (22 bins)

4.12.2.3 HCI_Lat HCI latitude (degrees)

time-varying

position>latitude

At timestamp. After Fraenz and Harper, PSS, 2002.

4.12.2.4 HCI_Lon HCI longitude (degrees)

time-varying

position>longitude

At timestamp. After Fraenz and Harper, PSS, 2002.

4.12.2.5 HCI_R Heliocentric distance (AU)

time-varying

position>radial

At timestamp. After Fraenz and Harper, PSS, 2002.

4.12.2.6 HGC_Lat HGC latitude (degrees)

time-varying

position>latitude

At timestamp. After Fraenz and Harper, PSS, 2002.

4.12.2.7 HGC_Lon HGC longitude (degrees)

time-varying

position>longitude

At timestamp. After Fraenz and Harper, PSS, 2002.

4.12.2.8 HGC_R Heliocentric distance (AU)

time-varying

position>radial

At timestamp. After Fraenz and Harper, PSS, 2002.

4.12.2.9 LET2_C_HCI HCI flow direction LET2C

Size: 3 time-varying

position>direction

Unit vector, after Fraenz and Harper, PSS, 2002.

4.12.2.10 LET2_C_PA Pitch angle LET2C (degree)

time-varying

position>angle

4.12.2.11 LET2_C_RTN RTN flow direction LET2C

Size: 3 time-varying

position>direction

Unit vector, after Fraenz and Harper, PSS, 2002.

4.12.2.12 LET2_C_SA Nominal Parker Spiral angle LET2C (degree)

time-varying

position>angle

Angle between particle direction and nominal outward Parker Spiral, based on 400km/s solar wind and corotation breakdown at 10Rs.

OTHER SUPPORT

PSP_ISOIS-EPIHI_L2-LET2-RATES300

ISOIS-EPIHI>Integrated Science Investigation of the Sun, Energetic Particle Instrument Hi

L2-LET2-rates300>Level 2 LET2 5-minute rates

EPI-Hi LET2 300 second rates cdf. Time tags indicate midpoint of integration.

Instrument paper: Integrated Science Investigation of the Sun (ISIS): Design of the Energetic Particle Investigation. McComas, D. J. et al (2016). Space Sci. Rev., doi:10.1007/s11214-014-0059-1

1 minute to 1 hour

Cite McComas et al (2016), doi:10.1007/s11214-014-0059-1

PRIMARY VARIABLES

OTHER DATA

4.13.2.1 HCI_Lat HCI latitude (degrees)
time-varying
position>latitude
At timestamp. After Fraenz and Harper, PSS, 2002.

4.13.2.2 HCI_Lon HCI longitude (degrees)
time-varying
position>longitude
At timestamp. After Fraenz and Harper, PSS, 2002.

4.13.2.3 HCI_R Heliocentric distance (AU)
time-varying
position>radial
At timestamp. After Fraenz and Harper, PSS, 2002.

4.13.2.4 HGC_Lat HGC latitude (degrees)
time-varying
position>latitude
At timestamp. After Fraenz and Harper, PSS, 2002.

4.13.2.5 HGC_Lon HGC longitude (degrees)
time-varying
position>longitude
At timestamp. After Fraenz and Harper, PSS, 2002.

4.13.2.6 HGC_R Heliocentric distance (AU)
time-varying
position>radial
At timestamp. After Fraenz and Harper, PSS, 2002.

4.13.2.7 LET2_C_HCI HCI flow direction LET2C
Size: 3 time-varying
position>direction

Unit vector, after Fraenz and Harper, PSS, 2002.

4.13.2.8 LET2_C_PA Pitch angle LET2C (degree)

time-varying

position>angle

4.13.2.9 LET2_C_R1_SECT_HCI HCI flow direction LET2CR1SECT

Size: 9×3 time-varying

position>direction

Unit vector, after Fraenz and Harper, PSS, 2002.

LET2_R1_SECTORS 0 – 8 (9 bins)

4.13.2.10 LET2_C_R1_SECT_PA Pitch angle LET2CR1SECT (degree)

Size: 9 time-varying

position>angle

LET2_R1_SECTORS 0 – 8 (9 bins)

4.13.2.11 LET2_C_R1_SECT_RTN RTN flow direction LET2CR1SECT

Size: 9×3 time-varying

position>direction

Unit vector, after Fraenz and Harper, PSS, 2002.

LET2_R1_SECTORS 0 – 8 (9 bins)

4.13.2.12 LET2_C_R1_SECT_SA Nominal Parker Spiral angle LET2CR1SECT (degree)

Size: 9 time-varying

position>angle

Angle between particle direction and nominal outward Parker Spiral, based on 400km/s solar wind and corotation breakdown at 10Rs.

LET2_R1_SECTORS 0 – 8 (9 bins)

4.13.2.13 LET2_C_R25_SECT_HCI HCI flow direction LET2CR25SECT

Size: 25×3 time-varying

position>direction

Unit vector, after Fraenz and Harper, PSS, 2002.

LET2_R25_SECTORS 0 – 24 (25 bins)

4.13.2.14 LET2_C_R25_SECT_PA Pitch angle LET2CR25SECT (degree)

Size: 25 time-varying

position>angle

LET2_R25_SECTORS 0 – 24 (25 bins)

4.13.2.15 LET2_C_R25_SECT_RTN RTN flow direction LET2CR25SECT

Size: 25 × 3 time-varying

position>direction

Unit vector, after Fraenz and Harper, PSS, 2002.

LET2_R25_SECTORS 0 – 24 (25 bins)

4.13.2.16 LET2_C_R25_SECT_SA Nominal Parker Spiral angle LET2CR25SECT (degree)

Size: 25 time-varying

position>angle

Angle between particle direction and nominal outward Parker Spiral, based on 400km/s solar wind and corotation breakdown at 10Rs.

LET2_R25_SECTORS 0 – 24 (25 bins)

4.13.2.17 LET2_C_RTN RTN flow direction LET2C

Size: 3 time-varying

position>direction

Unit vector, after Fraenz and Harper, PSS, 2002.

4.13.2.18 LET2_C_SA Nominal Parker Spiral angle LET2C (degree)

time-varying

position>angle

Angle between particle direction and nominal outward Parker Spiral, based on 400km/s solar wind and corotation breakdown at 10Rs.

4.13.2.19 R1C_CNO_SECT_Rate CNO sectored count rate R1C (counts s⁻¹)

Size: 1 × 9 time-varying

particle_flux>differential_directional_number_rate

Energy Bins for R1 CNO SECT 3 – 3 MeV/nuc (1 bins)

LET2_R1_SECTORS 0 – 8 (9 bins)

4.13.2.20 RIC_FeGroup_SECT_Rate FeGroup sectored count rate RIC (counts s⁻¹)

Size: 1 × 9 time-varying

particle_flux>differential_directional_number_rate

Energy Bins for R1 FeGroup SECT 3 – 3 MeV/nuc (1 bins)

LET2_R1_SECTORS 0 – 8 (9 bins)

4.13.2.21 RIC_NetoSi_SECT_Rate NetoSis sectored count rate RIC (counts s⁻¹)

Size: 1 × 9 time-varying

particle_flux>differential_directional_number_rate

Energy Bins for R1 NetoSis SECT 3 – 3 MeV/nuc (1 bins)

LET2_R1_SECTORS 0 – 8 (9 bins)

4.13.2.22 R25C_CNO_SECT_Rate CNO sectored count rate R25C (counts s⁻¹)

Size: 3 × 25 time-varying

particle_flux>differential_directional_number_rate

Energy Bins for R25 CNO SECT 6 – 23 MeV/nuc (3 bins)

LET2_R25_SECTORS 0 – 24 (25 bins)

4.13.2.23 R25C_FeGroup_SECT_Rate FeGroup sectored count rate R25C (counts s⁻¹)

Size: 3 × 25 time-varying

particle_flux>differential_directional_number_rate

Energy Bins for R25 FeGroup SECT 6 – 23 MeV/nuc (3 bins)

LET2_R25_SECTORS 0 – 24 (25 bins)

4.13.2.24 R25C_NetoSi_SECT_Rate NetoSis sectored count rate R25C (counts s⁻¹)

Size: 3 × 25 time-varying

particle_flux>differential_directional_number_rate

Energy Bins for R25 NetoSis SECT 6 – 23 MeV/nuc (3 bins)

LET2_R25_SECTORS 0 – 24 (25 bins)

OTHER SUPPORT

PSP_ISOIS-EPIHI_L2-LET2-RATES3600

ISOIS-EPIHI>Integrated Science Investigation of the Sun, Energetic Particle Instrument Hi

L2-LET2-rates3600>Level 2 LET2 hourly rates

EPI-Hi LET2 3600 second rates cdf. Time tags indicate midpoint of integration.

Instrument paper: Integrated Science Investigation of the Sun (ISIS): Design of the Energetic

Particle Investigation. McComas, D. J. et al (2016). Space Sci. Rev., doi:10.1007/s11214-014-0059-1

1 minute to 1 hour

Cite McComas et al (2016), doi:10.1007/s11214-014-0059-1

PRIMARY VARIABLES

4.14.1.1 C_H_Flux H flux side C ($\text{cm}^{-2}\text{sr}^{-1}\text{sec}^{-1}\text{MeV}^{-1}$)

Size: 24 time-varying

particle_flux>differential_directional_number

Energy Bins for H 1 – 35 MeV (24 bins)

4.14.1.2 C_He_Flux He flux side C ($\text{cm}^{-2}\text{sr}^{-1}\text{sec}^{-1}(\text{MeV}/\text{nuc})^{-1}$)

Size: 25 time-varying

particle_flux>differential_directional_number

Energy Bins for He 1 – 41 MeV/nuc (25 bins)

4.14.1.3 R1C_H_SECT_Flux H sectored flux R1C ($\text{cm}^{-2}\text{sr}^{-1}\text{sec}^{-1}\text{MeV}^{-1}$)

Size: 1×9 time-varying

particle_flux>differential_directional_number

Energy Bins for R1 H SECT 1 – 1 MeV (1 bins)

LET2_R1_SECTORS 0 – 8 (9 bins)

4.14.1.4 R1C_He_SECT_Flux He sectored flux R1C ($\text{cm}^{-2}\text{sr}^{-1}\text{sec}^{-1}(\text{MeV}/\text{nuc})^{-1}$)

Size: 1×9 time-varying

particle_flux>differential_directional_number

Energy Bins for R1 He SECT 1 – 1 MeV/nuc (1 bins)

LET2_R1_SECTORS 0 – 8 (9 bins)

4.14.1.5 R25C_H_SECT_Flux H sectored flux R25C ($\text{cm}^{-2}\text{sr}^{-1}\text{sec}^{-1}\text{MeV}^{-1}$)

Size: 3×25 time-varying

particle_flux>differential_directional_number

Energy Bins for R25 H SECT 3 – 11 MeV (3 bins)

LET2_R25_SECTORS 0 – 24 (25 bins)

4.14.1.6 R25C_He_SECT_Flux He sectored flux R25C ($\text{cm}^{-2}\text{sr}^{-1}\text{sec}^{-1}(\text{MeV}/\text{nuc})^{-1}$)

Size: 3×25 time-varying

particle_flux>differential_directional_number
Energy Bins for R25 He SECT 3 – 11 MeV/nuc (3 bins)
LET2_R25_SECTORS 0 – 24 (25 bins)

OTHER DATA

4.14.2.1 C_Al_Rate Al count rate side C (counts s⁻¹)

Size: 27 time-varying

particle_flux>differential_directional_number_rate
Energy Bins for Al 1 – 99 MeV/nuc (27 bins)

4.14.2.2 C_Ar_Rate Ar count rate side C (counts s⁻¹)

Size: 28 time-varying

particle_flux>differential_directional_number_rate
Energy Bins for Ar 1 – 117 MeV/nuc (28 bins)

4.14.2.3 C_C_Rate C count rate side C (counts s⁻¹)

Size: 25 time-varying

particle_flux>differential_directional_number_rate
Energy Bins for C 1 – 70 MeV/nuc (25 bins)

4.14.2.4 C_Ca_Rate Ca count rate side C (counts s⁻¹)

Size: 30 time-varying

particle_flux>differential_directional_number_rate
Energy Bins for Ca 1 – 140 MeV/nuc (30 bins)

4.14.2.5 C_Cr_Rate Cr count rate side C (counts s⁻¹)

Size: 31 time-varying

particle_flux>differential_directional_number_rate
Energy Bins for Cr 1 – 140 MeV/nuc (31 bins)

4.14.2.6 C_Fe_Rate Fe count rate side C (counts s⁻¹)

Size: 31 time-varying

particle_flux>differential_directional_number_rate
Energy Bins for Fe 1 – 140 MeV/nuc (31 bins)

4.14.2.7 C_H_Rate H count rate side C (counts s⁻¹)

Size: 24 time-varying

particle_flux>differential_directional_number_rate

Energy Bins for H 1 – 35 MeV (24 bins)

4.14.2.8 C_He_Rate He count rate side C (counts s⁻¹)

Size: 25 time-varying

particle_flux>differential_directional_number_rate

Energy Bins for He 1 – 41 MeV/nuc (25 bins)

4.14.2.9 C_Mg_Rate Mg count rate side C (counts s⁻¹)

Size: 27 time-varying

particle_flux>differential_directional_number_rate

Energy Bins for Mg 1 – 99 MeV/nuc (27 bins)

4.14.2.10 C_N_Rate N count rate side C (counts s⁻¹)

Size: 25 time-varying

particle_flux>differential_directional_number_rate

Energy Bins for N 1 – 70 MeV/nuc (25 bins)

4.14.2.11 C_Na_Rate Na count rate side C (counts s⁻¹)

Size: 27 time-varying

particle_flux>differential_directional_number_rate

Energy Bins for Na 1 – 99 MeV/nuc (27 bins)

4.14.2.12 C_Ne_Rate Ne count rate side C (counts s⁻¹)

Size: 27 time-varying

particle_flux>differential_directional_number_rate

Energy Bins for Ne 1 – 99 MeV/nuc (27 bins)

4.14.2.13 C_Ni_Rate Ni count rate side C (counts s⁻¹)

Size: 32 time-varying

particle_flux>differential_directional_number_rate

Energy Bins for Ni 1 – 166 MeV/nuc (32 bins)

4.14.2.14 C_O_Rate O count rate side C (counts s⁻¹)

Size: 26 time-varying

particle_flux>differential_directional_number_rate

Energy Bins for O 1 – 83 MeV/nuc (26 bins)

4.14.2.15 C_S_Rate S count rate side C (counts s⁻¹)

Size: 28 time-varying

particle_flux>differential_directional_number_rate

Energy Bins for S 1 – 117 MeV/nuc (28 bins)

4.14.2.16 C_Si_Rate Si count rate side C (counts s⁻¹)

Size: 28 time-varying

particle_flux>differential_directional_number_rate

Energy Bins for Si 1 – 117 MeV/nuc (28 bins)

4.14.2.17 HCI_Lat HCI latitude (degrees)

time-varying

position>latitude

At timestamp. After Fraenz and Harper, PSS, 2002.

4.14.2.18 HCI_Lon HCI longitude (degrees)

time-varying

position>longitude

At timestamp. After Fraenz and Harper, PSS, 2002.

4.14.2.19 HCI_R Heliocentric distance (AU)

time-varying

position>radial

At timestamp. After Fraenz and Harper, PSS, 2002.

4.14.2.20 HGC_Lat HGC latitude (degrees)

time-varying

position>latitude

At timestamp. After Fraenz and Harper, PSS, 2002.

4.14.2.21 HGC_Lon HGC longitude (degrees)
time-varying
position>longitude
At timestamp. After Fraenz and Harper, PSS, 2002.

4.14.2.22 HGC_R Heliocentric distance (AU)
time-varying
position>radial
At timestamp. After Fraenz and Harper, PSS, 2002.

4.14.2.23 LET2_C_HCI HCI flow direction LET2C
Size: 3 time-varying
position>direction
Unit vector, after Fraenz and Harper, PSS, 2002.

4.14.2.24 LET2_C_PA Pitch angle LET2C (degree)
time-varying
position>angle

4.14.2.25 LET2_C_R1_SECT_HCI HCI flow direction LET2CR1SECT
Size: 9×3 time-varying
position>direction
Unit vector, after Fraenz and Harper, PSS, 2002.
LET2_R1_SECTORS 0 – 8 (9 bins)

4.14.2.26 LET2_C_R1_SECT_PA Pitch angle LET2CR1SECT (degree)
Size: 9 time-varying
position>angle
LET2_R1_SECTORS 0 – 8 (9 bins)

4.14.2.27 LET2_C_R1_SECT_RTN RTN flow direction LET2CR1SECT
Size: 9×3 time-varying
position>direction
Unit vector, after Fraenz and Harper, PSS, 2002.
LET2_R1_SECTORS 0 – 8 (9 bins)

4.14.2.28 LET2_C_R1_SECT_SA Nominal Parker Spiral angle LET2CR1SECT (degree)

Size: 9 time-varying

position>angle

Angle between particle direction and nominal outward Parker Spiral, based on 400km/s solar wind and corotation breakdown at 10Rs.

LET2_R1_SECTORS 0 – 8 (9 bins)

4.14.2.29 LET2_C_R25_SECT_HCI HCI flow direction LET2CR25SECT

Size: 25 × 3 time-varying

position>direction

Unit vector, after Fraenz and Harper, PSS, 2002.

LET2_R25_SECTORS 0 – 24 (25 bins)

4.14.2.30 LET2_C_R25_SECT_PA Pitch angle LET2CR25SECT (degree)

Size: 25 time-varying

position>angle

LET2_R25_SECTORS 0 – 24 (25 bins)

4.14.2.31 LET2_C_R25_SECT_RTN RTN flow direction LET2CR25SECT

Size: 25 × 3 time-varying

position>direction

Unit vector, after Fraenz and Harper, PSS, 2002.

LET2_R25_SECTORS 0 – 24 (25 bins)

4.14.2.32 LET2_C_R25_SECT_SA Nominal Parker Spiral angle LET2CR25SECT (degree)

Size: 25 time-varying

position>angle

Angle between particle direction and nominal outward Parker Spiral, based on 400km/s solar wind and corotation breakdown at 10Rs.

LET2_R25_SECTORS 0 – 24 (25 bins)

4.14.2.33 LET2_C_RTN RTN flow direction LET2C

Size: 3 time-varying

position>direction

Unit vector, after Fraenz and Harper, PSS, 2002.

4.14.2.34 LET2_C_SA Nominal Parker Spiral angle LET2C (degree)

time-varying

position>angle

Angle between particle direction and nominal outward Parker Spiral, based on 400km/s solar wind and corotation breakdown at 10Rs.

4.14.2.35 RIC_CNO_SECT_Rate CNO sectored count rate RIC (counts s⁻¹)

Size: 1 × 9 time-varying

particle_flux>differential_directional_number_rate

Energy Bins for R1 CNO SECT 3 – 3 MeV/nuc (1 bins)

LET2_R1_SECTORS 0 – 8 (9 bins)

4.14.2.36 RIC_FeGroup_SECT_Rate FeGroup sectored count rate RIC (counts s⁻¹)

Size: 1 × 9 time-varying

particle_flux>differential_directional_number_rate

Energy Bins for R1 FeGroup SECT 3 – 3 MeV/nuc (1 bins)

LET2_R1_SECTORS 0 – 8 (9 bins)

4.14.2.37 RIC_H_SECT_Rate H sectored count rate RIC (counts s⁻¹)

Size: 1 × 9 time-varying

particle_flux>differential_directional_number_rate

Energy Bins for R1 H SECT 1 – 1 MeV (1 bins)

LET2_R1_SECTORS 0 – 8 (9 bins)

4.14.2.38 RIC_He_BIN RIC He Rates (counts)

Size: 5 × 16 time-varying

particle_flux>differential_directional_number_rate

Energy Bins for R1 He BIN 1 – 3 MeV/nuc (5 bins)

RIC_He_BIN_MASS_BIN 0 – 15 segment (16 bins)

4.14.2.39 RIC_He_SECT_Rate He sectored count rate RIC (counts s⁻¹)

Size: 1 × 9 time-varying

particle_flux>differential_directional_number_rate

Energy Bins for R1 He SECT 1 – 1 MeV/nuc (1 bins)

LET2_R1_SECTORS 0 – 8 (9 bins)

4.14.2.40 RIC_Ne_BIN RIC Ne Rates (counts)

Size: 5×8 time-varying

particle_flux>differential_directional_number_rate

Energy Bins for R1 Ne BIN 1 – 6 MeV/nuc (5 bins)

RIC_Ne_BIN_MASS_BIN 0 – 7 segment (8 bins)

4.14.2.41 RIC_NetoSi_SECT_Rate NetoS_i sectored count rate R1C (counts s⁻¹)

Size: 1×9 time-varying

particle_flux>differential_directional_number_rate

Energy Bins for R1 NetoS_i SECT 3 – 3 MeV/nuc (1 bins)

LET2_R1_SECTORS 0 – 8 (9 bins)

4.14.2.42 R25C_CNO_SECT_Rate CNO sectored count rate R25C (counts s⁻¹)

Size: 3×25 time-varying

particle_flux>differential_directional_number_rate

Energy Bins for R25 CNO SECT 6 – 23 MeV/nuc (3 bins)

LET2_R25_SECTORS 0 – 24 (25 bins)

4.14.2.43 R25C_FeGroup_SECT_Rate FeGroup sectored count rate R25C (counts s⁻¹)

Size: 3×25 time-varying

particle_flux>differential_directional_number_rate

Energy Bins for R25 FeGroup SECT 6 – 23 MeV/nuc (3 bins)

LET2_R25_SECTORS 0 – 24 (25 bins)

4.14.2.44 R25C_H_SECT_Rate H sectored count rate R25C (counts s⁻¹)

Size: 3×25 time-varying

particle_flux>differential_directional_number_rate

Energy Bins for R25 H SECT 3 – 11 MeV (3 bins)

LET2_R25_SECTORS 0 – 24 (25 bins)

4.14.2.45 R25C_He_SECT_Rate He sectored count rate R25C (counts s⁻¹)

Size: 3×25 time-varying

particle_flux>differential_directional_number_rate

Energy Bins for R25 He SECT 3 – 11 MeV/nuc (3 bins)

LET2_R25_SECTORS 0 – 24 (25 bins)

4.14.2.46 R25C_NetoSi_SECT_Rate NetoS i sectored count rate R25C (counts s $^{-1}$)

Size: 3 \times 25 time-varying

particle_flux>differential_directional_number_rate

Energy Bins for R25 NetoS i SECT 6 – 23 MeV/nuc (3 bins)

LET2_R25_SECTORS 0 – 24 (25 bins)

4.14.2.47 R2C_He_BIN R2C He Rates (counts)

Size: 7 \times 16 time-varying

particle_flux>differential_directional_number_rate

Energy Bins for R2 He BIN 2 – 16 MeV/nuc (7 bins)

R2C_He_BIN_MASS_BIN 0 – 15 segment (16 bins)

4.14.2.48 R2C_Ne_BIN R2C Ne Rates (counts)

Size: 8 \times 8 time-varying

particle_flux>differential_directional_number_rate

Energy Bins for R2 Ne BIN 3 – 32 MeV/nuc (8 bins)

R2C_Ne_BIN_MASS_BIN 0 – 7 segment (8 bins)

4.14.2.49 R3C_He_BIN R3C He Rates (counts)

Size: 5 \times 16 time-varying

particle_flux>differential_directional_number_rate

Energy Bins for R3 He BIN 8 – 32 MeV/nuc (5 bins)

R3C_He_BIN_MASS_BIN 0 – 15 segment (16 bins)

4.14.2.50 R3C_Ne_BIN R3C Ne Rates (counts)

Size: 6 \times 8 time-varying

particle_flux>differential_directional_number_rate

Energy Bins for R3 Ne BIN 16 – 91 MeV/nuc (6 bins)

R3C_Ne_BIN_MASS_BIN 0 – 7 segment (8 bins)

4.14.2.51 R45C_He_BIN R45C He Rates (counts)

Size: 5 \times 16 time-varying

particle_flux>differential_directional_number_rate

Energy Bins for R45 He BIN 8 – 32 MeV/nuc (5 bins)

R45C_He_BIN_MASS_BIN 0 – 15 segment (16 bins)

4.14.2.52 R45C_Ne_BIN R45C Ne Rates (counts)

Size: 6×8 time-varying

particle_flux>differential_directional_number_rate

Energy Bins for R45 Ne BIN 16 – 91 MeV/nuc (6 bins)

R45C_Ne_BIN_MASS_BIN 0 – 7 segment (8 bins)

OTHER SUPPORT

PSP_ISOIS-EPIHI_L2-LET2-RATES60

ISOIS-EPIHI>Integrated Science Investigation of the Sun, Energetic Particle Instrument Hi
L2-LET2-rates60>Level 2 LET2 1-minute rates

EPI-Hi LET2 60 second rates cdf. Time tags indicate midpoint of integration.

Instrument paper: Integrated Science Investigation of the Sun (ISIS): Design of the Energetic Particle Investigation. McComas, D. J. et al (2016). Space Sci. Rev., doi:10.1007/s11214-014-0059-1

1 minute to 1 hour

Cite McComas et al (2016), doi:10.1007/s11214-014-0059-1

PRIMARY VARIABLES

4.15.1.1 C_H_Flux H flux side C ($\text{cm}^{-2}\text{sr}^{-1}\text{sec}^{-1}\text{MeV}^{-1}$)

Size: 24 time-varying

particle_flux>differential_directional_number

Energy Bins for H 1 – 35 MeV (24 bins)

4.15.1.2 C_He_Flux He flux side C ($\text{cm}^{-2}\text{sr}^{-1}\text{sec}^{-1}(\text{MeV}/\text{nuc})^{-1}$)

Size: 25 time-varying

particle_flux>differential_directional_number

Energy Bins for He 1 – 41 MeV/nuc (25 bins)

4.15.1.3 R1C_H_SECT_Flux H sectored flux R1C ($\text{cm}^{-2}\text{sr}^{-1}\text{sec}^{-1}\text{MeV}^{-1}$)

Size: 1×9 time-varying

particle_flux>differential_directional_number

Energy Bins for R1 H SECT 1 – 1 MeV (1 bins)

LET2_R1_SECTORS 0 – 8 (9 bins)

4.15.1.4 R1C_He_SECT_Flux He sectored flux R1C ($\text{cm}^{-2}\text{sr}^{-1}\text{sec}^{-1}(\text{MeV}/\text{nuc})^{-1}$)

Size: 1×9 time-varying

particle_flux>differential_directional_number

Energy Bins for R1 He SECT 1 – 1 MeV/nuc (1 bins)
LET2_R1_SECTORS 0 – 8 (9 bins)

4.15.1.5 R25C_H_SECT_Flux H sectored flux R25C ($\text{cm}^{-2}\text{sr}^{-1}\text{sec}^{-1}\text{MeV}^{-1}$)
Size: 3×25 time-varying
particle_flux>differential_directional_number
Energy Bins for R25 H SECT 3 – 11 MeV (3 bins)
LET2_R25_SECTORS 0 – 24 (25 bins)

4.15.1.6 R25C_He_SECT_Flux He sectored flux R25C ($\text{cm}^{-2}\text{sr}^{-1}\text{sec}^{-1}(\text{MeV}/\text{nuc})^{-1}$)
Size: 3×25 time-varying
particle_flux>differential_directional_number
Energy Bins for R25 He SECT 3 – 11 MeV/nuc (3 bins)
LET2_R25_SECTORS 0 – 24 (25 bins)

OTHER DATA

4.15.2.1 C_Al_Rate Al count rate side C (counts s^{-1})
Size: 27 time-varying
particle_flux>differential_directional_number_rate
Energy Bins for Al 1 – 99 MeV/nuc (27 bins)

4.15.2.2 C_Ar_Rate Ar count rate side C (counts s^{-1})
Size: 28 time-varying
particle_flux>differential_directional_number_rate
Energy Bins for Ar 1 – 117 MeV/nuc (28 bins)

4.15.2.3 C_C_Rate C count rate side C (counts s^{-1})
Size: 25 time-varying
particle_flux>differential_directional_number_rate
Energy Bins for C 1 – 70 MeV/nuc (25 bins)

4.15.2.4 C_Ca_Rate Ca count rate side C (counts s^{-1})
Size: 30 time-varying
particle_flux>differential_directional_number_rate
Energy Bins for Ca 1 – 140 MeV/nuc (30 bins)

4.15.2.5 C_Cr_Rate Cr count rate side C (counts s⁻¹)

Size: 31 time-varying

particle_flux>differential_directional_number_rate

Energy Bins for Cr 1 – 140 MeV/nuc (31 bins)

4.15.2.6 C_Fe_Rate Fe count rate side C (counts s⁻¹)

Size: 31 time-varying

particle_flux>differential_directional_number_rate

Energy Bins for Fe 1 – 140 MeV/nuc (31 bins)

4.15.2.7 C_H_Rate H count rate side C (counts s⁻¹)

Size: 24 time-varying

particle_flux>differential_directional_number_rate

Energy Bins for H 1 – 35 MeV (24 bins)

4.15.2.8 C_He_Rate He count rate side C (counts s⁻¹)

Size: 25 time-varying

particle_flux>differential_directional_number_rate

Energy Bins for He 1 – 41 MeV/nuc (25 bins)

4.15.2.9 C_Mg_Rate Mg count rate side C (counts s⁻¹)

Size: 27 time-varying

particle_flux>differential_directional_number_rate

Energy Bins for Mg 1 – 99 MeV/nuc (27 bins)

4.15.2.10 C_N_Rate N count rate side C (counts s⁻¹)

Size: 25 time-varying

particle_flux>differential_directional_number_rate

Energy Bins for N 1 – 70 MeV/nuc (25 bins)

4.15.2.11 C_Na_Rate Na count rate side C (counts s⁻¹)

Size: 27 time-varying

particle_flux>differential_directional_number_rate

Energy Bins for Na 1 – 99 MeV/nuc (27 bins)

4.15.2.12 C_Ne_Rate Ne count rate side C (counts s⁻¹)

Size: 27 time-varying

particle_flux>differential_directional_number_rate

Energy Bins for Ne 1 – 99 MeV/nuc (27 bins)

4.15.2.13 C_Ni_Rate Ni count rate side C (counts s⁻¹)

Size: 32 time-varying

particle_flux>differential_directional_number_rate

Energy Bins for Ni 1 – 166 MeV/nuc (32 bins)

4.15.2.14 C_O_Rate O count rate side C (counts s⁻¹)

Size: 26 time-varying

particle_flux>differential_directional_number_rate

Energy Bins for O 1 – 83 MeV/nuc (26 bins)

4.15.2.15 C_S_Rate S count rate side C (counts s⁻¹)

Size: 28 time-varying

particle_flux>differential_directional_number_rate

Energy Bins for S 1 – 117 MeV/nuc (28 bins)

4.15.2.16 C_Si_Rate Si count rate side C (counts s⁻¹)

Size: 28 time-varying

particle_flux>differential_directional_number_rate

Energy Bins for Si 1 – 117 MeV/nuc (28 bins)

4.15.2.17 HCI_Lat HCI latitude (degrees)

time-varying

position>latitude

At timestamp. After Fraenz and Harper, PSS, 2002.

4.15.2.18 HCI_Lon HCI longitude (degrees)

time-varying

position>longitude

At timestamp. After Fraenz and Harper, PSS, 2002.

4.15.2.19 HCI_R Heliocentric distance (AU)
time-varying
position>radial
At timestamp. After Fraenz and Harper, PSS, 2002.

4.15.2.20 HGC_Lat HGC latitude (degrees)
time-varying
position>latitude
At timestamp. After Fraenz and Harper, PSS, 2002.

4.15.2.21 HGC_Lon HGC longitude (degrees)
time-varying
position>longitude
At timestamp. After Fraenz and Harper, PSS, 2002.

4.15.2.22 HGC_R Heliocentric distance (AU)
time-varying
position>radial
At timestamp. After Fraenz and Harper, PSS, 2002.

4.15.2.23 LET2_C_HCI HCI flow direction LET2C
Size: 3 time-varying
position>direction
Unit vector, after Fraenz and Harper, PSS, 2002.

4.15.2.24 LET2_C_PA Pitch angle LET2C (degree)
time-varying
position>angle

4.15.2.25 LET2_C_R1_SECT_HCI HCI flow direction LET2CR1SECT
Size: 9×3 time-varying
position>direction
Unit vector, after Fraenz and Harper, PSS, 2002.
LET2_R1_SECTORS 0 – 8 (9 bins)

4.15.2.26 LET2_C_R1_SECT_PA Pitch angle LET2CR1SECT (degree)

Size: 9 time-varying

position>angle

LET2_R1_SECTORS 0 – 8 (9 bins)

4.15.2.27 LET2_C_R1_SECT_RTN RTN flow direction LET2CR1SECT

Size: 9×3 time-varying

position>direction

Unit vector, after Fraenz and Harper, PSS, 2002.

LET2_R1_SECTORS 0 – 8 (9 bins)

4.15.2.28 LET2_C_R1_SECT_SA Nominal Parker Spiral angle LET2CR1SECT (degree)

Size: 9 time-varying

position>angle

Angle between particle direction and nominal outward Parker Spiral, based on 400km/s solar wind and corotation breakdown at 10Rs.

LET2_R1_SECTORS 0 – 8 (9 bins)

4.15.2.29 LET2_C_R25_SECT_HCI HCI flow direction LET2CR25SECT

Size: 25×3 time-varying

position>direction

Unit vector, after Fraenz and Harper, PSS, 2002.

LET2_R25_SECTORS 0 – 24 (25 bins)

4.15.2.30 LET2_C_R25_SECT_PA Pitch angle LET2CR25SECT (degree)

Size: 25 time-varying

position>angle

LET2_R25_SECTORS 0 – 24 (25 bins)

4.15.2.31 LET2_C_R25_SECT_RTN RTN flow direction LET2CR25SECT

Size: 25×3 time-varying

position>direction

Unit vector, after Fraenz and Harper, PSS, 2002.

LET2_R25_SECTORS 0 – 24 (25 bins)

4.15.2.32 LET2_C_R25_SECT_SA Nominal Parker Spiral angle LET2CR25SECT (degree)

Size: 25 time-varying

position>angle

Angle between particle direction and nominal outward Parker Spiral, based on 400km/s solar wind and corotation breakdown at 10Rs.

LET2_R25_SECTORS 0 – 24 (25 bins)

4.15.2.33 LET2_C_RTN RTN flow direction LET2C

Size: 3 time-varying

position>direction

Unit vector, after Fraenz and Harper, PSS, 2002.

4.15.2.34 LET2_C_SA Nominal Parker Spiral angle LET2C (degree)

time-varying

position>angle

Angle between particle direction and nominal outward Parker Spiral, based on 400km/s solar wind and corotation breakdown at 10Rs.

4.15.2.35 R1C_H_SECT_Rate H sectored count rate R1C (counts s⁻¹)

Size: 1 × 9 time-varying

particle_flux>differential_directional_number_rate

Energy Bins for R1 H SECT 1 – 1 MeV (1 bins)

LET2_R1_SECTORS 0 – 8 (9 bins)

4.15.2.36 R1C_He_SECT_Rate He sectored count rate R1C (counts s⁻¹)

Size: 1 × 9 time-varying

particle_flux>differential_directional_number_rate

Energy Bins for R1 He SECT 1 – 1 MeV/nuc (1 bins)

LET2_R1_SECTORS 0 – 8 (9 bins)

4.15.2.37 R25C_H_SECT_Rate H sectored count rate R25C (counts s⁻¹)

Size: 3 × 25 time-varying

particle_flux>differential_directional_number_rate

Energy Bins for R25 H SECT 3 – 11 MeV (3 bins)

LET2_R25_SECTORS 0 – 24 (25 bins)

4.15.2.38 R25C_He_SECT_Rate He sectored count rate R25C (counts s⁻¹)

Size: 3 × 25 time-varying

particle_flux>differential_directional_number_rate

Energy Bins for R25 He SECT 3 – 11 MeV/nuc (3 bins)

LET2_R25_SECTORS 0 – 24 (25 bins)

OTHER SUPPORT

PSP_ISOIS-EPIHI_L2-SECOND-RATES

ISOIS-EPIHI>Integrated Science Investigation of the Sun, Energetic Particle Instrument Hi
L2-second-rates>Level 2 one-second rates

EPI-Hi second rates cdf. Time tags indicate time of collection.

Instrument paper: Integrated Science Investigation of the Sun (ISIS): Design of the Energetic Particle Investigation. McComas, D. J. et al (2016). Space Sci. Rev., doi:10.1007/s11214-014-0059-1

1 minute to 1 hour

Cite McComas et al (2016), doi:10.1007/s11214-014-0059-1

PRIMARY VARIABLES

OTHER DATA

4.16.2.1 HCI_Lat HCI latitude (degrees)

time-varying

position>latitude

At timestamp. After Fraenz and Harper, PSS, 2002.

4.16.2.2 HCI_Lon HCI longitude (degrees)

time-varying

position>longitude

At timestamp. After Fraenz and Harper, PSS, 2002.

4.16.2.3 HCI_R Heliocentric distance (AU)

time-varying

position>radial

At timestamp. After Fraenz and Harper, PSS, 2002.

4.16.2.4 HET_A_Electrons_Rate Electrons rate HET A (counts s⁻¹)

Size: 3 time-varying

particle_flux>differential_directional_number_rate
Energy Bins for HET Electrons 1 – 3 MeV (3 bins)

4.16.2.5 HET_A_HCI HCI flow direction HETA

Size: 3 time-varying

position>direction

Unit vector, after Fraenz and Harper, PSS, 2002.

4.16.2.6 HET_A_H_Rate H rate HET A (counts s⁻¹)

Size: 2 time-varying

particle_flux>differential_directional_number_rate
Energy Bins for HET H 12 – 23 MeV (2 bins)

4.16.2.7 HET_A_PA Pitch angle HETA (degree)

time-varying

position>angle

4.16.2.8 HET_A_RTN RTN flow direction HETA

Size: 3 time-varying

position>direction

Unit vector, after Fraenz and Harper, PSS, 2002.

4.16.2.9 HET_A_SA Nominal Parker Spiral angle HETA (degree)

time-varying

position>angle

Angle between particle direction and nominal outward Parker Spiral, based on 400km/s solar wind and corotation breakdown at 10Rs.

4.16.2.10 HET_B_Electrons_Rate Electrons rate HET B (counts s⁻¹)

Size: 3 time-varying

particle_flux>differential_directional_number_rate
Energy Bins for HET Electrons 1 – 3 MeV (3 bins)

4.16.2.11 HET_B_HCI HCI flow direction HETB

Size: 3 time-varying

position>direction

Unit vector, after Fraenz and Harper, PSS, 2002.

4.16.2.12 HET_B_H_Rate H rate HET B (counts s⁻¹)

Size: 2 time-varying

particle_flux>differential_directional_number_rate

Energy Bins for HET H 12 – 23 MeV (2 bins)

4.16.2.13 HET_B_PA Pitch angle HETB (degree)

time-varying

position>angle

4.16.2.14 HET_B_RTN RTN flow direction HETB

Size: 3 time-varying

position>direction

Unit vector, after Fraenz and Harper, PSS, 2002.

4.16.2.15 HET_B_SA Nominal Parker Spiral angle HETB (degree)

time-varying

position>angle

Angle between particle direction and nominal outward Parker Spiral, based on 400km/s solar wind and corotation breakdown at 10Rs.

4.16.2.16 HGC_Lat HGC latitude (degrees)

time-varying

position>latitude

At timestamp. After Fraenz and Harper, PSS, 2002.

4.16.2.17 HGC_Lon HGC longitude (degrees)

time-varying

position>longitude

At timestamp. After Fraenz and Harper, PSS, 2002.

4.16.2.18 HGC_R Heliocentric distance (AU)

time-varying

position>radial

At timestamp. After Fraenz and Harper, PSS, 2002.

4.16.2.19 LET1_A_Electrons_Rate Electrons rate LET1 A (counts s⁻¹)

Size: 2 time-varying

particle_flux>differential_directional_number_rate

Energy Bins for LET Electrons 1 – 1 MeV (2 bins)

4.16.2.20 LET1_A_HCI HCI flow direction LET1A

Size: 3 time-varying

position>direction

Unit vector, after Fraenz and Harper, PSS, 2002.

4.16.2.21 LET1_A_H_Rate H rate LET1 A (counts s⁻¹)

Size: 3 time-varying

particle_flux>differential_directional_number_rate

Energy Bins for LET H 2 – 10 MeV (3 bins)

4.16.2.22 LET1_A_PA Pitch angle LET1A (degree)

time-varying

position>angle

4.16.2.23 LET1_A_RTN RTN flow direction LET1A

Size: 3 time-varying

position>direction

Unit vector, after Fraenz and Harper, PSS, 2002.

4.16.2.24 LET1_A_SA Nominal Parker Spiral angle LET1A (degree)

time-varying

position>angle

Angle between particle direction and nominal outward Parker Spiral, based on 400km/s solar wind and corotation breakdown at 10Rs.

4.16.2.25 LET1_B_Electrons_Rate Electrons rate LET1 B (counts s⁻¹)

Size: 2 time-varying

particle_flux>differential_directional_number_rate

Energy Bins for LET Electrons 1 – 1 MeV (2 bins)

4.16.2.26 LET1_B_HCI HCI flow direction LET1B

Size: 3 time-varying

position>direction

Unit vector, after Fraenz and Harper, PSS, 2002.

4.16.2.27 LET1_B_H_Rate H rate LET1 B (counts s⁻¹)

Size: 3 time-varying

particle_flux>differential_directional_number_rate

Energy Bins for LET H 2 – 10 MeV (3 bins)

4.16.2.28 LET1_B_PA Pitch angle LET1B (degree)

time-varying

position>angle

4.16.2.29 LET1_B_RTN RTN flow direction LET1B

Size: 3 time-varying

position>direction

Unit vector, after Fraenz and Harper, PSS, 2002.

4.16.2.30 LET1_B_SA Nominal Parker Spiral angle LET1B (degree)

time-varying

position>angle

Angle between particle direction and nominal outward Parker Spiral, based on 400km/s solar wind and corotation breakdown at 10Rs.

4.16.2.31 LET2_C_Electrons_Rate Electrons rate LET2 C (counts s⁻¹)

Size: 2 time-varying

particle_flux>differential_directional_number_rate

Energy Bins for LET Electrons 1 – 1 MeV (2 bins)

4.16.2.32 LET2_C_HCI HCI flow direction LET2C

Size: 3 time-varying

position>direction

Unit vector, after Fraenz and Harper, PSS, 2002.

4.16.2.33 LET2_C_H_Rate H rate LET2 C (counts s⁻¹)

Size: 3 time-varying

particle_flux>differential_directional_number_rate

Energy Bins for LET H 2 – 10 MeV (3 bins)

4.16.2.34 LET2_C_PA Pitch angle LET2C (degree)

time-varying

position>angle

4.16.2.35 LET2_C_RTN RTN flow direction LET2C

Size: 3 time-varying

position>direction

Unit vector, after Fraenz and Harper, PSS, 2002.

4.16.2.36 LET2_C_SA Nominal Parker Spiral angle LET2C (degree)

time-varying

position>angle

Angle between particle direction and nominal outward Parker Spiral, based on 400km/s solar wind and corotation breakdown at 10Rs.

OTHER SUPPORT

EPI-LO DECODER RING

We have produced a summary of the EPI-Lo data called the EPI-Lo Channel Definition “crib sheet”. The intent is to guide the user from a description of physical measurements to specific data products. Note that this relationship is time dependent and Figure 4 only applies during the first three orbits (launch until 21 November 2019, LUT Regime Index = 1). The time dependence is due to instrument configuration changes (e.g., changing definitions of species and energy bins due to adjustment to lookup tables or LUTs) and unplanned changes (e.g., sensitivity variations or background increase due to dust impacts admitting more light).

PSP / ISOIS / EPI-Lo Rate Channel Definitions			LUT Regime Index = 1 Orbits 1, 2, and TBD				TRIPLES (except T, U = DOUBLES)						
Mode	Channel / rate	Label	ChanID		species	mass	E (keV)		E (MeV/nuc)		Logical	Variable	comments
	mnemonic		low	high		amu	low	high	low	high	Source	Name	
IC	[P] Protons	High Res. Protons	P000	P040	H	1	60	8,990	0.060	8.990	psp_isois-epilo_l2-ic	H_Flux_ChanP	box not defined
IC	[P]	High Res. Protons	P041	P047									
IC	[C] Composition	Ions Group 1	C048	C093	He-3	3	84	20,000	0.028	6.667	psp_isois-epilo_l2-ic	He3_Flux_ChanC	
IC	[C]	Ions Group 1	C094	C140	He-4	4	72	20,000	0.018	5.000	psp_isois-epilo_l2-ic	He4_Flux_ChanC	box not defined
IC	[C]	Ions Group 1	C141	C145									
IC	[C]	Ions Group 1	C146	C186	O	16	227	20,600	0.014	1.288	psp_isois-epilo_l2-ic	O_Flux_ChanC	box not defined
IC	[C]	Ions Group 1	C187	C192									non-standard boxes
IC	[C]	Ions Group 1	C193	C197	Fe	Null							
IC	[C]	Ions Group 1	C198	C238	Fe	56	453	22,300	0.008	0.398	psp_isois-epilo_l2-ic	Fe_Flux_ChanC	box not defined
IC	[C]	Ions Group 1	C239	C239									
IC	[D] D = Comp. + 1	Ions Group 2	D240	D260	C	12	197	20,400	0.016	1.700	psp_isois-epilo_l2-ic	C_Flux_ChanD	box not defined
IC	[D]	Ions Group 2	D261	D351									
IC	[D]	Ions Group 2	D352	D366	Si	28	529	21,400	0.019	0.764	psp_isois-epilo_l2-ic	Si_Flux_ChanD	box not defined
IC	[D]	Ions Group 2	D367	D431									
IC	[T] TOF Only	Ion TOF	T000	T031	Ions	1	44,900	30	44,900	0.030	psp_isois-epilo_l2-ic	H_Flux_ChanT	no composition
IC	[R] R = Proton + 1	Hi Time Res Protons	R000	R014	H	1	60	8,320	0.060	8.320	psp_isois-epilo_l2-ic	H_Flux_ChanR	
IC	[R] skip Q = Q quadrant	Hi Time Res Protons	R015	R015	H	1	Null						non-standard boxes

PSP / ISOIS / EPI-Lo Rate Channel Definitions			LUT Regime Index = 1 Orbits 1, 2, and TBD				SINGLES (except X = DOUBLES)						
Mode	Channel / rate	Label	ChanID		species	mass	E (keV)		E (MeV/nuc)		Logical	Variable	comments
	mnemonic		low	high		amu	low	high	low	high	Source	Name	
PE	[E] Electron	High Res Electrons	E000	E000	deposited	null							hi/lo gain, no comp.
PE	[E]	High Res Electrons	E001	E047	deposited		15	327,000	0.015	327			hi/lo gain, no comp.
PE	[E]	High Res Electrons	E000	E016	e- cal		26	388	0.026	0.388	psp_isois-epilo_l2-pe	Electron_Flux_ChanE	hi/lo gain, no comp.
PE	[E]	High Res Electrons	E002	E031	H cal	1	399	10,200	0.399	10.2	psp_isois-epilo_l2-pe	H_Flux_ChanE	hi/lo gain, no comp.
PE	[F] F = Elect. + 1	High Time Res. Electrons	F000	F000	deposited	null							hi/lo gain, no comp.
PE	[F]	High Time Res. Electrons	F001	F015	deposited		35	327,000	0.035	327	psp_isois-epilo_l2-pe	Electron_Flux_ChanF	hi/lo gain, no comp.
PE	[F]	High Time Res. Electrons	F000	F011	H cal	1	399	10,200	0.399	10.2	psp_isois-epilo_l2-pe	H_Flux_ChanF (pending)	hi/lo gain, no comp.
PE	[G] G = Elect + 2	High Look Res Electrons	E000	G000	deposited	null							hi/lo gain, no comp.
PE	[G]	High Look Res Electrons	E001	G047	deposited		15	327,000	0.015	327	psp_isois-epilo_l2-pe	Electron_Flux_ChanG	hi/lo gain, no comp.

Figure 4: EPI-Lo Decoder Ring.

The upper table in Figure 5 references only data products that include time-of-flight TOF measurements and the lower table references only measurements that employ the energy/solid state detector (SSD) system. Both have the same columns. The Mode identifies one of four instrument modes: Ion Composition (IC), Particle Composition (PC), Ion Energy (IE) or Particle Energy (PE), (PC and IE are not included in Release 1) which relate to the types of measurements made. The instrument can cycle through up to eight different mode intervals (slots) per second. Typically the slot pattern covers all four modes in an alternating pattern (e.g., IC,PE,IC,IE,IC,PE,IC,PC). The next column is the channel/rate name and the associated mnemonic. Different channels can measure multiple types of particles, so it is useful to provide a non-descriptive, but memorable, name for the different data products to help avoid confusion like “During this period the Electron data are mostly protons” in favor of ‘During this period the [E] rates are mostly protons. The mnemonic and associated system is based largely on what we expect to see in each the given channel (e.g., [E] for electrons). The next column provides the official, descriptive label for each data type. The Channel ID provides the useful range and naming of individual channels associated with each data

type or sub group thereof. Species mass provides the species or type (or alternate information). The energy range associated with the channel ID list is given in keV and MeV/nuc (where applicable). The CDF data file needed to study the particles described on a given row are in the Logical Source. Within each file the variable name is given for physical units and counting rate. Finally, there are miscellaneous notes on each row in the last column. See Release Notes on details for variables and calibrated data products.

ACRONYMS

For detailed information on the various [coordinate systems](#), refer to [Franz and Harper \(2002\)](#).

ApID: Application Identifier
EPI-Lo: Energetic Particle Instrument - Low Energy
EPI-Hi: Energetic Particle - High Energy
FOV: Field of View
GSE: Geocentric Solar Ecliptic
GSM: Geocentric Solar Magnetospheric
HGC: Heliographic Coordinates
HAE: Heliocentric Aries Ecliptic
HCI: Heliocentric Inertial
HEE: Heliocentric Earth Ecliptic
HEEQ: Heliocentric Earth Equatorial
IC: Ion Composition
IE: Ion Energy
IS \odot IS: Integrated Science Investigations of the Sun
PC: Particle Composition
PE: Particle Energy
PSP: Parker Solar Probe
RTN: Heliocentric
TAI: International Atomic Time, defined by SI seconds
TOF: Time of Flight
TPS: Thermal Protection System
UTC: Coordinated Universal Time

REFERENCES

- McComas, D., et al. (2016). Integrated science Investigation of the Sun (ISIS): Design of the Energetic Particle Investigation. *SSRv*, 204:187–256. DOI 10.1007/s11214-014-0059-1.
- Hill, M., et al. (2019). in preparation.
- Szalay, J., et al. (2019). in preparation.
- Franz, M. and D. Harper (2002). Heliospheric Coordinate Systems. *Plan.Space Sci.*, 50, 217–233.